The degenerate human lumbar vertebral endplate – a mechanical, clinical and histological analysis

Tom Paul Marjoram
MBChB, FRCS(Tr&Orth)

A thesis submitted as a contribution of work for the award of Doctor of Medicine by the University of East Anglia Medical School.

July 2021

Abstract

Background

Low back pain is an increasingly common health problem. Treatment employs a range of surgical and non-surgical techniques. The adult intervertebral disc is one source of significant pain although each individual element of the functional spinal unit interacts with one another. The disc normally is largely avascular thus relying on nutritional support from the adjacent vertebral endplates. The vertebral endplate undergoes a process of degeneration alongside degeneration of the disc and has also been implicated in itself as a pain source. In a proportion of those with degeneration (but not exclusively) vertebral endplate changes can be seen on MRI imaging as described by Modic. There is little understanding of the changes in the degenerate endplate. An understanding of the changes seen at the endplate will contribute to the overall understanding of the process of degeneration in the spine.

Aims

This work aims to study the effects of degeneration of the human lumbar intervertebral disc on the endplate. The analysis incorporates the mechanical properties of indentation modulus and hardness, a clinical study exploring the translation of these mechanical properties into medical practice and a histological analysis exploring vascularity, inflammation and bone turnover.

Methods

Nano-indentation techniques have been applied to fresh, non-embedded human vertebral endplate samples taken at the time of surgery for symptomatic degenerative disc disease. Two sets of samples are included from those without degenerate discs for comparison.

Histological analysis has been performed on a representative selection of the same samples using immuno-stains for CD-3, CD-20, CD-31 and CD-56, giving unique mechanical and histological analysis of the same samples.

MRI study of each individual case had defined the clinical status of the disc and endplate. A parallel clinical analysis of post-operative lumbar interbody device subsidence at 12 months has been undertaken including patients from two independent tertiary specialist spinal surgery centres in order to bridge the basic science into clinical fields.

Results

Degeneration significantly increases the stiffness of the endplate by 26.4% (3.623GPa vs 4.581GPa) and the underlying trabecular bone by 19.8% (4.185GPa vs 5.014GPa) while also increasing the hardness of the trabeculae by 9.3% (0.150GPa vs 0.164GPa).

The presence of type 1 or type 2 Modic changes at the endplate is associated with an increase in indentation modulus and hardness at both the endplate and the underlying trabecular bone while type 3 changes showed the reverse with a decrease in indentation modulus and hardness in both regions.

Histological analysis showed degeneration to be associated with increased calcification of the cartilaginous portion of the endplate, increased vascularity in the region of the endplate and an increase in the number of CD-56 staining Osteoblast lineage cells.

Modic type 2 changes were found to be associated with an increase in endplate variability and Osteoblast lineage cells indicating a state of increased bone turnover.

Interbody fusion device subsidence was found to be highest in those with type 2 Modic changes and lowest in those with type 3 changes. This indicates that the increased hardness and stiffness in Modic 2 changes are detrimental to the mechanical stability of the device clinically.

Conclusions

Degeneration has been found to affect the mechanical properties of the human lumbar spine endplate. Modic pathology in degeneration has been shown to affect the mechanical properties which in turn (as a secondary outcome) affect the rate of clinical lumbar interbody fusion device subsidence: type 2 Modic changes have a detrimental effect and type 3 seem to offer some favourable mechanical properties. An increase in histological endplate calcification is accompanied by an increase in vascularity and markers of bone turnover, likely as a response to altered force transmission from the degenerating disc.

Acknowledgements

I would like to acknowledge and thank the institutions that have contributed towards the funding of this MD:

The Gwen Fish Trust whose trustees have been supportive and flexible, allowing me to navigate several issues.
Action Arthritis who contributed towards the MD Fees relieving the burden of this cost.
The British Association of Spinal Surgeons who contributed to the running costs of the project – specifically sample collection and transport.
The Ipswich Hospital Charitable fund for contributions towards hospital running costs.

I would like to thank my supervisors across all three institutions involved in this research. Without them the work would not have been possible: in the Cambridge Centre for Medical Materials, Prof. Ruth Cameron and Prof. Serena Best for their advice and support; Andrew Rayment (senior technical officer in material science, also from Cambridge) for his help and guidance with the nano-indentation; from the University of East Anglia, Prof. Iain McNamara and Prof. Alex McGregor for the supervision and support of the MD Process; from the Norwich Biorepository, Roxanne Brunton-Sim, Dr Rachael Stanley and Prof. Mark Wilkinson for facilitation of the sample collection, processing and histological staining methods; from the Norfolk and Norwich University Hospital; from Ipswich Hospital Spinal Surgery Unit, Mr Saajid Kaleel for his support with the sample collection and multiple discussions about the implications of the research. Finally, also from Ipswich, Mr David Sharp who is responsible for the initial conception of the project and my recruitment into it. We have spent many hours discussing the intellectual aspects of the project and many more despairing about the hurdles that we have overcome to make it all happen.

Lastly, I would like to thank my wife Rebecca for her support and tolerance. She has (and no doubt will continue to) suffered many evenings waiting for me to finish working. She has listened to the many challenges that this project has created with patience and without complaint. Without her support I would not have been able to complete this work.

Table of Contents

Index of Tables

Index of Figures

Index of Equations

5.1-1 to 5.1-7 describe the Oliver Pharr method. 6.1-1 describes the Dabbs method of radiological measurement.

1 Introduction

This introduction aims to provide a background of information to explain the nature of the issues surrounding this research, the current knowledge, gaps in this knowledge and a basis for technique utilisation and development. It contains work that has been published with open access and this work is referenced in the appendix.

1.1 Low back pain

Low back pain is an established and significant health problem[1,2] with not only health but also economic impacts. Wynn-Jones used pooled estimates to find 32% of the working age population suffering with low back pain will not have returned to work after one month [3]. In Europe the economic cost of back pain due to time lost from work is estimated to be €12 billion, affecting up to 47% of working age men [4]. Cheung et al. found 40% of those under 30 displayed MRI evidence of lumbar disc degeneration which increased to 90% by 55 years of age[5] they also found a strong correlation between disc degeneration and low back pain. The causes for low back pain are multifactorial and this reflects the range of therapies that have been employed including psychological approaches [6], physical therapies [7], pain management techniques and surgical intervention.

1.2 Treatment for low back pain

Therapy in the UK for low back pain initially employs a combination of non-surgical and pharmacological methods provided by primary care physicians including physical therapy. 93.3% of people with acute low back pain will have recovered well enough to return to work by 6 months [3]. This leaves 6.7% of the population that will not respond. In the UK, once a person has been on incapacity-related welfare benefit for 1 year, they are more likely to die or retire than return to work [4].

The surgical management of low back pain for degenerative disc disease is reserved for those that do not respond to or are unable to manage their symptoms with non-surgical and pharmacological methods. It employs some key concepts. The principle of the 'functional spinal unit' [8] describes the spine in terms of motion segments acting as a functional unit. Each functional unit is comprised of the intervertebral disc and its adjacent (cranial and caudal) vertebral bodies which are connected via posterior articulations of facet joints. The

disc is a vital part of this functional unit, conveying stability but allowing movement which transfers forces to the adjacent vertebral bodies.

Fusion for non-specific chronic low back pain is currently not recommended by NHS England [9]. A recent systematic review and meta-analysis did, however, find good evidence that surgical fusion for chronic non-responsive low back pain was a good option [10]. NHS England do, however, recommend fusion for low back pain if there is concurrent nerve compression causing pain of a radicular nature[9].

Once the decision to operate has been made, a well-recognised treatment for degenerative disc disease is the use of a surgical implant to restore height, sagittal balance and create fusion [11]. The propensity for fusion depends on both the mechanical stability of the implants, which is reliant on the adjacent endplates, and also the nutritional availability to the region such that a fusion can occur.

The posterolateral portion of the endplate has been demonstrated to be the strongest, and it is recommended that implants are placed here to avoid subsidence [12,13]. This is, however, mechanically less advantageous than placing the device anterior in the disc space when one considers the correction of deformity and sagittal balance which are well known to be vital to the success of fusion constructs [14]. Anterior placed devices are further from the fulcrum of correction and thus are able to exert a greater corrective force.

Cell based regeneration of the disc attracts large amounts of attention. Animal studies have shown some promise with increased matrix production in both animal studies and some human studies. The exact lineage of stem cells that will work best is, however, yet to be realised, and further work is needed before this becomes a viable treatment option[15]. Others have explored the stimulation of existing cells as a potential therapeutic intervention, but these are some way from being clinically useful despite some initial promising results [16]. Other potential strategies in regenerative approaches to the degenerate disc include injectable hydrogels to try to re-hydrate the disc and improve the mechanical environment and have the potential for incorporation of cell therapy cultures into the matrix. A recent review of repair and regeneration of the degenerate disc concludes that such therapies are ‘more a fiction than a fact’[17].

Undoubtably a key to the concept of regeneration is the nutritional availability to the region in which the cells are expected to thrive. It has been shown that the cartilaginous endplate plays a crucial role in disc nutrition [18–20]. If we are to expect new cells inserted into a

degenerate disc to survive and regenerate the disc, they will require the nutrients to do so[21]. The process of disc degeneration has been shown to significantly affect the diffusion across the endplate[22]. A cadaveric study analysing the micro-architecture of the endplate and subchondral bone in a range of discs showed that while the thickness of the endplate does increase this is also accompanied by an increase in porosity [23]. They surmised that altered nutritional availability may be due to the quality of the underlying capillaries as opposed to a decrease in the permeability. This may be an oversimplification, making the assumption that porosity is proportional to diffusion. The findings from a study correlating porosity with the diffusion of metabolites found them to be independent of each other [24]. Wu et al. used a finite element model to demonstrate that the endplate is critical for nutritional availability to the intervertebral disc and calcification of the endplate reduces the available nutrients. They comment that cell injection increases the nutritional demands[21]. Simply injecting cells into the disc without an understanding of the effect of degeneration on nutrition is unlikely to be successful. A more in-depth structural and mechanical knowledge of the endplate in symptomatic diseased humans will provide valuable information in the utilisation and development of this treatment in the population in which it is intended to be used.

There is currently no consensus on the ideal treatment for low back pain [25]. Our understanding of the pathological processes involved in the degeneration of the human disc causing pain continues to develop, but evidence can be conflicting. The true underlying pathological process is likely to be variable and multifactorial. We must consider the mechanical environment of the disc, the chemical and immunological changes that occur with the degenerative process, and the link with infective processes, especially in pre-disposed individuals. There is no doubt that a greater understanding of the adjacent endplates and surrounding bone will play a key role in this further understanding.

Key to the utilisation of therapy of any kind, especially surgical intervention and intradiscal therapies, is the ability to use clinical information with the application of basic principles and evidence-based medicine to identify those patients who are most suitable for the available treatment pathways. Clinical application of basic science concepts and findings rely on a greater understanding of the interpretation of clinical investigations; key to the assessment of the spine is the MRI. A correlation of MRI changes in clinically symptomatic patients and the mechanical structure of the endplate may provide a key link between the clinical and basic science.

1.3 An introduction to the disc

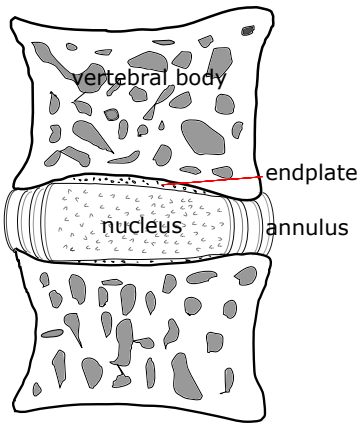

Figure 1.3.1 A diagram of the intervertebral disc.

The adult intervertebral disc is an avascular structure relying on the adjacent vertebral endplate for nutritional support [18,25]. Macroscopically the disc consists of an outer annulus fibrosis and a central nucleus pulposus. It develops in utero at approximately day 30. The anulus fibrosis arises from sclerotome origin while the nucleus pulposus forms from a process of involution of the notochord which has a mesodermal origin[26].

The outer annulus connects to the endplate via specialised type 1 collagen fibres with elastin bundles known as Sharpey's fibres [27]. The annulus fibrosus consists of collagen fibres arranged in layers of fibres alternating at 30° angles [28], which serve to resist circumferential stresses transmitted from the nucleus pulposus while allowing a limited range of motion to occur at the disc in the coronal and sagittal planes as well as some rotation. The outer portion of the normal annulus fibrosis contains the majority of the nociceptive pain fibres of the disc endplate complex and the remainder of the healthy disc is normally aneural. In the degenerative disc it has been shown that the density of neurones increases and that areas of the disc that usually have no innervation can become populated with neurones [19,29,30]. This implicates the disc as a source of pain in the process of degeneration.

The nucleus pulposus consists of collagen fibres within an extracellular matrix containing aggrecan and elastin which in the healthy disc is highly hydrated. This serves to aid the even transfer of applied forces to the endplate.

Degeneration of the intervertebral disc and its adjacent endplates is complex and multifactorial with genetic and environmental influences[31,32]. Loss of disc height that occurs with degeneration is also known to increase the forces passing through the posterior facet

joints contributing to accelerated degeneration and pain. We know that severe back pain prevalence increases with age [2]. The study of the ageing disc has shown evidence of significant biochemical changes including the loss of proteoglycans (which attract water). The reduction in hydration has been shown to significantly alter the stress transfer to the vertebral endplate causing failure and re-modelling, altering the nutrient transfer which further contributes to degeneration [33].

On a cellular level, degeneration of the disc has been shown to be a progressive phenomenon with the formation of fibrous tissue and degeneration of the normal disc matrix and a reduction in cell density[19]. Le Maitre et al. describe an increase in the expression of degradation enzymes including matrix metalloproteinases and ADAMTS (a disintegrin and metalloprotease with thrombospondin motifs) relative to their inhibitors. They suggest that this represents a dysregulation of the normal homeostasis of the disc.[34]. Implicated signalling molecules that have been shown to play a key role in the regulation of this pathway include interleukin 1 and TNF-α. IL-1 knockout mice displayed typical features of human disc degeneration when examined adding to the observation of an imbalance with the normal levels of IL-1 in relation to its natural inhibitor IL-1Ra seen in human disc degeneration [35]. Degeneration of the disc is therefore likely to represent a disruption of the homeostasis of the normal function of a healthy disc. This may be precipitated by excessive load which has been shown to inhibit the normal synthesis of extracellular proteins [36] , infection, or changes to the mechanical or biological environment in genetically susceptible individuals. Restoring this complex balance may hold some promise but identifying the correct patients in whom a favourable environment can be achieved will rely on greater understanding of the pathological changes and their correlation with imaging modalities.

1.4 An introduction to the endplate

The interface between the disc and the vertebral body, the endplate, plays a key role in the maintenance of a healthy motion segment. The endplate acts as an anchorage system for the disc with fibrils crossing the cartilaginous and bony portion. Mechanically these are more resistant to failure in compression and shear than in tension [37]. The endplate has been shown to be the vulnerable aspect of the intervertebral disc[38]. Mechanical failure of the endplate has been shown to produce pain and to cause changes on a cellular level that further alter the mechanical environment, creating a cycle of degeneration [19]. Breaches of the endplate in degeneration were described in 1927 by Schmorl [39]. He later noted these to be herniations of

nucleus material through the endplate[40]. Most resolve spontaneously but some seem to be a pain generator. They are more common in the degenerate spine and theories as to their origin include mechanical overload, degenerative weakening of the endplate and a developmental defect (as there is notochordal tissue present in the developing vertebra)[41].

The normal adult disc has a low density of cells and an acid environment due to the low oxygen tension leading to anaerobic metabolism and a build-up of lactic acid. Nucleus cells can survive in this oxygen deplete environment, but a lack of glucose is tolerated poorly[19].

The nutritional supply to the disc is dependent on the free diffusion between the capillaries in the subchondral bone of the vertebral body and the disc across the endplate [20]. The implications of interrupting this this normal diffusion not only apply to the degenerative process but must also be considered when conceiving novel therapies regarding the regeneration of this disc.

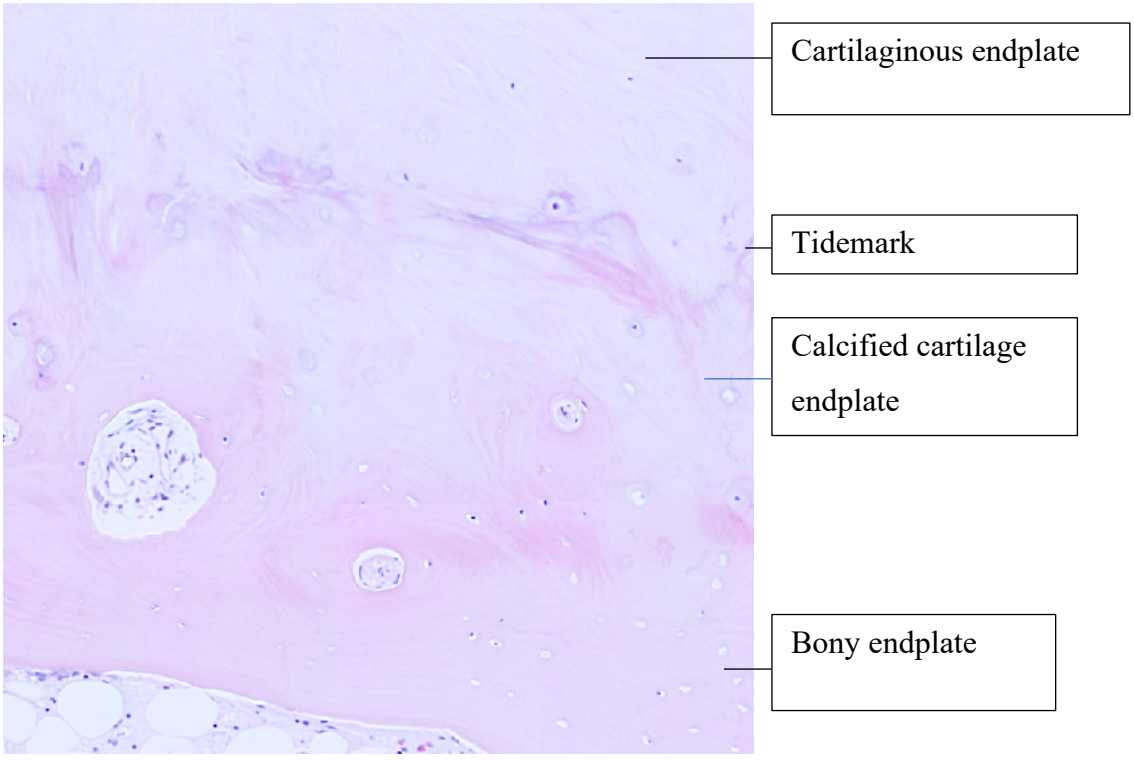

Figure 1.4.1 Histological section of the human vertebral endplate

The endplate has two components, the cartilaginous and the bony portions. The cartilaginous endplate is closer to the disc and has a higher concentration of collagen (as opposed to proteoglycans) in the periphery, suggesting more structural importance here[42]. As one ages the cartilaginous endplate undergoes a process of calcification and resorption. This, in conjunction with age related changes to the nutrient canals, reduces the diffusion across the

endplate by a value in the region of 50% [43,44]. The calcified cartilaginous endplate is delineated from the uncalcified portion by a tidemark which is visible on histological sections. Figure 1.4.1 offers an illustration of the histological section of the human endplate.

The bony endplate consists of an epiphyseal rim/ring peripherally and a separate central portion which is more porous[12]. It is not clear if the endplate represents specialised cortical bone or merely a confluence of trabecular bone; perhaps it is neither and instead is a unique form of specialised bone.

Stiffness and strength increase as one moves peripherally and also increase throughout the endplate generally in the more caudal spinal levels. Interestingly it is preferentially the peripheral epiphyseal rim that undergoes changes in degeneration resulting in a 40% decrease in stiffness and 25% decrease in strength overall [45]. A retrospective MRI study focusing on the disc in osteoporosis did, however, demonstrate that the presence of osteoporosis was associated with a much lower incidence of disc degeneration [46]. This would imply that the decrease in endplate stiffness and strength seen by Liu et al. is a consequence of the degenerative process rather than a cause.

A detailed analysis of the human endplate by Wang et al. produced some interesting findings in cadaveric degenerate discs (defined by discography). It found that increased thickness of the endplate was associated with more disc degeneration but not bone mineral density, size or concavity. More strongly it associated lesions of the endplate (Schmorl's nodes, fracture, calcification and erosions) with degeneration of the disc. Degeneration was also more strongly correlated with abnormalities of both the cranial and caudal endplates of a disc rather than in isolation [47]. The work investigated the overall morphology of the endplate and found no statistical correlation with a difference of the shape of the endplate (concave/flat/convex) and adjacent disc degeneration. The analysis involved a large (over 200) number of endplates for detailed analysis, providing valuable information on which to build. This is cadaveric work, however, based upon degeneration as a discographic entity rather than a disease process. Translation of this work into clinical practice requires the analysis of the endplate in clinically symptomatic individuals and to build upon it using clinical imaging to correlate findings in order to allow application to surgical practice.

1.5 The bone

Bone gains its strength, much like any other structure, through a composite of the structural properties and the material properties. Bone, as a living tissue, is able to re-model and repair itself in response to a variety of stimuli, including responding to chemical signalling pathways and directly responding to the load exerted upon it.

The basic components of bone can be subdivided into organic and inorganic compounds. The principle organic components being collagenous proteins (principally type I) in matrix proteins. Collagen is known to form a triple helical structure (type 1 containing two $\alpha 1$ and one $\alpha 2$ chains). These microfibrils align with a quarter stagger pattern to form fibrils of collagen essential to the formation, turnover and structure of the bone, especially tensile strength. The other organic components of bone are cellular: Osteocytes are thought to have a regulatory function in response to mechanical stimulus, communicating to osteoblasts through dendritic connections via gap junctions, they are former Osteoblasts, which are cells with a mesenchymal origin which lay down new osteoid matrix; and Osteoclasts develop from myeloid haematopoietic stem cells that resorb bone by creating lacunae in which the pH is low, increasing the solubility of hydroxyapatite and then secreting proteolytic enzymes (such as cathepsin K) to degrade the inorganic matrix. The inorganic component of the bone matrix is principally Hydroxyapatite (HA) ($Ca_{10(}PO_{4)6}(OH)_2$) a crystalline structure often referred to as plate-like (dimensions approx. 50nm x 15nm x 5nm). The numerous impurities found in bone HA change both the mechanical properties and the solubility which are understood to aid the process of homeostasis [48].

The organisation of the organic and inorganic components allows a further classification into two main types: woven bone in which there is a random organisation of the components and lamellar bone in which the collagen and inorganic matrix are laid down in an ordered fashion (in response to the mechanical environment). Woven bone is often a precursor to lamellar bone; it is found in the developing skeleton in zones of transition from the cartilaginous physis to the more ordered lamellar bone. Woven bone is also found in areas of pathology including in callus after fracture. Work by Bromage et al.[49] with polarised light microscopy demonstrated that the orientation of collagen within lamellar bone is variable in response to the type of force predominating in that region of the bone. Lamellar bone can exist in two distinct macrostructural subtypes: cortical and trabecular. Cortical bone is dense lamellar bone consisting of a system of osteons. An osteon is centred on the Haversian canal and

consists of concentric layers of lamellar bone interspersed with Osteocytes. Each osteon is connected with its neighbour via a cement line and Haversian canals are interconnected via Volkmann's canals forming an interconnected system for the passage of nutrients, waste and signalling molecules. Each osteon is a cylinder about 200–250μm in diameter[50]. Cortical bone most often forms the outer portion of a bone and is responsible for much of the mechanical strength. The cortical shell can be of varied thickness depending on the mechanical demands of the bone and physiological conditions. The second macrostructural sub classification of lamellar bone is trabecular bone. This is often referred to as 'spongy' bone and consists of spaces between struts of bone that contain bone marrow (among other things) which is essential to haematological function. It is important not to underestimate the mechanical function of trabecular bone, however; for instance the proximal part of the femur, which is able to withstand significant forces, is predominantly trabecular bone. Mechanically, bone displays anisotropic properties (displaying differing mechanical properties in differing axis of testing)[50], but its material properties also change depending on the site of the bone (due to the ability of the bone to rearrange its extracellular components depending on its mechanical environment). This variation is described as being orthotropic[51].

Bone exists in a state of constant turnover and adaptation to the forces applied on it. This turnover is influenced by both local and systemic factors, including mechanical load and the homeostasis of various elements such as calcium. It is well established that bone formation is strongly linked with the number of Osteoblasts in a given area[52]. Osteoblasts are cells of mesenchymal origin that are the principle cell responsible for the deposition of bone matrix [53]. Differentiating from osteoprogenitor cells, the Osteoblasts synthesise bone matrix initially by secreting the organic components of the matrix (type 1 collagen, proteoglycans and other proteins). This is followed by the mineralisation of the inorganic component relying on the formation of hydroxyapatite crystals within vesicles in response to calcium release from the degradation of proteoglycans and phosphate ions through the action of Alkaline phosphatase (ALP)[54]. Mature Osteoblasts, which are cuboidal in shape, can undergo a process of apoptosis, can become Osteocytes embedded within the bone or become bone lining cells which are spindle shaped cells thought to represent a resting phase and perhaps act as a barrier to the action of Osteoclasts (which resorb the bone matrix) and which can retract to allow access [55].

Osteoblasts have a strong effect on bone resorption (as well as formation). Through the RANK ligand signalling pathway they can stimulate the activation of Osteoclasts, thus

increasing the rate of bone resorption. Localised inflammatory processes have been shown to activate the RANKL pathway stimulating the activation of Osteoclasts and increasing the resorption of bone[56]. Pacios et al. [57], using genetically modified mice, demonstrated that this inflammatory upregulation in bone resorption (in this case secondary to a dental biofilm) was dependant on the presence of functioning Osteoblasts. Activation of the RANKL pathway as a contributing factor in subchondral bone resorption in cartilage degeneration (in an equine population) has been demonstrated by Bertuglia et al. [58].This study also demonstrated a release of RANKL from the damaged hyaline cartilage which perhaps represents a direct signal pathway between this and the underlying bone. The correlation between the severity degeneration and the scale of bone remodelling around the knee has been demonstrated by work from Bobinac[59]; they showed that in early degeneration the trabecular thickness and trabecular bone volume were decreased while this seemed to be the opposite in more advanced degeneration of the overlying cartilage. In this more advanced stage of degeneration, it was found that the overall number of trabeculae was decreased despite an increase in the overall trabecular volume. Animal model work found a fall in subchondral bone mineral density with degeneration, while also finding that osteoporosis contributed to degeneration of the cartilage [58,60]. The process of synovial joint degeneration is a separate process from that of spinal disc degeneration; however, there are similarities in the histological structure. The subchondral bone in the synovial joint is of a 'plate like' configuration with trabecular bone below but continuous with this[61]. Histologically the chondral layer has a tidemark separating it from the calcified cartilage and a secondary tidemark separating the calcified cartilage from this plate-like bone layer. Risk factors for both diseases are similar and include age, high body mass index, genetic predisposition and injury through work or sport [61–65], indicating that drawing comparisons with caution might be appropriate.

In the vertebrae of the spine the cortical shell is often thin and comprises a very small percentage of the thickness of the bone. The trabecular bone makes up the vast proportion of the vertebral bone content. Perhaps one of the best known and most common processes to affect this structural level of the bone composition is osteoporosis. This disease process is separate from the ageing process and is characterised by a reduction in bone density. It is the thickness of the trabecular and cortical bone that decreases, resulting in an overall reduction in bone density as measured by dual energy X-ray absorptiometry (DEXA) when compared to either predicted peak bone density or age matched normal values.

The function of bone is not purely mechanical. It has a key role in mineral homeostasis (principally but not exclusively calcium and phosphate), and the bone marrow that it contains is an essential site for haematopoiesis. It is under influence of both systemic and local signalling pathways as well as being able to respond directly to mechanical stimuli (a process commonly referred to as Wolff's law[66]). It is this variable mechanical property that will be investigated with the nano-indentation methods I will be using, specifically with reference to how the process of degeneration in the lumbar spine alters these properties.

1.6 Mechanical testing of bone

The mechanical properties of bone have been investigated using multiple techniques.

Values for the Elastic Modulus vary depending on the method of testing, the preparation and the type of bone. Trabecular bone has a range from 1-13GPa in the previous literature[67,68]. Testing has taken the form of micro-indentation and progressed to nano-indentation which has been combined with other characterisation methods, including Fourier transform infrared micro spectroscopy, micro-CT and Raman spectroscopy [69–73].

Choi in 1990[67] used 3 point bending to determine the elastic modulus of subchondral bone (1.15GPa), trabecular bone (4.59 GPa) and cortical bone (5.44GPa) from the human tibia. In the trabecular bone they did not find any significant difference in the mechanical properties of the bone when considering the anatomical orientation (horizontally orientated compared with vertically orientated).

Liu et al. compared cadaveric spine samples with micro-CT and 3mm spherical tip indentation to findings of degeneration in MRIs of cadaveric specimens [45]. They calculated load to failure data and stiffness from the loading curve data, concluding that stiffness and strength as defined in their study both decreased with signs of degeneration. They found correlations between this reduction and the presence of Modic changes but no differences between the 3 types of Modic change. Further investigating Modic changes, Perilli et al. biopsied trabecular bone through a transpedicular approach performing an architectural analysis with micro-CT and histological analysis. They found that there was an increase in trabecular fraction moving from Modic type 1 to Modic type 3 and decreasing evidence of bone turnover with this same progression [74]. This work suggests Modic type 1 to be an active phenomenon with type 3 to represent a less active (in terms of bone turnover) stage of the disease process. In 2012, Hou et al. performed micro-indentation with a 1.5mm spherical

indenter on cadaveric specimens determining load to failure. They found that the inferior lumbar endplate withstood a higher load to failure; they also found that the peripheral endplate regions had a higher load to failure than the central regions. They found a non-uniform decrease in load to failure in those with degenerate discs (degeneration being decided upon by macroscopic inspection); interestingly the peripheral regions were less affected than the already weaker central regions, further exaggerating the relative difference between the central and the peripheral regions. They also measured bone mineral density with DEXA and found that with a decrease in bone density came a uniform decrease in load to failure [13]. This is a distinctly different finding from their degeneration analysis which seems to preferentially affect the central region of the endplate.

A review by Arnold at al. into micro-indentation techniques applied to bone commented as follows: 'One of the main obstacles facing micro-indentation as a testing method is recognising what part of the complex hierarchical structure of bone is being tested'[72]. They recommended the use of a spherical tip at this scale to reduce the amount of plastic deformation that occurs at the indenter tip. The papers included in this review were using indentation tips on a millimeter scale (3mm for the vertebral samples) and indentation loads of 10-20N (one paper using 250N on cortical bone). Plastic deformation with this load would clearly be an issue to take into consideration. Considering the loads being applied and the size of the tip in comparison with the average trabecular size (2mm) it is likely that micro-indentation of trabecular bone is producing a composite of the structural properties as well as the material properties of the samples. This may be desirable in some cases, especially when considering osteoporosis and trabecular thinning, and it does provide some valuable information when mapping the regions of the vertebrae which may help to guide implant design and position for instance. One way to reduce the effect of both plastic deformation and structural properties affecting the results is to reduce the scale and use nano-indentation to assess the structural properties of the bone. With a smaller tip contact area relative to the trabecular size and a lower force of indentation it is unlikely that the structural properties will alter the data. Nano-indentation is, however, more sensitive to the rough surface of biological samples; the preparation of the samples and the mounting of the samples are all important considerations when undertaking this work.

Nano-indentation has become an increasingly used method of mechanical testing and material science. Key to understanding this is work from Oliver and Pharr where they describe a technique for calculating the Young's modulus from the unloading data of an

indentation commonly referred to as the Oliver-Pharr method [75]. Applying this method requires a knowledge of the geometry and material properties of the indentation tip and its surface area of contact at any given depth, which allows calculation of the hardness of the tested material, and from an extrapolation of the initial portion of the unloading curve (typically at 90% unloading) the indentation modulus can be calculated.

Rho et al. employed nano-indentation to cortical and trabecular bone that was dehydrated and embedded followed by a process of progressive polishing. They used a diamond indenter with a force of 20mN and a rate of 1mN/sec and a hold time of 10s [50]. They found the modulus of cortical bone to be 22.4GPa in the osteon and 25.7GPa in the interstitial region. Focusing on trabecular bone they found a modulus of between 15GPa and 19.4GPa depending on the orientation.

Pawlikowski et al. employed micro-scale indentation on trabecular (femoral) bone. The sample preparation in their work was different in that they used samples stored in 70% alcohol, only letting them drain before mechanical testing. They used a spherical 0.2mm tip loading to 500mN with minimal hold time [68]. This is a significantly larger load than the work of Rho and others which will produce a larger indentation. This larger indentation profile is required to overcome the initial inaccuracies that would be present with a non-polished testing surface (it is not practical to polish fragile trabecular bone without embedding). The issue with a larger indentation profile in trabecular bone is the concern is that the results could be influenced by the structural properties of the bone rather than purely representing the material properties. The orientation and structures of the underlying trabecular bone will impact these indentation results even considering that 500mN is within the normal working limits of bone. The results from Pawlikowski et al. produced a Young's modulus of 3.8 to 6.18GPa which is on the lower end of the spectrum of previously published results (but still within the range). This result in the lower end of the spectrum is to be expected given that both dehydration and embedding are known to increase the measured modulus[76].

Nano-indentation of human vertebral tissue was explored by Dall'ara et al. on dry and embedded cadaveric vertebral tissue [77]. This work investigated the anisotropy of the vertebral structures (cortical bone, trabeculae and endplate) as well as investigating the material properties of the osteophytes in incidentally degenerate samples. They found the osteophytes to have a lower elastic modulus (10.9GPa) and also that there were demonstrable differences in the modulus depending on the direction of the applied force

(axial/radial/circumferential) with axial indentation providing the higher modulus (14.6GPa axial, 12.3GPa circumferential and 8.3GPa radial) as one would expect given this is the direction of normal physiological load. The implication of this work for those undertaking mechanical testing would suggest that it is necessary to consider osteophytes as a separate entity and not representative of the overall vertebra. One should also ensure that one is performing indentations in comparable planes with relation to the anatomical orientation of the vertebral body when testing different sample groups as alterations in this could produce significantly different values in itself.

In addition to standardising the orientation of the indents due to the anisotropic properties of bone there are other variables to consider, including the preparation of the samples. Many studies have embedded their bone samples to allow them to be manipulated and polished (especially with fragile trabecular bone). The benefits of avoiding embedding and polishing have been previously explored by Hoffler et al. who compared cortical lamellar bone specimens from 4 human subjects. Samples were dry (dehydrated), wet or wet (rehydrated) and embedded. They found when looking at indentation depth that, even with these polished samples, the larger (500nm) indentations were the most reliable with a variation of 29%. When examining their results for preparation they found that the dry samples had a significantly higher elastic modulus: 25.5GPa for dry samples, 21.1GPa for the wet samples and 20.2GPa for those wet and embedded. Interestingly their measurement deviations were between 4.6 and 8.0GPa. [78]. The small number of subjects in this work (3) is its main limitation; however, the effect of drying the sample reached significance despite this.

Embedding cortical bone would be expected to have less effect than if it were applied to trabecular bone. Wolfram et al.[79] compared wet and dry samples taken from human vertebral biopsy. They found a 29% increase in the dry elastic modulus. Mittra et al. explored the effect of embedding on canine trabecular bone, comparing different embedding materials and also different indentation profiles [80]. Their work found that it did not affect the modulus of the tested material with different embedding substances; there was, however, a significant increase in hardness as the modulus of the embedding material increased. This would suggest that if one were to consider embedding a trabecular bone sample to look at modulus alone then there is no significant difference; however, if one is to consider hardness the choice of embedding material will play a role. When looking at their results on indentation rate and maximum load they were not able to demonstrate any significant difference between the variations tested (Loads of 250/500/750μN and Rates of 200/500/800μN/s). These tested loads

are comparably low when considering other published data [50,68,78,81] concerning bone indentation. Table 1.6.1 displays a summary of bone indentation methodologies and results to illustrate the differences between techniques and results.

Table 1.6.1 Bone indentation methodologies in previously published work

Author	Sample	Preparation	Tip	Depth/Load	Rate	Hold	Modulus (GPa)
Follon E[82]	Human Cortical bone	Embedded	Berkovich	1mN	0.05mN/sec	10s	10.8-22.6
Dall'ara et al.[77]	Human Vertebrae	Embedded	Berkovich	2.5μm	60mN/min	60s	8.3-14.6
Grant et al. [83]	Human Vertebrae	Fresh	Spherical	3mm	0.2mm/sec	-	Stiffness 100-250 N/mm
Boughton et al. [73]	Human Cortical bone	Fresh	Spherical	10N	100mN/sec	60s	13
Hoffler et al.[84]	Human Cortical Bone	Combination	Berkovich	100-500nm	5-20 nm/sec	0	17.7-19.3
Hou et al. [13]	Human Vertebrae	Fresh	Spherical	To Failure – 100 - 160N	0.2mm/sec	0	Not Calculated
Hengsberger et al. [85]	Human femur	Embedded	Berkovich	5mN/550nm	0.33mN/sec	10s	18-22.5
Wolfram et al. [79]	Human Vertebrae	Embedded, rehydrated	Berkovich	2.5μm	120mN/min	30s	6.5-12.4
Ojanen et al.[71]	Human Trabecular (femur)	Wet USS treated	Berkovich	30mN	5mN/sec	60s	10.41
Pawlikowski et al. [68]	Human Trabecular (femur)	Alcohol treated	Spherical	500mN	500mN/min	0	3.84-6.18

Rho et al. [50]	Human Vertebrae and Tibia	Embedded	Berkovich	20mN	1mN/Sec	10s	18.6-21.3
Zhang et al.[86]	Primate Vertebrae	Embedded	Spherical & Berkovich	1-100mN	400μm/sec	10s	12.2-17.8

Zhang et al. found that the load contact time made little difference to the calculated values of bone Young's modulus. They noted that a spherical tip gave a higher modulus in comparison to the Berkovich tip. It was suggested that a standardisation of the conditions of indentation would be beneficial to allow some form of comparison between results, especially when considering the effect of medical treatments. Based on their study this recommendation was '10 mN maximum load, 400 mN/s load/unload rate, and a 10 s hold time' [86]. Further considering the sample preparation, one must consider the storage of the sample prior to testing. The effect of freezing on the mechanical properties (as tested by indentation) of bone has been investigated previously and has been found to have no statically significant effect when compared with tissue that has not been frozen [100]. It is clear that the preparation and conditions of testing can have a significant impact on the results of indentation experimentation; therefore a clear and consistent methodology is essential when comparing samples.

1.7 Clinical Imaging (MRI)

The use of MRI (Magnetic Resonance Imaging) in clinical practice has increased dramatically in recent times. It works on the principle that the application of a magnetic field to the polarised water molecules present in the tissue of the body brings them into alignment (or phase) with the applied field. A radiofrequency pulse is then used to move the molecules out of phase. Once the pulse is removed energy is released by the molecules returning to their in-phase alignment. This released energy is measured at specific points in the realignment process to produce the MRI image. The principal benefit of the technology is that is does not use ionising radiation and therefore does not come with the risks associated with this. MRI is excellent at imaging the pathology within soft tissue but less good at imaging of the bone. An MRI is more expensive (although the cost is decreasing as the technology develops) than a CT scan and takes longer to perform. Finally, an MRI scan cannot be performed on those with any incompatible metal within their body due to the strong magnetic fields applied.

Correlation of pathology with symptom profiles is not straight forward. Analysis of a randomised control trial in patients with sciatica, in which patients were randomised to operative or non-operative management, showed that 39% of those in the control group went on to need surgery. Analysis of their MRIs, however, did not show any statically significant MRI differences in those that went on to require surgery versus those who did not [88].

The changes seen in degeneration (dehydration, endplate changes and re-modelling) can be visualised clinically on conventional MRI scans. Degenerate discs appear 'dark' on T2 weighted images, representing the relative low concentration of water in the nucleus pulposus. In more advanced degenerative disease disc height is reduced and characteristic changes are seen in the endplate, including Schmorl's nodes [41] and changes within the adjacent bone known as Modic changes [89]. Both described phenomena are present in asymptomatic individuals, however. One common way of classifying these degenerative appearances of the disc is the method first described by Pfirrmann et al.[152] (and thus the classification is known as the Pfirrmann classification). The original description is based on mid-sagittal images on T2 weighted MRI and reads as follows.

'Grade I: The structure of the disc is homogeneous, with a bright hyperintense white signal intensity and a normal disc height. Grade II: The structure of the disc is inhomogeneous, with a hyperintense white signal. The distinction between nucleus and anulus is clear, and the disc height is normal, with or without horizontal gray bands. Grade III: The structure of the disc is inhomogeneous, with an intermediate gray signal intensity. The distinction between nucleus and anulus is unclear, and the disc height is normal or slightly decreased. Grade IV: The structure of the disc is inhomogeneous, with an hypointense dark gray signal intensity. The distinction between nucleus and anulus is lost, and the disc height is normal or moderately decreased. Grade V: The structure of the disc is inhomogeneous, with a hypointense black signal intensity. The distinction between nucleus and anulus is lost, and the disc space is collapsed.' [152]

1.8 Modic changes

An initial description of the signal changes seen on MRIs around the endplate and underlying trabecular bone was made by Roos et al. in 1987[90] . Modic, in 1988, classified them into 3 patterns of visible changes in the endplate and adjacent trabecular bone on MRI[91]: type 1 showing as dark on T1 and bright on T2, representing bone marrow oedema and inflammation; type 2 showing bright on both T1 and T2, representing a process of replacement of the usual red marrow with fatty marrow; type 3 (a later addition) showing dark on both (see figures 1.8.1-1.8.3) [89].

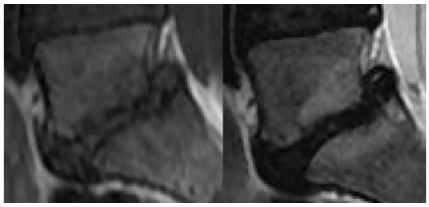

Figure 1.8.1 T1 and T2 weighted MRI images showing type 1 Modic changes

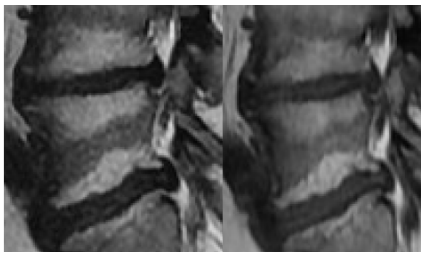

Figure 1.8.2 T1 and T2 weighted MRI images showing type 2 Modic changes

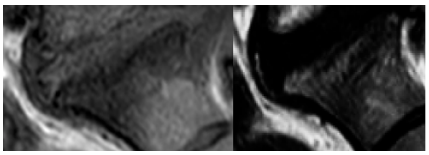

Figure 1.8.3 T1 and T2 weighted images showing type 3 Modic changes

It has been shown that Modic changes can transition from one type to another and that there is an increased incidence of radiological degenerative disc disease in those discs surrounded by Modic type changes in the adjacent vertebral bodies [92,93] It has been hypothesised that Modic changes progress from type 1 to type 3; however, studies have shown that this is not always the case [94]. We know that type 2 Modic changes are most prevalent in the symptomatic population and more common in degenerate disc disease and in the presence of spondylolisthesis [95,96]. Esposito et al. [97] undertook a cohort study analysing the outcomes of patients undergoing fusion for degenerative disc disease and found that type 1 Modic changes

were associated with a better outcome and the most common type 2 changes with a significantly worse one. The mechanisms underlying this are poorly understood and prior reviews have suggested the reverse[98,99]. The overall evidence about the clinical significance of Modic changes remains unclear[98]. One MRI study over a 3 year period found Modic changes did not correlate with the onset of low back pain [62]. They did, however, find evidence that depression was a strong predictor for back pain. The clinical picture regarding Modic changes remains unclear. It is well established, however, that asymptomatic individuals can display Modic changes on an MRI

There are several mechanisms proposed as the driver for Modic changes, including mechanical changes as a consequence of disc degeneration resulting in abnormal load and shear stresses [100]. Another proposed mechanism is an autoimmune response to disc material originating from the nucleus pulposus that enters the vertebral body through microfractures in the endplate which are known to occur in degenerative disc disease [101]. Histological and CT analysis of bone taken from transpedicular biopsy in patients exhibiting Modic changes on MRI found that Modic type 1 changes were associated with changes that one would expect in high bone turnover situations. Modic type 2 changes showed reduced bone turnover/remodelling, and Modic type 3 showed changes consistent with a sclerotic/stable phase [74,102]. Analysis using DEXA to assess the composition of the vertebral body and its fat distribution concluded Modic type 2 changes may have a metabolic component to its aetiology [103].

Ohtori et al. [104] used immunohistology to stain for TNF and PGP 9.5 and found both to be increased suggesting inflammation and nerve in-growth could be a contributing factor for pain. Antonacci worked on bone sustaining osteoporotic fractures (not degeneration) finding that in areas of fracture there is new bone formation as one would expect but also neovascularisation alongside an increase in localised nerve density when staining for PGP 9.5 [105]. We could extrapolate from this (taking into account the work from Ohtori) that it is the inflammation associated with the fracture that stimulates this increase.

The presence of inflammation is further supported by work from Rannou [106] who took serum high-sensitivity CRP (hsCRP) measurements in those with different Modic type changes. They found that the hsCRP levels were significantly higher in those with Modic type 1 changes on MRI. Dudli et al. [107] demonstrated in their rat model that the bone marrow (with some inflammatory upregulation from Il-1) mounts a response when exposed to nucleus

pulposus cells, potentially contributing to Modic changes. This is in keeping with work from the same group [108] in humans displaying Modic changes in which 'pro-inflammatory cross-talk between the bone marrow and adjacent discs' was found when comparing marrow and disc aspirated from levels displaying Modic changes or no changes in the same patients. Extrapolating this into clinical work, the results of a Randomised Controlled Trial comparing anti-TNF medication to a placebo for back pain did not show any significant benefit [109], suggesting that the process is either not reversible or the true mechanism is not yet understood. It has been shown that intra-discal corticosteroids do improve pain, again supporting the inflammation hypothesis [110].

Khot et al. in 2004 did not find any difference between intradiscal steroid or an intradiscal saline placebo in a prospective randomised control trial treating low back pain [111]. Buttermann et al. analysed the effect of intradiscal steroid injections, comparing those with and without inflammatory endplate changes (Modic type 1)[112]. Their prospective follow up found that those with Modic type 1 changes had a greater improvement in outcome than those that did not have inflammatory endplate changes. It is worth noting that they excluded patients with a disc prolapse, spondylolisthesis or stenosis and that all patients were treated by the same clinical team without randomisation.

Stirling et al. in 2001 proposed these MRI changes could represent a form of chronic vertebral osteomyelitis associated with *Propionibacterium acnes* [113]. Their paper found 53% of included patients with herniated lumbar discs were found to have anaerobic organisms isolated from samples taken at the time of surgery.

Albert (2013) took nuclear disc material from 61 patients undergoing lumbar discectomy. Patients were grouped according to their microbiological cultures (aerobic, anaerobic or no growth). 46% of these patients had microbiological growth. Those with 80% anaerobic growth, 0% aerobic growth and 44% of those with no growth developed new Modic changes, respectively[114]. *Propionibacterium acnes* was the most cultured organism. It is worth noting that this study had very strict inclusion criteria limiting its extrapolation into the general population.

McLorinan et al. [115] did not find a significant correlation between this colonisation and symptomatic individuals and found *P.acnes* in samples from the skin, wound tissue and wound washings suggesting that the positive results are more likely to represent contamination than a true infection.

The truth is likely to be that there is more than one stimulator of the same pathological pathway that results in the characteristic MRI and histological changes that we see in painful degenerate discs, which would be in keeping with work from Adams et al. [116] who propose 2 main mechanisms of disc degeneration with a final common pathway.

In summary, Modic changes seem to represent a disease process. The underlying aetiology for the process is likely to be multifactorial but is clearly associated with symptomatic degeneration of the disc. A recent review [117] concludes new models, classification and a clarification of the pathogenesis are still required, adding that the underlying pathology could be a target for the treatment of low back pain in the future.

1.9 Histology of Modic changes

The original classification by Modic et al. in 1988 described 2 types of altered MRI signal in the vertebral subchondral bone[91]. Part of this work included 3 histological specimens from each type and concluded that type 1 was inflammatory (disruption and fissuring of the endplates and vascularised fibrous tissue) and type 2 represented yellow marrow replacement. A more recent (2015) histological analysis of 40 patients who underwent transpedicular biopsy at the time of pedicle screw insertion showed a higher bone volume fraction and trabecular thickness in Modic type 3 when compared with either type 1 or type 2 samples [74]. Histological analysis from the same specimens analysed the osteoid surface proportion and the ratio of osteoid and eroded bone surface. They found an increase in the osteoid relative to total surface and relative to eroded bone. Osteoid is laid down by Osteoblasts and is a precursor to mature bone; it therefore indicates an increase in the formation rate of new bone. Erosions on the bone represent osteoclastic activity which form ‘pits’ of erosion, which are of an acid pH to allow optimum function of degradation enzymes such as Cathepsin K and Matrix metalloproteinases. These ‘pits’ can be seen as erosions on microscopy and can be used as an indicator of bone resorption. These two processes constantly exist in unison with each other under complex biological control hence the need to interpret their values as a ratio either to each other or to the total bone volume. The study found that Modic type 3 displayed an increase in osteoid and relative decrease in erosions indicating increasing bone formation and reduced bone resorption.

In a study, Ohtori et al. in 2006 performed histological analysis on samples from patients expressing Modic type 1 or type 2 changes on MRI, comparing this with those showing no Modic pathology. They found when staining for PGP 9.5 (a protein originally found to be

localised to neurones and neuro-endocrine cells [118]) that none of their control samples stained positive, but 12 of their 14 patients with back pain had positive staining for this nerve marker. The majority of the nerves were found to be in the cartilaginous portion of the endplate and very few in the marrow. They also found that Modic type 1 or type 2 changes had a higher density of nerve fibres. This correlated with a significant increase in TNF staining cells in those displaying Modic changes but also a higher TNF expression in those with type 1 Modic changes when compared with type 2[104]. This increase in TNF expression would seem to indicate that inflammation plays a role in the pathology of Modic changes (as was suggested in the original description) and that inflammation brings with it new nerve fibres that are a potential source of pain.

The finding that the presence of and percentage of endplate involvement of Modic changes both correlated with the presence of cartilaginous endplate in the extruded material in a study by Schmid et al.[119] would infer that the pathology responsible for Modic changes weakens the anchorage of the cartilaginous endplate, increasing the likelihood of it detaching from its bony portion. What we do not know, however, is the site of this weakness. Does the apparent inflammation associated with degenerative disc disease weaken the bone, making it more susceptible to shear and tension forces, or does the inflammation itself weaken the anchoring fibres? Perhaps the inflammation is a mere consequence of the mechanical overload or failure.

The pathological process of Modic changes has yet to be fully understood. Histological analysis has, however, shown a correlation with markers of inflammation and nerve in-growth associated with type 1 changes. Histology has also shown features indicating that there is an alteration in the mechanical environment in which Modic changes exist; it is not clear if this is a cause or effect style relationship. Further work to investigate the pathology of Modic changes may prove to be important in the clinical treatment of back pain.

1.10 Histology of the endplate in degeneration and ageing

We know from the work of Adams that the disc undergoes an ageing process and distinguishing this from a process of degeneration can be difficult [19]. The same author in another piece of work summarises as follows: ‘Spinal tissues can age biochemically without becoming degenerated or painful. However a combination of genetic inheritance, ageing and loading history can make some tissues more vulnerable to injury or repetitive loading so that they become disrupted’ [120].

Within the degenerate disc there are several changes taking place, including the matrix production changes in the nucleus with alterations in the collagen production (more type I collagen; less type II) and a reduction in aggrecan (a proteoglycan essential to the maintenance of disc hydration) levels. To compensate for a loss of cells due to apoptosis the existing cells replicate to form clusters. Dehydration leads to alterations of the force transmission through the disc and the endplate, leading to further changes in matrix production. The integrity of the endplate is key to the function of the disc. It is established that the disc does not have its own blood supply and relies on diffusion of metabolites and water across the endplate[20]. Vertebral endplate architecture studies have shown that blood vessels do not enter the disc itself and that the endplate canal system is complex and highly interconnected[20,121]. Ageing has been shown to affect the nutritional supply to the disc with an increase in calcification of cartilaginous layer and detrimental changes to the vascular structures of the vertebral body[43]. Work by Boos et al. established that ageing affects the blood supply to the endplate in a detrimental way [122]. By investigating the changes found in cadaveric samples from a very wide age range (foetal to 88 years), they conclude that their work 'provided clear histologic evidence for the detrimental effect of a diminished blood supply on the endplate, resulting in the tissue breakdown beginning in the nucleus pulposus and starting in the second life decade'.

Nucleus pulposus cells have been shown to be sensitive to changes in glucose and pH levels, the latter being affected by both diffusion of oxygen into the disc and diffusion of lactic acid out of the disc[123]. A focus on diffusion and perfusion of the disc will therefore be key in the understanding of degenerate disc disease. Atherosclerosis of the Aorta has been shown to correlate strongly with the presence of lumbar disc degeneration and back pain[124]. Perhaps unsurprisingly, smoking and high levels of LDL cholesterol were also linked to disc degeneration. On a smaller scale, Benneker et al.[125] showed that the density of vascular openings at the endplate was reduced in those discs that displayed properties of degeneration. The inference from this is that the density of vascular openings has an effect on the perfusion of the disc. Investigating nutrition of the disc further, using in vitro dye to demonstrate the diffusion around the annulus fibrosis of human disc material, Nachemson et al. demonstrated a decrease in the permeability of the endplate in those discs that showed signs of degeneration[22]. This correlates with the decrease in vascular openings at the endplate previously mentioned. Their findings suggest that these vascular openings cease at the boundary between the mineralised and non-mineralised parts of the endplate.

Histological and permeability analysis of the degenerate cartilaginous endplate has been undertaken by DeLucca et al. They found that with degeneration the cartilaginous endplate permeability decreases. This not only would decrease the transport of nutrients into the disc but inhibit the transport of lactic acid out of the disc [44]. This is contrary to work by Rodriguez et al. who found when looking at degenerate discs that 'vertebral endplate porosity increased between 50% and 130%'[23]. They also commented that perfusion increased, suggesting the issue was not one of poor perfusion but more likely a cellular process. Cytokine IL-1 among others has been shown to increase within the disc in degeneration, and in turn this has been shown to increase nerve growth factor (NGF) and vascular endothelial growth factor (VEGF) which are key signalling molecules in vascular and nerve growth[126]. Other work has suggested that it is a loss of the inhibitory effect of aggrecan and its inhibition of endothelial cell adhesion and sensory nerve growth within the disc itself [127].

Vascular openings do not provide the entire explanation for a decrease in disc nutrition. The composition of the cartilaginous portion of the endplate has been shown to affect the diffusion of a variety of solutes across the endplate. Roberts et al. demonstrated that the shape and size (larger and long chain molecules diffusing more slowly) of molecules affected the diffusion through the cartilage matrix of the endplate. The composition of the endplate also played an important role on the rate of transport of substances through the endplate: calcification of the chondral matrix restricted the movement of solutes and so did an increase in the collagen content and proteoglycan content.

Calcification of cartilaginous endplate and the disc have been demonstrated to affect perfusion. Analysis of calcification of the endplate and its association with degeneration showed that a decrease in pore number correlated with an increase in disc degeneration [128]. They did, however, find this correlation for pores <300µm and most strongly for those between 10-50µm, suggesting this correlation is not as straight forward as it initially appears. Simple diffusion occurs most effectively across the small (10-50µm), thin-walled capillaries and while the larger diameter channels will have a greater flow their thicker walls will inhibit the process of simple diffusion that has been established as the mechanism for disc nutritional supply across the endplate[20].

Malandrino found porosity and diffusion of metabolites into the disc were not dependant on each other [24]. This was based principally on computer modelling, demonstrating that the

diffusion of water (therefore nucleus pulposus hydration, crucial to the hydrostatic dissipation of load across the endplate) was increased in the presence of an increased porosity.

It has been established since the 1970s that vertebral trabecular bone adjacent to the endplate undergoes a process of micro-fracture and healing [129]. These changes in the endplate will naturally affect the porosity as well as the disc mechanics, resulting in a depressurisation effect of the nucleus which reduces its effective ability to dissipate forces and therefore increases the damage to the endplate further. This alteration also increases the damage to the surrounding annulus tissue which Boos et al. noted to increase with age[122]. A change in the mechanics of the disc affects the remainder of the structures in that functional spinal unit, with facet joint hypertrophy, ligamentum flavum hypertrophy and foraminal compression due to loss of disc height all being hallmarks of advanced degenerative conditions of the spine. Added to this is the concept of adjacent level disease which is noted especially after fusion type procedures [130] and is one justification for those supporting the use of disc replacement implants and is a common benchmark for its success [131].

The accepted teaching by Orthopaedic Surgeons is that bone tissue itself contains very few meaningful nerve fibres. The pain that is associated with damage to the bone is taught to originate from the periosteum which is rich in nerve endings. For the spine, at least, we have evidence that this is not the case. We know that in the normal spine the outer third of the annulus and the vertebral body contain nerve fibres[29]. A study of 69 samples using haematoxylin and eosin (H&E) staining noted the following: 'Neurovascular bundles and intraosseous nerves were routinely identified within human vertebral bone' [132]. The nerves were seen throughout the vertebral body, including the marrow. They concluded that the presence of the nerve fibres could suggest the vertebrae themselves are a potential source of pain. These were, however, normal samples from 23 individuals and further work on diseased samples would be the next logical step. Prior to this it had been well established that the outer one-third of annulus fibrosus contains nerve fibres.

Freemont et al. used diseased human disc specimens to perform immunohistostaining using PGP 9.5 to stain for nerve fibres and Substance P immunostaining as a marker of nociception. They found that in their group of control samples the nerve fibres seemed to be exclusively limited to the outer third of the annulus as expected; however, in the diseased group the nerve fibres were seen to extend into the middle and inner thirds in 46% of samples. Both groups of nerves expressed Substance P, suggesting that they could be involved in nociception. [133].

This finding that there is an increase in nerve fibres in the annulus fibrosis surrounding the diseased disc not only explains the clinical picture of pain from the degenerate or damaged disc but also highlights a biological process of neoinnervation associated with degeneration that may also be the case in the vertebral body. It would also support the clinical entity of an annular tear seen as an area of high signal in the annulus and often associated with significant back pain.

In a study by Brown et al. 15 patients (mean age 36) with degenerative disc disease were included in histological analysis of samples collected at surgery. They stained for substance P, calcitonin gene-related peptide (CGRP), neuropeptide Y (NPY) and PGP 9.5 representing autonomic (PGP 9.5 and NPY) and sensory nerve fibres (PGP 9.5, substance P and CGRP). The results were compared with presumed normal cadaveric control specimens (mean age 61). They showed that vascular channels around the endplate were accompanied by nerves of autonomic origin, which they conclude suggests that perfusion to the area and hence nutrition of the disc are under autonomic control. They found 'very localised' areas of increased nerve fibres staining for sensory neuropeptide CGRP, but PGP 9.5 staining did not show an overall difference between the nerve density of diseased and control samples. The increase in localised staining for CGRP could represent one possible mechanism for pain in these patients, while the vascular perfusion seeming to be closely related to autonomic nerve control suggests that nerve control of the disc perfusion may play a role in the degenerative process[134]. There are several limitations including the small number of samples and the clear age difference between the control and disease groups; could the clear difference in age in itself be a confounding factor? The identification of nerve fibres within the vertebral body being of both autonomic and sensory type is an important potential area for further research.

Ohtori et al. performed histological analysis on samples from patients expressing Modic type 1 or type 2 changes on MRI, comparing this with those showing no Modic pathology. They found when staining for PGP 9.5 that none of their control samples stained positive but 12 of their 14 patients with back pain had positive staining for this nerve marker. The majority of the nerves were found to be in the cartilaginous portion of the endplate and very few in the marrow, slightly contradicting other work. They also found that Modic type 1 or type 2 changes had a higher density of nerve fibres, but no difference was seen between these types. This correlated with a significant increase in TNF staining cells in those displaying Modic changes but also a higher TNF expression in those with type 1 Modic changes when compared with type 2[104]. This increase in inflammation suggests inflammation plays a role

in the new nerve formation. As previously mentioned; Antonacci et al. worked on bone sustaining osteoporotic fractures (not as part of a degenerative process) finding that in areas of fracture there is new bone formation as one would expect but also neovascularisation alongside an increase in localised nerve density when staining for PGP 9.5 [105]. We could surmise from this (taking into account the work from Ohtori) that it is the inflammation associated with the fracture that stimulates this increase. They also commented that Avascular Necrosis was seen in their samples and new bone formation adjacent to this even in non-fractured osteoporotic bone suggests microfracture as an underlying mechanism. This work would suggest that ageing (and osteoporosis) especially is a confounding factor when considering the histological analysis of specimens and that the mechanical and biochemical processes are likely to be strongly linked.

This view is supported in the literature by Niv et al. who comment that vertebroplasty cement while acting to improve mechanical strength is also toxic to those nerve fibres found within the vertebral body [135]. This, in their view, would explain the immediate relief of pain that patients often report and the observation that effect is not linked to technique or volume of cement infusion as one might expect it to be if it were a purely mechanical finding. Histological analysis of degeneration in the spine has indicated nerve in-growth deeper into the annulus and nerve in-growth within the vertebral body or perhaps the cartilaginous endplate, all of which could be a source of pain. Correlation of this with some clinical application would support this hypothesis. The studies are, however, limited in number but also in size, especially when one considers separately work with symptomatic patients. Further work to investigate these findings would add valuable information to the understanding of the nerve supply and its alteration in degeneration, the endplate and surrounding bone is likely to be key to this understanding.

A review by Moore indicates that the endplate is an important part of the system that maintains the health of the spine and this system faces mechanical and physiological challenges. This work concludes that ‘the challenge we face as scientists is to learn more about it so that we can confront the problems that arise due to this inevitable failure’[136].

My work will use samples from those with symptomatic (rather than incidental) degeneration of the lumbar spine to explore areas in which there is limited published research: the micromechanical properties of the bone at the endplate and how this varies in degeneration; the effect of Modic pathology on these properties; and a clinical translational study to explore the clinical impact of these findings and the underlying histological changes in the same

sample group with specific attention to vascularity, inflammation and histological structure. The ultimate aim is to better understand how degeneration affects the endplate of the lumbar spine in symptomatic individuals.

2 Thesis aims

The overarching aim of this work is to explore the effect of degeneration on the bony portion of the endplate and its mechanical and histological properties with some translation into clinical practice. Work on the degenerate human spine is limited and the main body of existing work concentrates on incidental degeneration in cadaveric tissue. My work will have the unique perspective of samples from symptomatic individuals undergoing surgery for this degeneration, an essential novel aspect to the work.

2.1 Nano-indentation testing

The primary aim of the nano-indentation testing is to characterise the changes at the endplate and the underlying trabecular bone that are seen in the presence of symptomatic degeneration.

The secondary aim of the indentation testing is to assess the impact of Modic type pathology on the material properties of the endplate and underlying trabecular bone in degeneration.

2.2 Clinical Study Subsidence

This clinical analysis of lumbar interbody cage subsidence has the primary aim of assessing the impact of the MRI evidence of Modic changes on radiological subsidence of lumbar interbody fusion devices.

2.3 Histology

Histological analysis of the samples has the primary aim of characterising the changes seen in the presence of symptomatic degeneration. Analysis of the vascular anatomy, markers of inflammation and endplate anatomy aims to further the understanding of the pathological degeneration at the endplate.

The secondary aim of the histological analysis is to explore the effect of Modic pathology on these same parameters in the presence of disc degeneration.

3 Hypothesis

3.1 Indentation testing

The presence of symptomatic degeneration is expected to change the indentation properties of both the endplate and the trabecular bone. It would be expected that the stiffness and hardness of both would increase in advancing degeneration as a response to the increased mechanical loading that one would expect in disc degeneration.

3.1.1 Indentation testing secondary hypothesis

Modic changes have been associated with an increase in the trabecular thickness. Thus, the hypothesis is that the presence of Modic changes will be associated with an increase in the modulus and the hardness of the endplate and underlying trabecular bone, representing an environment of increased mechanical load. As Modic changes are most commonly seen in the trabecular bone I hypothesise that these changes will be greater in the trabecular bone than at the endplate.

3.2 Clinical Study

Radiological analysis of subsidence is hypothesised to show that the presence of Modic changes does affect the rate of interbody fusion cage subsidence. Type 1 changes have been thought to represent inflammation and therefore I hypothesise that the subsidence rate will increase when compared to those without Modic changes. Type 2 changes are hypothesised to have a lower rate of interbody cage subsidence than those without Modic changes as they have been associated previously with an increase in trabecular thickness. Type 3 changes should have a lower rate of interbody cage subsidence when compared to those without Modic changes on their MRI as they have been associated with a process of sclerosis which should increase the ability to withstand mechanical load.

3.3 Histological analysis

Histological analysis is hypothesised to show a process of thickening of the calcified portion of the endplate according to degeneration, an increase in vascularity with erosions through the endplate, inflammation associated with the degeneration process and an increase in Osteoblast numbers which are part of the remodelling process in response to the abnormal mechanical loads.

In those samples taken from individuals displaying modic changes it is hypothesised that type 1 and 2 changes will demonstrate an increase in inflammatory cells, vascularity, and erosions in keeping with the process of inflammation that they have been associated with. Type 3 changes are hypothesised to show an increase in calcification and Osteoblast numbers in association with the process of sclerosis that they have been associated with.

4 Clinical study – the samples

4.1 Surgical samples

Full approval from the NHS Research and Ethics committee was granted prior to the start of any work (IRAS 174756). This approval covers the collection of the diseased specimens from patients undergoing anterior lumbar fusion for degenerative disc disease causing pain +/- malalignment. The surgical procedure involves mobilisation of the abdominal viscera and the great vessels that lie immediately anterior to the spine. The annulus of the disc is then incised, and the disc material removed. After preparation of the disc space a 'cage' is inserted to maintain or restore the intervertebral height and improve the alignment. In this study all institutions use a PEEK (Polyether ether ketone) device. This device is secured using trans fixation screws, the holes for which are usually created with a drill and debris washed away. Our ethical approval allows the use of a 3mm trephine instead of this drill to create the guide hole for the screw insertion (see Figure 4.1.1 as an illustration) providing us with up to 3 samples (depending on clinical judgment) from the adjacent endplates and vertebral trabecular bone. The exact positioning of these can be determined both at the time of surgery and also on the usual post-operative X-ray images which allows correlation with the MRI morphological findings. All participating patients were consented in line with NHS Good Clinical Practice guidelines.

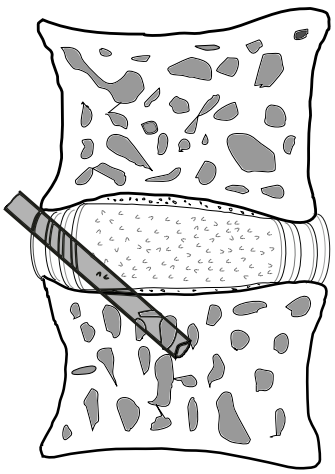

Figure 4.1.1 An illustration of the trephine sample collection

4.2 Cadaveric control sample

Control samples are invaluable for comparison of data. The collection of samples from a non-degenerate spine with no other pathology is, however, rare. Collection from live individuals with a normal spine would not be ethical. We therefore rely on cadaveric tissue; this by its very nature is often not 'normal' tissue. Our control samples were collected from cadaveric tissue purchased from the United States of America by the Norfolk and Norwich University Hospital for use in medical teaching. It is therefore subject to different ethical laws. The responsible person for the material contacted the supplier of the tissue for clarification and permission to use the tissue for research and this was granted. Two cadavers were identified; however, one was known to have metastatic breast cancer with spinal involvement and was therefore was excluded. The included cadaver was a 68-year-old female with no known spinal conditions or consultations for back pain. The cause of death was respiratory failure and co-morbidities listed were obstructive pulmonary disease and heart failure; there was no recorded history of osteoporosis or anti-osteoporotic medication.

The cadaver was transported frozen from the United States of America at -20°C. It was stored at this temperature until thawing, which was undertaken for a period of 4 days at 3-4°C. The cadaver underwent an MRI with a 3 Tesla scanner at the Norfolk and Norwich Hospital which was reviewed for signs of inflammation or degeneration. No significant pathological lesions were identified. There was, however, some minor degeneration in the high and mid lumbar spine as might be expected with someone of this age. Two radiologically normal disc levels were identified and their 4 surrounding vertebral endplates. 8 samples were then collected (2 from each level at cranial and caudal endplates) using the same approach and trephine as used for the diseased specimens. This tissue was then deposited into the Norwich Research Park Biorepository (Research and Ethics Committee Reference; 08/h0304/85+5) and frozen until use. The treatment of these samples is identical to those of the diseased samples thereafter.

4.3 Included Surgical Samples

Samples have been collected from 14 individual donors including 1 individual who had anterior lumbar surgery in the presence of normal discs (without signs or symptoms of degeneration) and one cadaveric donor who did not have any documented history of back pain and no MRI evidence of degeneration. MRI images from each of these individuals is found in the Appendix section 11.3. Table 4.3.1 summarises the characteristics of each individual and the changes found at the endplates at each level (cranial and caudal nomenclature relates to the

vertebral body rather than in relation to the disc). Sample 05 was not collected as the patient withdrew consent prior to collection and sample 22 is the cadaveric control samples.

Table 4.3.1 Included patient sample data

Sample	Age	Gender	Diagnosis requiring surgery	Level	Pfirrmann grade	Modic Changes	Erosions
01	44	Male	Psoriatic Arthropathy with degenerative disc disease.	L4 Caudal	5	2	3
				L5 Caudal	4	2	0
				S1	4	2	0
02	44	Female	Recurrent disc prolapses (previous discectomy)	L5 Caudal	5	2	0
				S1	5	2	0
03	37	Male	Lytic Spondylolisthesis	S1	4	0	0
04	52	Male	2 previous discectomies Recurrent prolapses	L4 Caudal	5	2	1
				L5 Cranial	5	0	1
06	33	Female	Lytic Spondylolisthesis	S1	4	0	2
07	35	Male	Lytic Spondylolisthesis	L5 Caudal	4	1	3
				S1	4	1	3
08	29	Female	Sagittal deformity	L5 Caudal	1	0	0
				S1	1	0	0
09	42	Female	Degeneration with foraminal stenosis	L5 Caudal	5	1	3
				S1	5	1	3
10	51	Male	Recurrent Disc prolapse (previous discectomy)	L5 Cranial	4	3	2
				L5 Caudal	5	3	2
				S1	5	3	2
11	40	Female	Degeneration with foraminal stenosis	L5 Caudal	5	1	2
				S1	5	1	2
12	40	Male	Recurrent disc prolapses (previous discectomy)	L5 Caudal	5	2	2
				S1	5	2	2
13	48	Male	Lytic Spondylolisthesis	L4 Caudal	4	0	0
				L5 Caudal	5	2	0
14	30	Male	Recurrent disc prolapses (previous discectomy)	L5 Caudal	4	0	0
				S1	4	0	0
22	62	Female	Normal spine (Cadaver)	L4 Caudal	1	0	0
				L5 Cranial	1	0	0
				L5 Caudal	1	0	0
				S1	1	0	0

5 Indentation testing

5.1 The Oliver-Pharr Method

Oliver and Pharr[75] described a method that allows the calculation of the Young's Modulus (E) and Hardness (H). Their work was based on adaptations from work undertaken by Sneddon [137]. The work described the elastic penetration of indenters with different geometries (flat, conical, cylindrical) finding the relationship;

$$P = \alpha h^m$$

Where P is the load applied to the indenter tip, h is the elastic displacement occurring at the tip α and m are constants accounting for the geometry of the tip, the elastic modulus and Poisson's ratio of both the tip and the sample.

With this information an indentation load displacement curve can be produced, consisting of a loading portion, a period of hold (which can be 0 if required) and an unloading portion. The loading portion of the curve represents increasing excursion of the tip into the sample and measures mixed elastic-plastic deformation. The hold period results in creep under the tip while held at the defined maximum load. The unloading section of the curve represents a reduction in the applied force and a return of the elastic portion of the deformation of the tissue.

Measurement of the indentation stiffness (the material's elastic resistance to displacement) is calculated from the initial portion of the unloading curve. Early analysis techniques applied a linear fit gradient to this initial portion of the curve. However, Oliver and Pharr[75] realised that the initial part of the unloading curve is not straight – it is in fact a curve. They therefore employed a power law fit to the initial part of the unloading curve. This application of the power law fit provided a small increase in the measured modulus when compared to the assumed linear analysis and is represented by the relationship

$$P = \alpha(h - h_f)^m \qquad (5.1\text{-}1)$$

(Where h_f is the final indentation depth. See Figure 5.1.1)

Oliver and Pharr[75] also developed the concept of the reduced modulus which includes the modulus of both the material and the indenter. It is represented by the equation;

$$\frac{1}{E_r} = \frac{1 - v_s^2}{E_s} + \frac{1 - v_i^2}{E_i} \tag{5.1-2}$$

Where E represents the modulus, v the Poisson's Ratio, r representing reduced modulus, s the sample and i the indenter.

The relationship of E_r to the stiffness of the sample (or the power law fit of the initial part of the unloading curve) can be described using the following equation;

$$E_r = \frac{\sqrt{\pi S}}{2\sqrt{A}} \tag{5.1-3}$$

Where S is the experimentally measured stiffness and A is the projected area of the elastic contact. A knowledge of the geometry of the indenter tip and data from the load displacement curve giving the contact depth allows the calculation of the contact area. This relationship can be described as;

$$A = F(h_c) \tag{5.1-4}$$

Where F is a function of the area of the indenter tip geometry and h_c is the contact depth (assuming that the indenter tip is made of a sufficiently hard material that it does not deform significantly). F has to be established prior to the calculation of any results with calibration experiments. Work from Sneddon[137] established the relationship;

$$h_c = h_{max} - h_s \tag{5.1-5}$$

Where h_{max} is the depth of displacement with maximum experimental load and h_s is the displacement at the perimeter of the contact surface. A schematic representation of these measurements was published by Oliver and Pharr[75]:

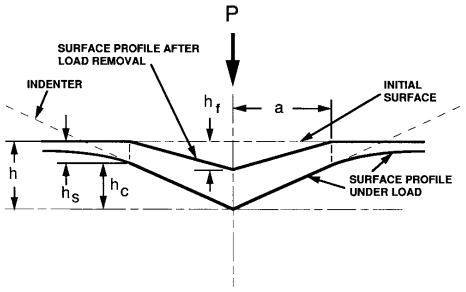

Figure 5.1.1 A diagram of the indentation contact surface from Oliver and Pharr[75]

Sneddon[137] found that h_s was dependant on the geometry of the indenter via the relationship;

$$h_s = \epsilon \frac{P_{max}}{S} \tag{5.1-6}$$

In this case ϵ is a constant specific to the geometry of the indentation tip which for a conical indenter is 0.72, for a flat punch 1 and for a paraboloid of revolution 0.75. P_{max} represents the maximum indentation load.

Hardness can also be calculated from the load displacement curves using the simple relationship below;

$$H = \frac{P_{max}}{A} \tag{5.1-7}$$

P_{max} representing the maximum indentation load, A the projected area of contact at peak load as calculated from the aforementioned equation $A = F(h_c)$.

Using this method of calculation, the Young's modulus and hardness can be calculated with knowledge of the geometric and mechanical properties of the indenter tip from the load displacement data produced during indentation experiments of a test material.

It is important to ensure before testing that calibrations are undertaken regularly to ensure accuracy of the data in terms of machine compliance and tip area function. The machine compliance is particularly important with samples of a high modulus of elasticity and can contribute to the calculation of the Young's modulus. By providing the reduced modulus (as detailed previously) the compliance can be taken into account. The machine compliance is calculated by performing indentations on a sample of known properties (fused silica) from which data can be used to indirectly calculate the indenter compliance. The precise geometry of the indenter tip can change over time (especially for pyramidal tips); this has a larger proportional impact on the results of small indentations (sub micrometre). Using the previously described relationship $A = F(h_c)$, a series of indents of different depths into fused silica can be used to plot the contact area.

Assumptions

There are some assumptions one must accept while using this method to calculate hardness and Young's modulus:

1. The Poisson's ratio is established – Bone = 0.3
2. The material displays predominantly isotropic properties. While it can also be assumed that the direction of the indentation is the predominant direction of deformation, it is not the only direction of deformation with surface indentation. Bone has been shown to display anisotropic properties[50]. The minimisation of the impact of this anisotropy in this testing is undertaken by ensuring that indentations are performed in the same anatomical plane (in relation to the vertebral endplate)
3. h_c (the contact area) is the same as the plastic area which in practice is unlikely to be precisely the case.
4. The area in contact with the indenter tip during removal of the load remains constant. This can be affected by creep, to minimise this effect a hold time at maximum load can be used until creep ceases or multiple loading/unloading cycles can be employed (the original method using 3 cycles[75])

Efforts to account for and minimise the effect of these assumptions have been addressed in the development of the methodology. The preparation and testing of all samples have been standardised and multiple indentations within the same region of the same sample have been employed to counter the effects of residual inaccuracies associated with the use of bone as a sample tissue.

Application of this technique produces an indentation curve (see figure 5.1.2). The first part of the curve is the loading portion which shows the displacement in nm of the tip into the surface of the sample with the increasing load. The *Pmax* is the maximum force of indentation which is maintained for 10 seconds in this example. The ongoing displacement at this constant load is representative the process of creep. A line depicting a representation of the gradient of the initial part of the unloading portion of the curve is shown in green and this gradient is the foundation of the calculation in the Oliver-Pharr method. Finally a period of holding at the final point of the unloading curve is employed for the calculation of corrections for variations.

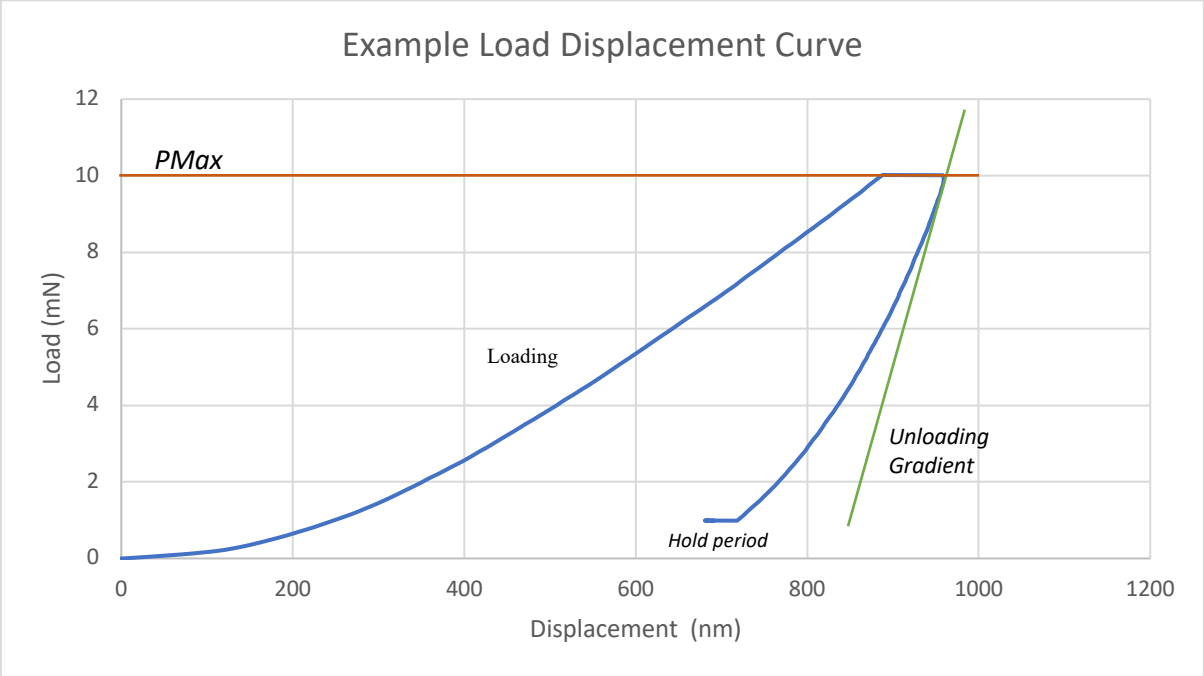

Figure 5.1.2 Example load displacement curve

5.2 Initial Sample Processing

Nano-indentation is a well-established method for calculating the material properties of a compound and has become an increasingly used method of mechanical testing and material science. Key to understanding this is work from Oliver and Pharr where they describe a technique for calculating the Young's modulus from the unloading data of an indentation commonly referred to as the Oliver-Pharr method [75]. This method utilises the unloading curve of indentation testing to calculate the elastic modulus of the material tested. Sample preparation for nano-indentation testing on biological samples has traditionally been to dehydrate the sample and embed it to allow the sample's surface to be sequentially polished. Embedding and dehydration both have been shown to significantly affect the indentation properties of bone. Hoffler et al.[78] explored this by looking at dry (dehydrated), wet, or wet (rehydrated) and embedded bone. They found when looking at indentation depth that, even with these polished samples, that the larger (500nm) indentations were the most reliable with a variation of 29%. When examining their results for preparation they found that the dry samples had a significantly higher elastic modulus: 25.5GPa for dry samples, 20.2GPa for the wet samples and 21.1GPa for the wet and embedded. Avoiding the process of embedding and

dehydration that this process requires would be ideal. This has been performed on trabecular bone by Pawlikowski et al.[68], who performed indentation on femoral fresh trabecular bone. It is worth noting, however, that they used a much larger force (and therefore larger indents) for their work. The benefit of this larger indentation is that the size of the indentation relative to the surface asperities is increased, decreasing the effect of the asperities. The issue with increasing the force and size of indent are that one could be entering a range where the structural properties of the sample begin to impact the results rather than producing a pure measurement of the material properties. In addition, when one is considering trabecular bone, a larger indentation would have a higher risk of involving the edge of the trabecula, giving an inaccurate result. Indentations on fresh samples of a smaller magnitude would have the benefit of using fresh bone while avoiding some of these issues. This study therefore developed a technique to enable the use of freshly defrosted samples without dehydration or embedding while producing a surface with as few asperities as possible to allow the use of smaller indentation forces.

In the ideal situation mechanical testing would be performed on samples that are as fresh as possible after collection from their biological environment and that have been subjected to the minimum number of processes prior to this testing. This is the situation that is most likely to give a true representation of the tissue properties. This ideal situation has several practical drawbacks. As this work is a collaboration between Ipswich hospital, the Department of Materials Science and Metallurgy in Cambridge and the Histopathology Department at the Norwich Research Park (itself a collaboration of different institutions including the University of East Anglia) it is not possible to collect and test all specimens immediately. As the samples are organic their useful lifespan is limited, cell damage, protein degeneration and the release of lytic lysosomal enzymes irreversibly damage the tissue[138]. Histological analysis also needs to be undertaken and for this the specimens are commonly fixed in formalin. Work has been done to explore the effect of formalin on bovine bone mechanics[139], finding that there is a 12% decrease in the measured Young's modulus with formalin fixation. Freezing the specimens is another well-established method of preservation. The effect of freezing on the mechanical properties (as tested by indentation) of bone has been investigated previously and has been found to have no statically significant effect when compared with tissue that has not been frozen [87]. This work used a combination of bovine and human tissue with reference point indentation testing to find no significant change in indentation depth with freezing to -20°C. Freezing does, however, have some impact on the

histological analysis of bone. Andrade et al. explored the effects of freezing and found that there was denaturing of the collagen proteins and some cell necrosis as a result of the freezing process [140]. It is well known that repeated freeze-thaw cycles allow water molecules to align and form crystals of ice which create destructive voids in the tissue on histological analysis. On balance, considering the effects of both freezing and formalin fixing of the samples, considering the handling of the samples for the mechanical testing and the significant effects formalin would have on the mechanical properties, it was decided for this project to first freeze the samples for one cycle only.

5.3 Ovine methodology development

Methodological development has been completed using ovine spine samples. Ovine tissue was obtained from the University of Cambridge Department of Veterinary Medicine as surplus from other research. The rare and valuable nature of the surgical samples from human subjects was therefore preserved.

After thawing the samples are divided longitudinally to allow both histological analysis and indentation to be undertaken on the same sample. The part destined for histological analysis being fixed in formalin for 6-12 hours. After fixation the sample is then transferred to 70% ethanol for storage while it is transported to the site of histological testing. The remaining half is available for further mechanical testing.

The longitudinal division of the sample to allow for both histology and mechanical testing has been utilised as an opportunity to prepare the surface of the trabecular bone and the bony endplate without the need for polishing and embedding.

A custom designed sample holding device to house 3mm cylinders of trephine biopsy bone was manufactured (Figure 5.3.1). The sample was bonded to the holding device to confer suitable stability to allow mechanical testing to be performed using cyanoacrylate. This process was undertaken in an enclosed environment with maximum humidity to prevent dehydration. Samples were weighed before and after the process to determine the water loss. Appendix 11.4 displays the hydration data for the human samples included in the analysis.

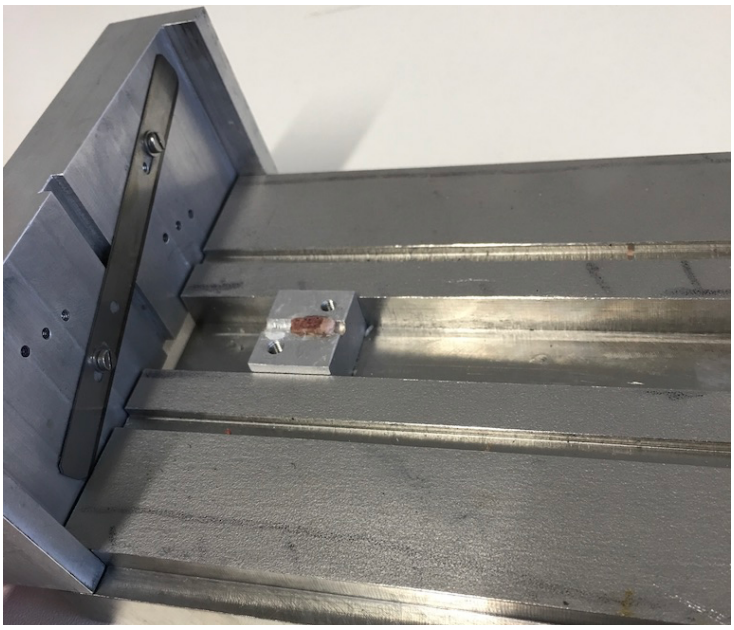

Figure 5.3.1 An image demonstrating the sample holding and sectioning custom made device

The mechanical testing has been undertaken on the ‘MTS Nano Indenter XP’. This is a computer controlled vertical indenter with an optical microscope to allow individual indentation site identification. It consists of a magnetic coil array for motion and force detection, controlled by passing current through the magnetic coils which is directly proportional to the applied force with a resolution of 50nN. In addition it consists of a lateral drift sensor and capacitors for detection of motion that work with two plates fixed to the housing and a third plate between them fixed to the indenter module itself; a change in distance between these produces a change in voltage that can be used to determine displacement. The maximum displacement for this machine is 2mm with a theoretical resolution of 0.01nm.

This indenter machine contains a vibration isolation table on which the equipment is housed; this is to minimise the effect of any external vibrations. Accompanying this, the housing contributes to environmental control, including temperature control to minimise the effect of thermal changes. A pause of 75 seconds is used in the methodology at the final part of the unloading curve to calculate the thermal drift. The machine automatically applies this to the data produced. The indenter is situated in a closed environment with temperature control and sound/vibration proofing to minimise the effect of the external environment, access to the room is restricted to minimise vibration and noise.

The sensitive nature of the nano-indentation equipment requires regular calibration checks. Initial calibration of a ruby spherical indenter tip with diameter 50μm was performed

according to the machine manufacturer's guidelines. Fused silica with a known modulus of 73GPa was indented with a 10x5 grid array of indentations 50μm apart. From the known indentation force and displacement with a known elastic modulus the geometry of the indenter tip can be calibrated.

For the purpose of this experimentation the same fused silica sample is used at the start of each cycle of indentations to first calibrate the indenter tip position, ensuring correlation with the microscope to ensure accuracy of indentation site. Secondly, indentations are made to check the accuracy of the machine for calculating the known modulus of the fused silica. Only once these calibration steps are satisfactorily complete can testing of the biological samples commence.

5.3.1 Indentation tip selection

The tip is interchangeable. Available for testing we have the spherical and Berkovich tip. The Berkovich has specific geometry corresponding to a uniform increase in surface area contact with an increase in indentation depth. This tip is in line with previous work in this lab and also in line with the recommendations made by Zhang et al.[86]. It is different from the tip used in the fresh trabecular testing by Pawlikowski et al. [68] who used a spherical indenter which has the theoretical benefit of producing less plastic deformation at the tip for a given load as the initial surface area of contact is higher. This theoretical increased initial contact area reduces the chance of the tip being affected by any surface imperfections that are smaller than the tip of the sphere. For these reasons the spherical tip is frequently used in the composite biological materials.

Trabecular bone samples from the same vertebral body were tested with the same loading parameters (10mN maximum load, 0.5mN/Second loading and 10 Second hold time). The results (table tip) demonstrated that the Berkovich tip produced a slightly lower elastic modulus, which is in keeping with published results from Zhang et al.[86] The spherical tip produced a lower standard deviation (analysis 3.43 compared to 3.54) and with the application of the student t-test the difference between the data reached statistical significance ($p=0.032$). The remainder of the indentation testing was carried out with the spherical indenter.

Table 5.3.1 Indentation tip comparison

	Berkovich	**Spherical**
Mean Modulus (GPa)	5.4613 (n=50)	7.0083 (n=50)
Standard Deviation	3.5455	3.4314
	p=0.0326	

5.3.2 Indentation Force

Previous work in this laboratory (PhD thesis unpublished [82]) used nano-indentation assessment of cortical femoral bone that was polished but not embedded to establish hardness and Young's modulus data.

The methodology from this previous work has some translation into the methods of this current piece of work in the bone of the lumbar spine.

The first translatable methodological parameter regards creep. Testing was undertaken with varied hold times (see Appendix 11.1) concluding that after 1 hour of hold creep was still occurring at a measurable rate. There was, however, no difference in the rate of creep from 10-240 seconds. As a result, a short but consistent hold time of 10 seconds was employed to minimise thermal drift. This is in keeping with the findings from other work on bone nano-indentation. Turner et al. used a holding time of 10 seconds for their work on embedded femoral trabecular bone[141] . Work from Zhang et al. explored the conditions of indentation in embedded primate vertebral bone; exploring variations in load, hold time and tip geometry, they conclude that a Berkovich indenter with a 10 mN maximum load, a 400 mN/s load/unload rate and a 10 second hold time are the recommended conditions of testing. Testing fresh (non-embedded) trabecular femoral bone, Pawlikowski et al.[68] used a 0 second hold time but a much larger force (500mN) and a spherical tip to obtain their results.

The nano-indenter in use for this series of experiments has a maximum experimental load of 500mN. This is in keeping with the previously mentioned work by Pawlikowski et al. [68] who used a 500mN load to produce their indentations, producing indentation depths of over 4000nm. Previous work within this laboratory used indentation methods on embedded cortical bone to indent individual osteons and found that a force of 1mN produced the most reproducible results. Within the literature there are a range of methodological forces [71,77,78,82,85]. With fragile trabecular bone this methodology was developed with the aims of producing indentations with a magnitude such that it is able to overcome the surface asperities that come with testing fresh biological samples but without entering the range in

which it would be expected that the structural properties of the bone itself (rather than the material properties) start to become tested.

Tests on ovine vertebral tissue (from the same vertebral body) were undertaken to establish the most reliable (the force with the lowest standard deviation) indentation force. The testing load with a combination of the lowest standard deviation and the highest rate of successful indentation (as a percentage of the overall number of planned indentation sites) being the most desirable. Tests were performed at 1mN, 5mN, 10mN and 20mN and results are displayed in Table 5.2.2.

Testing at 1mN is in line with previous work in this group on embedded cortical bone. 1mN testing in this fresh trabecular bone produced a comparatively low elastic modulus value (3.24GPa) with a standard deviation of 2.282 (which equates to 70% of the mean). When analysing hardness measurements the value again is comparatively low with a high deviation when taken as a proportion of the mean. The pre-published values for indentation modulus have been, on average, higher than these measurements even considering the sample is fresh and not embedded. The indentation success rate for 1mN load was 57%.

Testing with 5mN indentation force produced an average indentation modulus of 5.20GPa with a standard deviation measuring 3.53 (or 68% of the mean) and a success rate of 60%. Hardness measurement for 5mN loading was higher than that measured at 1mN with a deviation of 51% of the mean. 10mN testing produced a higher indentation modulus (6.52GPa) with a standard deviation of 2.78 (42% of the mean). Hardness was similar to that at 5mN loading with a similar deviation as a proportion of the mean (50%). The indentation success rate was 62%. 20mN load produced a higher indentation modulus again: 7.86 with a standard deviation of 3.19 (41% of the mean). The indentation success rate reduced to 53%, however.

Given the higher success with a lower standard deviation of modulus measurements with hardness measurements that are consistent with the lower 5mN load (accepting that 20mN load has a lower deviation as percentage due to the significantly higher mean hardness it measures) a load of 10mN has been selected for use being the most likely to produce both modulus and hardness values that reflect the true values.

Table 5.3.2 Load Comparison – displaying success as a proportion of programmed indentations with mean values and standard deviations expressed as a proportion of the mean.

Load	1mN	5mN	10mN	20mN
Success (%)	57% (n=50)	60% (n=50)	62% (n=50)	53% (n=50)
Mean Modulus (GPa)	3.236	5.202	6.519	7.861
SD of Modulus (% Mean)	2.282 (70.5%)	3.526 (67.8%)	2.780 (42.6%)	3.199 (40.7%)
Mean Hardness (GPa)	0.0472	0.154	0.166	0.264
SD of Hardness (% Mean)	0.0301 (63.7%)	0.078 (50.6%)	0.083 (50%)	0.085 (32%)

5.3.3 The rate of loading

It is possible and important to control the rate of the indentation process. Previous work in the same laboratory has been performed using a force of 1mN found that a loading rate of 0.05mN/s was best for their testing[82]. Other published work varies significantly and depends on the indentation forces being used in the methodology, presumably representing a combination of reliability and practicality: a high load at low rate would significantly increase the time taken for each indentation.

To establish the most suitable loading rate for this methodology a series of indentations at varying rates were performed on trabecular bone from the same region of one ovine vertebral body. The results are detailed in Table 5.3.3.

A rate of 0.1mN/s produced the highest mean modulus (11.65GPa) with a standard deviation of 2.68 the indentation success was 60%, hardness measured 0.184GPa with a low standard deviation. 0.5mN/second loading rate produced a lower mean modulus (7.60GPa) with a standard deviation close to that at 0.1mN/s (2.73) the indentation success rate (the successful number of indentations as a percentage of the total number of attempted indentations) was 10% higher at 70%, hardness measurement was higher at 0.197 with a slightly higher standard deviation of these data. 1mN/sec loading rate showed the same trend in reduction of mean modulus with increasing rate (6.64GPa) and a slightly higher Standard deviation (2.92) but a success rate of only 40%, hardness was comparable with 0.5mN/s loading rates with a higher deviation of 0.091. Finally, a rate of 2mN/s continued on the trend towards an inverse relationship between rate and modulus with a mean of 6.48. The standard deviation was also

low at 1.78; however, the success rate reached only 25%. Hardness values at this rate continued to increase (0.241) with a low deviation (0.047).

Reviewing these results, the comparatively low success rates of 1mN/s and 2mN/s make them unsuitable for this methodology due to the limitation in the tissue availability. 0.1mN/s and 0.5mN/s have a comparable standard deviation of the modulus and 0.1mN/s has a lower standard deviation in hardness measurement; however, the indentation success is higher with a rate of 0.5mN/s. A further practical consideration is the increased time for each indentation (from 20s for 10mN final load at 0.5mN/s to 100s at 0.1mN/s), which is especially important when working with this fresh frozen tissue with a limited working time. On balance the 0.5mN/s rate more is desirable and more practical.

Table 5.3.3 Loading Rate – Success as a proportion of programmed indentations with standard deviation at selected loading rates on samples taken from the same ovine vertebral body.

	0.1mN/s	**0.5mN/s**	**1mN/s**	**2mN/s**
Success rate (%)	60% (n=30)	70% (n=30)	40% (n=30)	25% (n=30)
Mean Modulus (GPa)	11.65	7.60	6.64	6.48
SD Modulus	2.68	2.73	2.92	1.78
Mean Hardness (GPa)	0.184	0.197	0.192	0.241
SD Hardness	0.05	0.079	0.091	0.047

5.3.4 Final indentation method

In summary the conditions of testing as a result of a combination of previously described work on creep and methodological development specific to the conditions and materials of this work produced a set of conditions as follows: Spherical indentation tip, 10mN load, 10 second hold at maximum load with a loading rate of 0.5mN/s.

To maximise the use of the samples, indentations are undertaken for as many sites as possible. This does, however, mean that a small number of the indentations are performed a longer period of time after preparation than others. Analysis of the sheep data for trabecular bone and endplate results, with the indentation conditions as defined above, was undertaken with indents split into those performed before and after 6 hours from initiation. This analysis

revealed no statistically significant differences between the two groups. There was, however, a trend to slightly lower average modulus values for the group tested after a 6-hour window (7.84 > 6hs, 9.01 < 6hrs ((p=0.763)). Considering these results, the methodology has been adapted and the preparation process co-ordinated to ensure the minimum time delays between each part of the process. The indentation process will be designed to produce the maximum number of indentations within the 6-hour window to minimise the effect of tissue degradation during the experiment. All indentations were performed a minimum of 50μm from each other to minimise the effect on the tissue from the previous indentation and also 50μm from the edge of any structures (i.e. in the more central regions) to try to mitigate the effect of the 3D structural properties affecting the results.

5.4 Indentation Testing Results

Analysis of the mechanical testing data has been undertaken using SPSS version 25 (IBM Corp. 2018). Where analysis includes or excludes any samples (for example the 'normal' samples) this is clearly stated in the explanation of each section. Analysis has been undertaken and has kept the two anatomical regions (EP and TB) independent for each comparison.

Statistical analysis of samples has been performed on a basis of each individual having equal representation in the analysis to give an 'n=1' scenario. As the key to the methodology is the 'fresh' nature of the samples and the time in which the indentations have been performed has been shown to affect the results analysis has been performed on the first 20 successful indentations to represent each sample/individual. This has been undertaken to give an even representation of each individual or sample within the analysis.

To decide if the data is suitable for analysis from the test that can be applied to data of a 'normal distribution' a combination of visual analysis with the use of histograms and application of the Kolmogorov-Smirnov test were employed. As the data are displaying characteristics suggesting normal distribution, the student t-test has been utilised for statistical comparison of the means using a probability value of 0.05 as the determinant of significance as is standard practice in biological sciences to account for the natural variation in biological materials.

Where multiple samples are available for the same endplate level in the same patient only the best sample was tested (as based on micro-CT analysis as part of a concurrent project). A

better sample is one with less fragmentation due to the trephine and the sample collected most perpendicular to the endplate.

Within the 6-hour window for preparation and indentation testing an average of 15-20 indentation points were possible at each of the two anatomical sites (endplate (EP) and trabecular bone (TB)) making a total of 30-40 indentations per sample with one sample per endplate level per patient. As each indentation produces values for the indentation modulus and the indentation hardness of the bone, the results will be displayed split into the 4 sections that these 2 categories form (Indentation Modulus and Hardness for each endplate and the trabecular bone).

There are 13 surgical patients included in the study, 8 male and 5 female, with an additional cadaveric sample from another female patient (patient 22). It is important to note that both of the patients with 'normal' samples which are being used as a control group are female. The indentation results for each individual patient are displayed in Table 5.4.1.

Table 5.4.1 Mean indentation results for the endplate and trabecular bone of each individual

Patient	**Endplate (EP) or Trabecular (TB)**	**Indentation Modulus (GPa)**	**Range (GPa)**	**Standard Deviation**	**Indentation Hardness (GPa)**	**Range (GPa)**	**Standard Deviation**
1	EP	4.321	1.219-7.646	1.868	0.135	0.093-0.234	0.0406
	TB	6.475	2.845-11.394	2.754	0.206	0.097-0.279	0.0538
2	EP	5.483	3.064-8.703	1.508	0.167	0.080-0.253	0.0458
	TB	5.930	1.007-13.057	3.443	0.200	0.103-0.339	0.0654
3	EP	3.238	1.606-5.851	1.178	0.142	0.077-0.237	0.0510
	TB	4.948	3.069-6.192	0.850	0.145	0.082-0.206	0.0332
4	EP	4.996	2.246-7.480	1.381	0.174	0.076-0.315	0.0557

	TB	4.347	1.685-7.631	1.496	0.174	0.076-0.358	0.0712
6	EP	4.029	2.132-5.649	1.064	0.154	0.102-0.198	0.0278
	TB	5.075	2.302-7.842	1.418	0.172	0.080-0.266	0.0492
7	EP	5.589	1.787-7.678	1.231	0.180	0.079-0.263	0.0481
	TB	7.115	2.385-12.620	2.246	0.185	0.077-0.304	0.0688
8	EP	3.312	0.774-6.404	1.238	0.156	0.093-0.376	0.0481
	TB	3.485	0.914-8.192	1.708	0.163	0.079-0.303	0.0524
9	EP	4.887	2.264-7.698	1.366	0.143	0.091-0.192	0.0293
	TB	5.821	1.021-8.862	1.882	0.156	0.081-0.240	0.0461
10	EP	2.645	1.423-5.293	0.814	0.120	0.075-0.175	0.0309
	TB	2.172	1.087-3.338	0.594	0.103	0.065-0.149	0.0213
11	EP	4.207	1.911-11.429	2.214	0.157	0.076-0.386	0.0816
	TB	4.816	2.051-5.785	1.021	0.157	0.079-0.299	0.0507
12	EP	5.372	1.817-8.692	1.535	0.170	0.092-0.288	0.0477
	TB	5.628	3.013-7.935	1.476	0.156	0.081-0.219	0.0389
13	EP	5.768	3.211-12.293	1.903	0.167	0.098-0.342	0.0511
	TB	5.282	3.259-8.345	1.306	0.167	0.102-0.242	0.0353
14	EP	3.796	2.196-6.075	0.727	0.115	0.082-0.103	0.0263
	TB	4.316	2.233-6.833	1.392	0.150	0.076-0.206	0.0550

22	EP	3.773	0.849-7.790	1.843	0.150	0.076-0.321	0.0691
	TB	4.506	0.907-10.405	2.778	0.144	0.075-0.327	0.0632

Figure 5.4.1 displays the individual mean indentation modulus values with 95% confidence intervals for both the bone of the endplate and the underlying trabecular bone. Figure 5.3.2 displays the individual mean hardness values with 95% confidence intervals for the endplate and underlying trabecular bone.

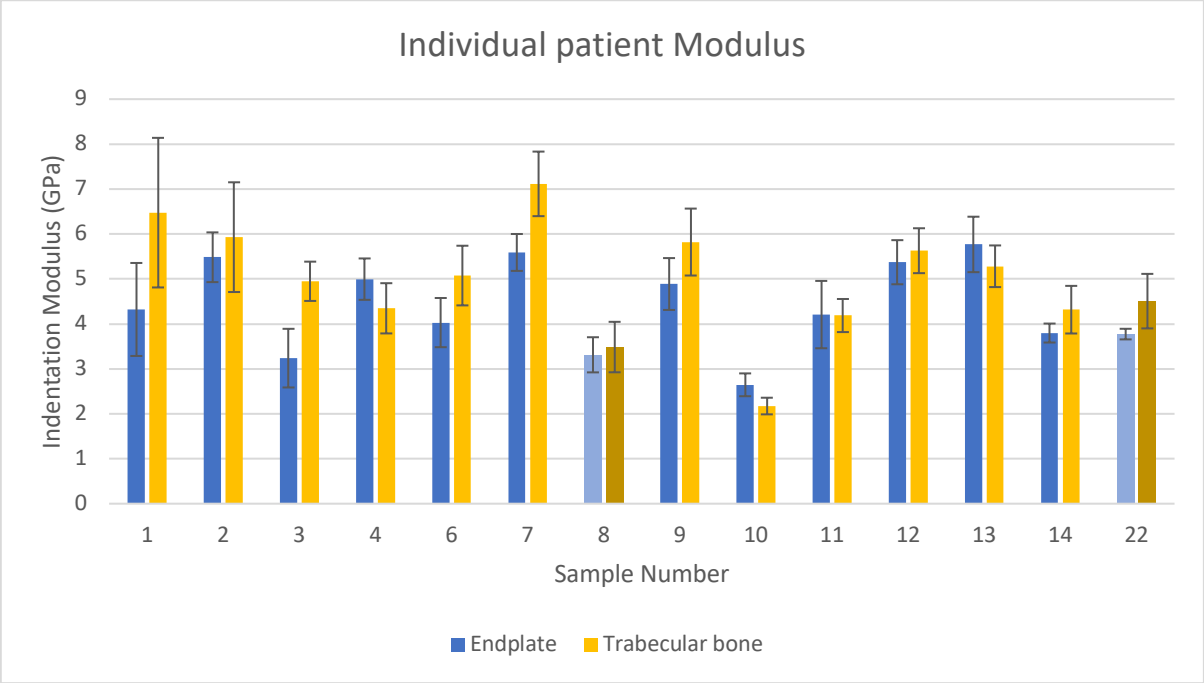

Figure 5.4.1 A graph displaying the individual indentation modulus of the endplate and trabecular bone with 95% confidence intervals.

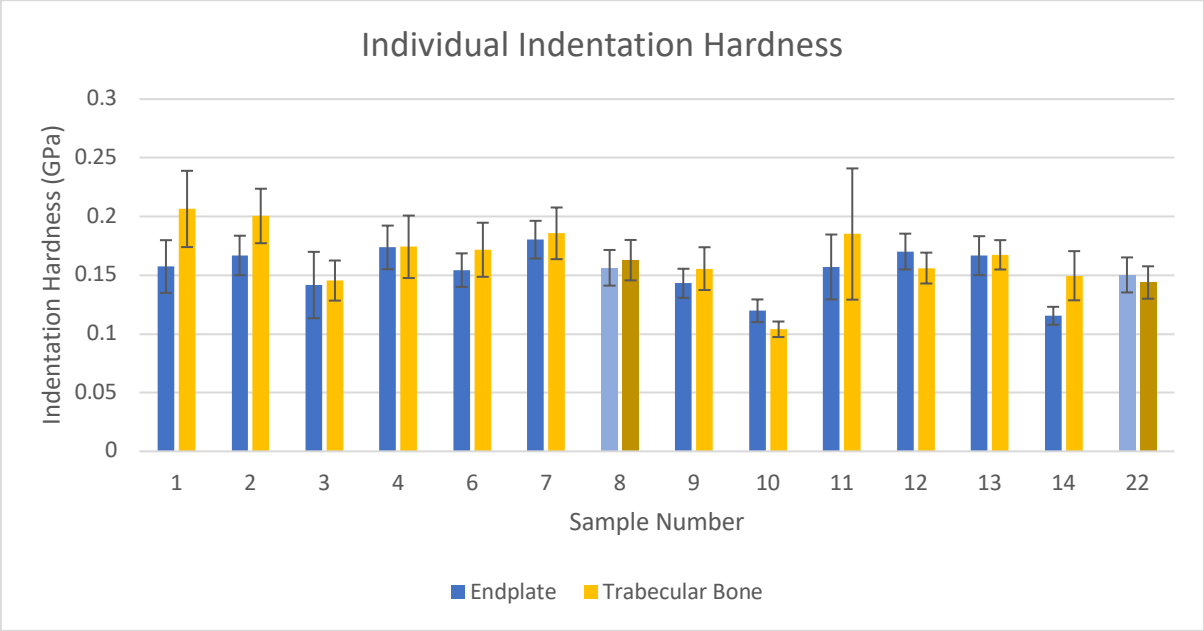

Figure 5.4.2 A graph displaying indentation hardness values with 95% confidence intervals.

5.4.1 Indentation values based on Gender

The mean indentation modulus and indentation hardness for the endplate and trabecular bone for the male and female patients (with the control samples separate) are displayed in Table 5.4.2. We can see that the male and female patients (excluding the two female controls) have only very small differences in the values for indentation modulus of both the endplate and the trabecular bone. Indentation hardness of the endplate does not show any significant difference. When considering the indentation hardness for the trabecular bone it is apparent that the female patients have a higher mean value (0.172GPa compared to 0.151GPa). When the t-test is applied this difference is the only difference between the male and female cohorts that reaches statistical significance (p=0.02).

Table 5.4.2 Mean indentation values based on gender

Location	Sex	Indentation Modulus (GPa)	Standard Deviation	Indentation Hardness (GPa)	Standard Deviation
Endplate	Male (n=160)	4.535	1.727	0.152	0.050
Endplate	Female (n=80)	4.696	1.774	0.176	0.056
Endplate	t-test p-value	0.423		0.451	
Trabecular	Male (n=160)	4.903	2.192	0.151	0.057
Trabecular	Female (n=80)	5.253	2.330	0.172	0.057
Trabecular	t-test p-value	0.172		0.020	

5.4.2 Indentation values and age

Analysis of the effect of the age of the patient at the time of sample collection on the mechanical testing is displayed in Table 5.4.3. The results in this table do not include the two control patients so that the effect of age on the endplate adjacent to a degenerate disc can be explored. Application of the t-test to the data categories revealed significant differences between all comparisons of indentation modulus in both the endplate and the trabecular bone (Tables 5.4.4 and 5.4.5). In the trabecular bone the modulus is similar between those in their 30s and 40s but decreases compared to those in their 50s. Analysis of the indentation

hardness of the endplate showed a significant difference between those in their 30s and 40s (p=0.006) and 40s with 50s n(p=0.02) but not when comparing those in their 30s with those in their 50s (p=0.995) (See Table 5.4.6). Analysis of the indentation hardness of the trabecular bone revealed significantly lower hardness of the patients aged 50-59 years when compared with those in their 30s (p=0.001) or 40s (p=0.002); however, there was not a significant difference when comparing those in the 30s with those in the 40s (p=0.421) (See Table 5.4.7).

Table 5.4.3 Mean indentation values categorised by decade of age

Location	**Age (number of individuals)**	**Indentation Modulus (GPa)**	**Standard Deviation**	**Indentation Hardness (GPa)**	**Standard Deviation**
Endplate	30s (n=80)	4.326	1.341	0.145	0.046
Endplate	40s (n=120)	5.099	1.843	0.162	0.054
Endplate	50s (n=40)	3.746	1.619	0.145	0.052
Trabecular	30s (n=80)	5.752	2.028	0.166	0.053
Trabecular	40s (n=120)	5.318	2.186	0.171	0.052
Trabecular	50s (n=40)	3.078	1.511	0.133	0.060

Table 5.4.4 p-values from application of the t-test to indentation modulus of the trabecular bone categorised by age

Age	**30**	**40**	**50**
30s	NA		
40s	0.001	NA	
50s	0.009	0	NA

Table 5.4.5 p-values from application of the t-test to indentation hardness of the trabecular bone categorised by age.

Age	**30**	**40**	**50**
30s	NA		
40s	0.09	NA	
50s	0.001	0.001	NA

Table 5.4.6 p-values from application of the t-test to indentation modulus of the endplate categorised by age

Age	30	40	50
30s	NA		
40s	0.006	NA	
50s	0.995	0.02	NA

Table 5.4.7 p-values from application of the t-test to the indentation hardness of the endplate categorised by age

Age	30	40	50
30s	NA		
40s	0.421	NA	
50s	0.001	0.002	NA

5.4.3 Indentation comparison of the endplate and trabecular regions of bone

Comparison of the results for indentation modulus and the indentation hardness of the endplate when compared with the underlying trabecular bone has been undertaken to explore the hypothesis that the endplate is either cortical bone or a separate specialised bone structure rather than a confluence of trabecular bone. The results of this comparison are displayed in Table 5.4.8. as well as Figures 5.4.3 and 5.4.4. There is a significant increase in the trabecular indentation modulus when compared with the endplate (p=0.004). There is also a significant increase in the hardness of the trabecular bone when compared to the hardness of the endplate (p=0.034).

Table 5.4.8 Mean indentation data for the endplate and trabecular regions of bone

	Indentation Modulus (GPa)	Standard Deviation	Indentation Hardness (GPa)	Standard Deviation
Endplate	4.581 (n=240)	1.740	0.153	0.052
Trabecular Bone	5.014 (n=240)	2.239	0.162	0.057
t-test p-value	0.004		0.034	

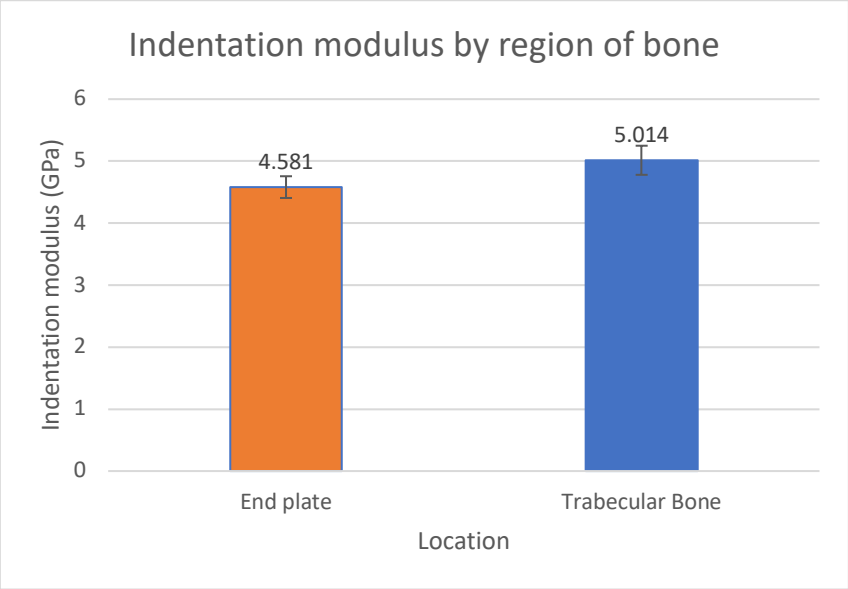

Figure 5.4.3 A graph displaying the indentation modulus of the endplate and trabecular bone with 95% confidence intervals

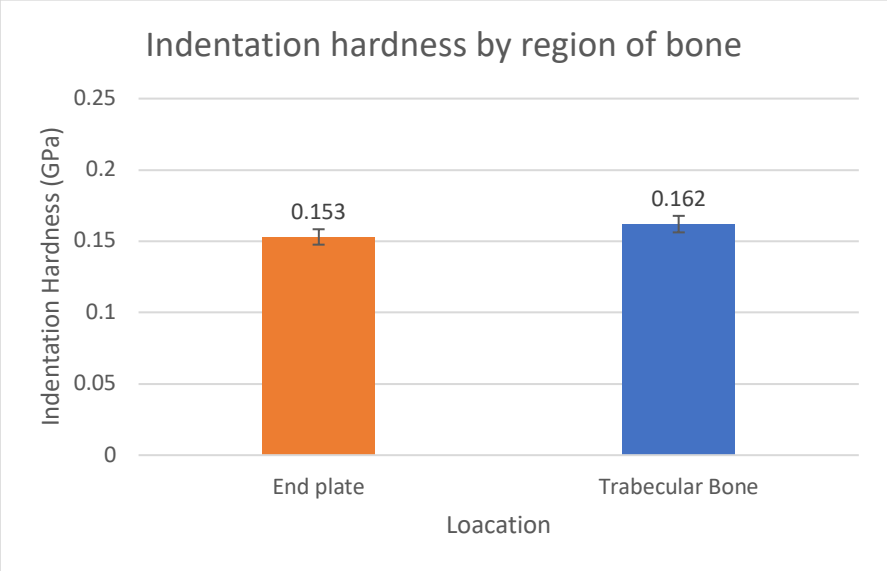

Figure 5.4.4 A graph displaying the indentation hardness by region of bone with 95% confidence intervals

5.4.4 Degeneration and indentation properties

In order to consider the effect of degeneration of the adjacent disc on the material properties of the endplate and the trabecular bone underlying it, a comparison was made between those with degeneration of the disc (as defined by Pfirrmann grade 4 or 5) and those without degenerative discs on MRI (Pfirrmann grade 1). The results of this comparison are displayed in Table 5.4.9. Those with degenerate discs have a significantly increased indentation

modulus of both the endplate (p=0.000) and the underlying trabecular bone (p=0.001). The hardness of the endplate is not altered by the presence of degeneration in the disc (p=0.844) but the trabecular bone is significantly harder in those samples taken from a degenerate disc (p=0.048).

Table 5.4.9 Mean indentation results categorised according to the presence of degeneration

Location	Pfirrmann Grade	Mean Indentation Modulus (GPa)	Standard Deviation	t-test p-value	Mean Indentation Hardness (GPa)	Standard Deviation	t-test p-value
Endplate	>4 (n=240)	4.581	1.740	0.000	0.153	0.052	0.844
Endplate	1 (n=40)	3.623	1.697		0.152	0.062	
Trabecular	>4	5.014	2.239	0.001	0.164	0.072	0.048
Trabecular	1	4.185	2.529		0.150	0.060	

5.4.5 Modic changes and indentation properties

In order to explore the changes that occur at the endplate and the underlying trabecular bone the mechanical testing results have been analysed, comparing groups of degenerate patients according to the type of Modic changes present at that level on the MRI. It has been established during this analysis that the endplate and the trabecular bone are mechanically different from each other. Therefore, for the purpose of this comparison the endplate and the underlying trabecular bone have been separated. Table 5.4.10 displays the mean indentation modulus and hardness with respective standard deviations when split by the type of Modic changes displayed on pre-operative MRI. The p-values from the application of the t-test are displayed in Tables 5.4.11-5.4.14.

Table 5.4.10 Indentation data categorised by the type of Modic changes present in MRI scan

Location	Modic Type	Indentation Modulus (GPa)	Standard Deviation	Indentation Hardness (GPa)	Standard Deviation
Endplate	0(n=60)	4.368	1.728	0.141	0.004
Endplate	1(n=60)	4.903	1.779	0.162	0.006
Endplate	2(n=100)	5.156	1.452	0.168	0.004
Endplate	3(n=20)	2.645	0.814	0.120	0.004
Trabecular	0	5.002	1.570	0.158	0.004
Trabecular	1	5.652	2.302	0.181	0.012
Trabecular	2	5.572	2.366	0.181	0.005
Trabecular	3	2.172	0.594	0.103	0.003

Table 5.4.11 p-values from the application of the t-test to the indentation modulus of the endplate categorised by Modic changes

Modic type	**0**	**1**	**2**	**3**
0	NA			
1	0.029	NA		
2	0.001	0.24	NA	
3	0.001	0.001	0.001	NA

Table 5.4.12 p-values from the application of the t-test to the indentation modulus of the trabecular bone categorised by Modic changes

Modic Type	**0**	**1**	**2**	**3**
0	NA			
1	0.044	NA		
2	0.05	0.814	NA	
3	0.001	0.001	0.001	NA

Table 5.4.13 p-values from application of the t-test to the indentation hardness of the endplate categorised by Modic changes.

Modic Type	**0**	**1**	**2**	**3**
0	NA			
1	0.005	NA		
2	0.001	0.45	NA	
3	0.01	0.001	0.001	NA

Table 5.4.14 p-values from application of the t-test to indentation hardness of the trabecular bone categorised by Modic changes

Modic Type	**0**	**1**	**2**	**3**
0	NA			
1	0.093	NA		
2	0.001	0.98	NA	
3	0.001	0.001	0.001	NA

The indentation modulus of the endplate in those displaying type 1 or 2 Modic changes is higher than those without any Modic changes in the presence of degeneration (p=0.029 and 0.001 respectively). Those with type 3 Modic changes had a significantly lower indentation modulus than those without Modic changes (p=0.001).

Those displaying type 1 or type 2 Modic changes have a higher trabecular bone indentation modulus than those without Modic changes (p=0.044 and 0.05 respectively). The trabecular bone indentation modulus in those with type 3 Modic changes again had a significantly lower indentation modulus than those without Modic changes (p=0.001). The results have not shown any significant difference between the indentation modulus of those with type 1 and those with type 2 Modic changes in the endplate (p=0.24) or the trabecular bone (p=0.814).

The indentation modulus of those with type 3 Modic changes is significantly different at both the endplate and the trabecular bone indentation sites when compared with type 1 (p=0.001 endplate and p=0.001 trabecular) and those with type 2 Modic changes (p=0.001 endplate and p=0.001 trabecular bone).

The indentation hardness of the samples follows a similar pattern to the indentation modulus. Those samples without Modic changes have a lower indentation hardness than those with type 1 changes, but this did not reach significance in the trabecular bone (p=0.093), whereas it did in the endplate (p=0.005). Those with type 2 Modic changes again had a significantly higher indentation hardness than those without Modic changes at both the endplate (p=0.001) and the trabecular bone (p=0.001). Those with type 1 Modic changes did not have any significant difference in indentation hardness at the endplate (p=0.45) or trabecular bone (p=0.98) when compared with those displaying type 2 changes. Those with type 3 Modic

changes showed a significantly lower indentation hardness than those without Modic changes (p=0.01 endplate; p=0.001 trabecular), those with type 1 Modic changes (p=0.001 endplate and trabecular) and those with type 2 Modic changes (p=0.001 endplate and trabecular bone).

5.5 Discussion

Surgical samples of this nature are difficult to obtain due to the nature of the surgery. Much of the previous work on human spines has been undertaken on cadaveric tissue that has been found to be incidentally degenerate. The samples used in my work are from individuals undergoing surgery for a symptomatic disease process that requires specialist surgery; they also have pre-operative MRI investigations which allows vital in vivo classification of the disease process. The samples are therefore unique and very valuable to the research.

Just as difficult to obtain have been the samples for comparison with 'normal' discs. One from a patient undergoing the same surgical procedure but without degeneration of the disc and another from a cadaver who has no history of degeneration and no degeneration or pathological changes on MRI. The difficulty in identifying suitable 'normal' samples restricts the number available from different individuals (just as does the difficulty collecting diseased samples of this nature). As a result, the number of samples for different individuals in the diseased cohort is 12 and in the normal cohort is 2.

Both 'normal' individuals are coincidentally female; it is therefore important to explore the effect of gender on the results of the experimental testing undertaken. Again, coincidentally the normal cohort represent both the oldest and youngest individuals in this work. The effect of age needed to be explored with respect to the experimental data collected to identify its potential impact.

5.5.1 Gender and Indentation properties.

The gender comparison has been an important issue in the planning of the study to address this issue as a potential confounding factor in the subsequent results. No significant difference with respect to gender between the indentation modulus of the endplate or trabecular regions of the bone was identified. The mean ages are 43.1 for the male samples and 39.7 for the female samples with the average Pfirrmann grade 4.4 in the male samples and 4.6 in the female. This is in keeping with previous work by Liu[45] who did not find a significant difference between the material properties of the endplate on indentation testing between sexes. Wolfram[79] used nano-indentation on vertebral trabecular bone and found no

significant difference in the elastic modulus between the male and female samples in either wet or dry conditions.

Dall'ara et al. [77] found when indenting trabecular bone that the female patients had a slightly lower indentation modulus than the male: the total number of samples was only 6, however. Neither of these pieces of work are designed to assess the effect of gender on the mechanical properties of the spine as a primary outcome and therefore caution should be taken when applying the results.

In my results demonstrable difference was noted between the hardness measurements of the trabecular bone with the female patients having the harder bone in these degenerate samples.

One possible explanation for this is the combination of the slightly younger age and the slightly higher average degeneration classification in the female group of patients. It is also possible that the presence of Modic changes could have an effect on the material hardness as the female patients have only one sample collected from a patient that does not have Modic type changes on MRI compared with 7 from the female cohort.

The effect of age, degeneration and Modic pathology combined might explain this identified difference between the groups. Similar to previous work in the area, the effect of gender was not a primary intended outcome for this work and therefore interpretation should be undertaken with caution.

More detailed analysis of the data produced in this testing has explored the effect of these parameters to improve the understanding of the effect of degeneration and of Modic type changes on the material properties of the degenerate human lumbar spine.

5.5.2 Ageing in degeneration and indentation properties

Work by Liu[45] found that the effect of age on the endplate was only evident in the outer portion of the endplate and at this site only was there a significant decrease in stiffness in the female patients. Dall'ara et al.[77] did not specifically look into the effect of age on trabecular modulus and all of the patients were over 68 years of age. Despite the youngest being 68 there remains an age variation of 20 years to the eldest patient. This 20 year span of ages did not demonstrate an effect on the results.

My results show an increase in indentation modulus at the endplate between those in their 30s and those in their 40s, but this then decreases in the 50s. The modulus of the trabecular bone is similar in the 30s and 40s but decreases in those in their 50s. In an attempt to explain this,

we can explore the characteristics of the patients in their 50s further. One of the two individuals displays type 3 Modic changes and is the only patient in the study to do so. This could have some bearing on the differences seen between the two groups rather than the age difference representing the only factor. An analysis of the effect of Modic changes has been undertaken in section 5.5.5. When considering the hardness of the endplate, the trends follow a very similar pattern to the indentation modulus as we would expect. Due to the rare and unique nature of the samples, the number of individuals representing each age group is small and this is not one of the primary outcomes of the work; therefore caution is required when drawing conclusions about the effect of the ageing process. It is an important evaluation of the data to explore the effects of age (as is the case with the effects of gender) to recognise their impact on the further analysis of degeneration and Modic changes.

The samples are all from individuals with degenerate disc disease, and therefore we are artificially separating out the process of ageing within degeneration. Establishing the effect of ageing within the samples is important when considering the analysis of degeneration compared to non-degenerate samples: although not causally related the incidence of DDD increases with age. Specific to this work, the nature of the non-degenerate samples is important when considering age. With one sample from a donor in their 60s (older than any of our operative samples) and another in her late 20s, the non-diseased samples represent both the oldest and youngest samples collected. While it would be ideal for them to match the degenerate disease cohort in every way the nature of the samples and difficulties collecting from the lumbar spine endplate from 'normal' discs have to be taken into account, these samples are the best available to me for comparison, and therefore the imperfect match has been accepted as the best possible comparison.

5.5.3 Indentation properties of the endplate and trabecular bone

It has been shown by Choi[67] that subchondral tibial bone has a lower elastic modulus than trabecular bone. They hypothesised that this might be partly due to the presence of calcified cartilage in the samples. Of course, subchondral bone in the tibia is not the same as vertebral bony end plate. Rho[50] used nano-indentation on dry embedded trabecular vertebrae and tibiae to find that trabecular bone has a lower indentation modulus than cortical bone.

Dall'ara[77] looked at the indentation modulus of the endplate and the trabecular bone independently rather than making a comparison in their dry embedded samples. Their data for the endplate had a range of 9.19 to 14.27GPa; for the trabecular bone transverse

compression (which is comparable to the direction of indentation used in my work) the indentation modulus was found to be 8.36-13.84GPa. The small sample size in this work makes comparison unlikely to have reached significance. This comparison was not explored in the original work and the samples were not classified as to the degeneration of the adjacent disc. As discussed in my introductory review, there has been very little additional work exploring the vertebral endplate and trabecular bone as separate entities from a material properties perspective.

My results find that in the lumbar spine with the presence of degenerative disc disease the trabecular bone and endplate have different material properties (with the trabecular bone having a significantly higher indentation modulus and hardness). This material assessment suggests that there is an underlying difference in the microstructural make-up of the two regions.

The material properties of bone depend on the hydration, mineral content, collagen content and the organisation of these within the bone[142]. The collagen content, alignment and degree of cross linking between collagen fibres alters the measured material properties of bone [143,144]. We know that alterations to type 1 collagen genes (COL1A1) have clinically significant impacts on the mechanical properties of the bone, for example in the condition Osteogenesis Imperfecta. Wang [145] used heat to denature collagen in human bone and demonstrated a reduction in toughness and yield strength but less change in the elastic modulus, suggesting collagen has more role in the plastic phase of bone deformation rather than the elastic phase.

The cross links between collagen fibrils as well as intermolecular bonds have also been shown to affect bone elasticity by up to 30%[146]. We also know that ageing affects the collagen content and function within bone[147]. The mineral content of human trabecular bone has been shown to directly affect the elasticity of the bone independently of the structure or bone volume, with the higher mineral content increasing the stiffness[148]. The hydroxyapatite inorganic component of bone exists in a crystal plate type structure with crystals of varying size. It would seem that the greater the variation in crystal size the more favourable the material properties, with such bone having less preponderance to fracture[149]. Both age of the crystals (older crystals being larger) and collagen fibre content and orientation can affect the size and alignment of hydroxyapatite crystals within bone.

The elastic modulus and hardness would seem to be more dependent on the inorganic (rather than organic) components of bone[143], although the reality is likely a complex interdependency between the two elements. This illustrates the immense complexity of working with bone, in particular the small structures that are the endplate and trabeculae. However, in particular the techniques used in this study have proved to be an important method for assessment of how clinical pathology affects the bony structure in the spine.

Considering the possibility of structural effects on the results, forces of 10mN applied to a 50µm spherical indentation tip should not reach the point where structural properties start to impact the results. If we were to see evidence of this in the load displacement curves produced, one would expect a significant increase in displacement in the higher loads representing the compliance of the structure increasing. An example of the indentation curves on the endplate and trabecular bone is seen in Figure 5.5.1. We do not see any evidence of a change in compliance at the higher loads, making it less likely that structural properties are represented at this force. If the effect of structure were to start to affect the measurements one would expect the endplate to have a greater stiffness and hardness measurement than the individually thinner, and therefore more likely to be affected, trabecular bone. This is contrary to the results found in my work which found the endplate to have a lower elastic modulus and lower hardness measurements.

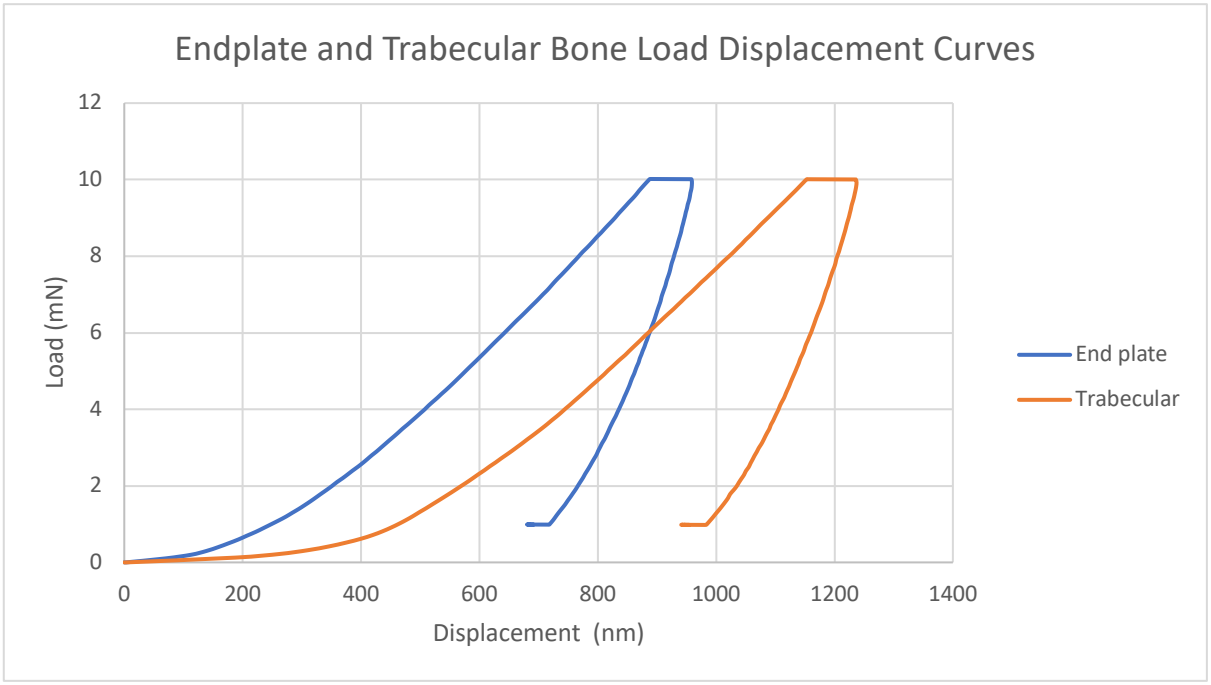

Figure 5.5.1 A load displacement graph showing representative curves for the endplate and underlying trabecular bone

It is well known that bone is anisotropic. Dall'ara found the endplate to exhibit these properties less so than the underlying trabecular bone [77] with transverse indentation of the trabeculae giving values on average 2.8GPa less than with longitudinal indentation. Could this anisotropy account for the differences that I have seen? The indentation has taken place at an angle perpendicular to the usual axis of anatomical loading. This orientation has been consistent for all sample testing. A variation in the collagen alignment or osteon orientation at the endplate in comparison to the trabecular bone (which is known to be along its long axis) might contribute to the differences seen between the endplate and trabecular bone on nano-indentation. If the work by Dall'ara is to be applied, then one would expect the transverse indentation of the trabeculae to represent the lower measured values accounting for the anisotropic properties. Orientation of the osteons in the endplate to one more perpendicular to the axial load (as one would expect to account for radial and shear stress) would lead to higher nano-indentation measurement values accounting for the anisotropy of the bone. If this is the case, then the detected difference in this work could be an underestimation of the true differences in the material properties between the two regions of bone.

One possible explanation for the lower indentation modulus and lower hardness of the endplate is the possibility that some of the indentations are being performed in cartilage or calcified cartilage rather than the bony endplate. If this were the case one might expect the endplate to have a lower elastic modulus and hardness (which is the case).

The sample preparation involves careful removal of the cartilaginous portion of the endplate after the sample is carefully split with the microtome blade. It is still theoretically possible that some of the calcified cartilage endplate or cartilaginous endplate remain. Caution was taken at the time of testing not to indent at the immediate disc facing edge of the endplate to mitigate for this phenomenon. If there were distinctly different materials contributing to the results one would expect two peaks in frequency charts plotting the values for the endplate. These are displayed in Figure 5.5.2.

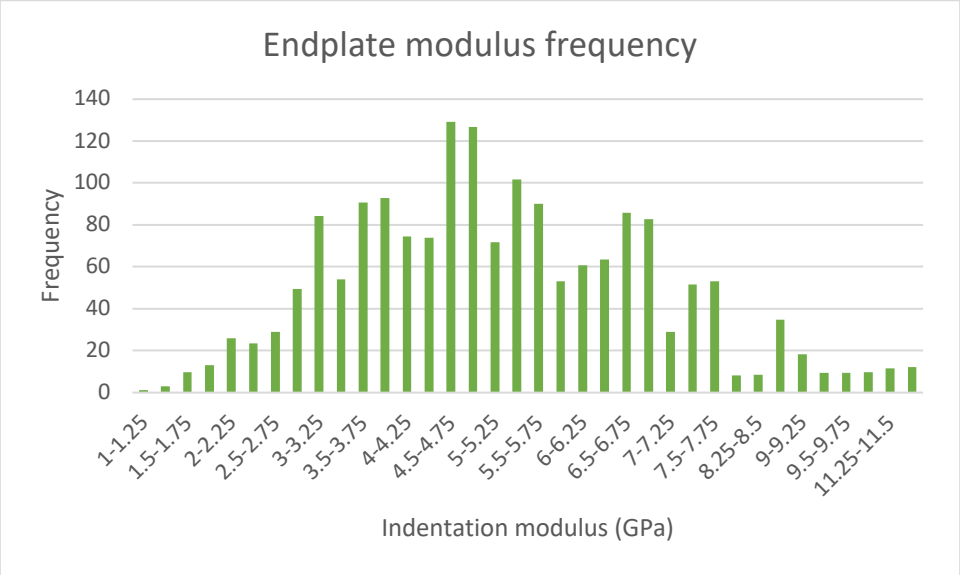

Figure 5.5.2 A graph displaying the range of results for the indentation modulus of the endplate

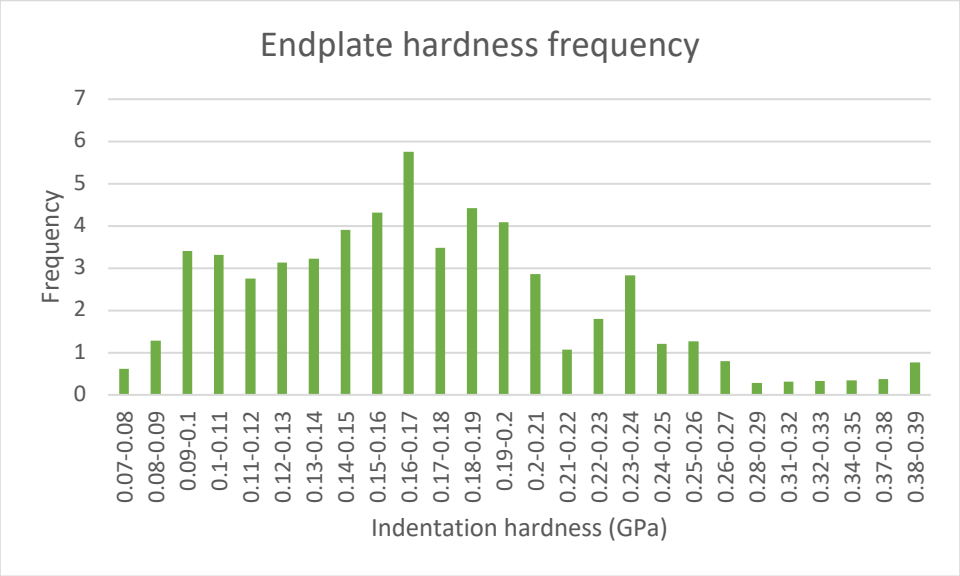

Figure 5.5.3 A graph displaying the range of results for endplate indentation hardness.

From the graph seen in Figure 5.5.2, it is evident that there is no clear division of the frequency values that would indicate a separation of 2 indentation materials. In the graph seen in Figure 5.5.3, there is a possible second peak for values 0.09-0.11 which was not seen in the indentation modulus. A comparison with the values for the trabecular bone (see the graphs in Figures 5.5.4 and 5.5.5) reveals patterns that are very similar to those seen in the endplate regions, and it is evident in the hardness measurements that the separate possible peak at 0.09-0.11 also occurs in the trabecular bone. The trabecular bone is not adjacent to the cartilaginous endplate (CEP) or calcified cartilaginous endplate (CCEP). Therefore if this

were to be the explanation for the lower endplate values on testing, we would not expect a similar pattern to be seen in the trabecular bone. One possible explanation for this apparent smaller peak at this lower modulus could be that the constant state of remodelling of the bone has an effect on a number of the indentations. During the process of bone remodelling bone is resorbed by Osteoclasts and new bone laid down by Osteoblasts in its immature stage. This new osteoid consists of small hydroxyapatite crystals that increase in size and become more heterogenous as they mature (which increases the stiffness and hardness)[149]. It would not be possible to identify this on the nano-indentation machinery, but it is possible that a proportion of the indentations might have occurred in this area of recent osteoid deposition, therefore potentially explaining the smaller second peak at the lower hardness values.

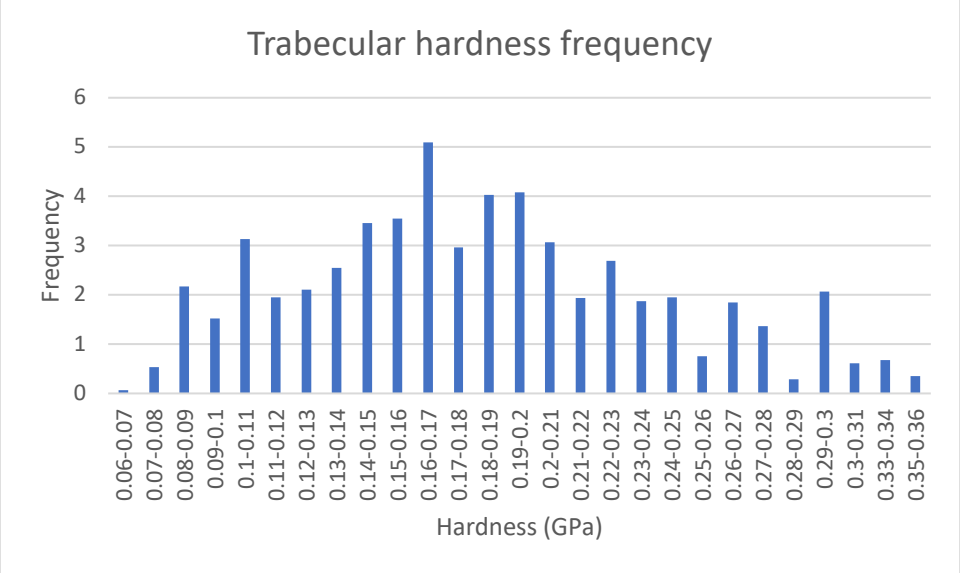

Figure 5.5.4 A graph displaying the range of results for indentation hardness of the trabecular bone.

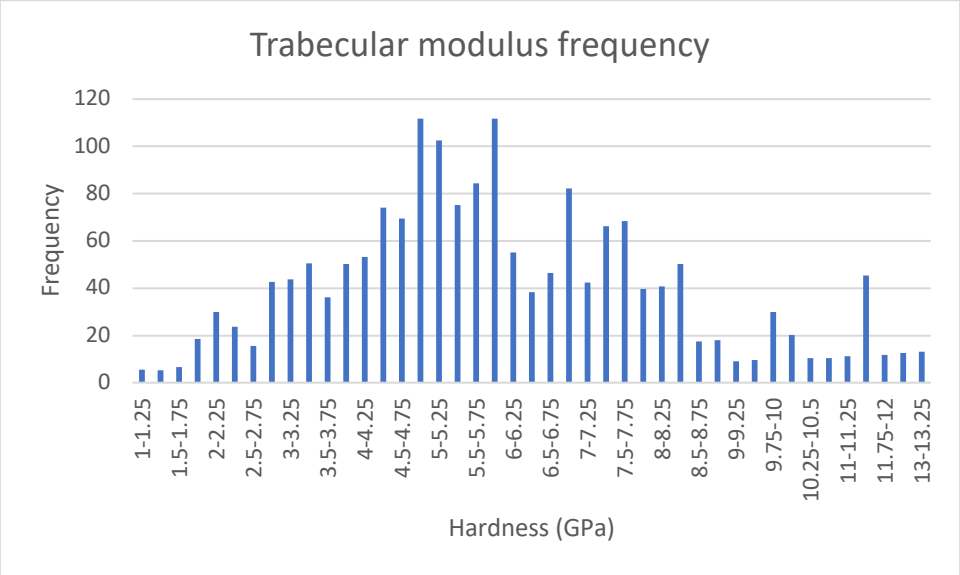

Figure 5.5.5 A graph displaying the range of results for the indentation modulus of trabecular bone

The reduction in stiffness and hardness seen at the endplate in comparison to the trabecular bone could be explained by a decrease in mineral composition, alterations in collagen content, orientation or cross links or an alteration in the hydroxyapatite crystal size variation. All of these factors are interdependent, and the differences seen between the endplate and trabecular bone material properties are likely to represent differences across the entire structure rather than in one isolated element.

5.5.4 Degeneration and indentation properties

We know that in the degenerating disc there is an alteration in collagen and other proteins due to a change in cell function and hydration[133]. Histologically there are notable changes at the endplate complex (cartilaginous endplate, calcified cartilaginous endplate, bony endplate) including a decrease in permeability and porosity, changes in thickness, neoinnervation and calcification [18,22,47,128,133,150]. A process of microfracture of the bony endplate and trabecular bone was demonstrated by Vernon-Roberts and Adams[151][129] in response to abnormal loading due to the degenerate disc. When considering the process of degeneration, each element must be considered in the context of the degeneration of the other parts of the functional spinal unit.

My work has focused on the bony endplate and trabecular bone as an area that was felt to be key to the health of the disc. Many people have signs of degeneration on investigational imaging without attributable symptoms. The samples tested here have been collected from

those with attributable symptoms, thus representing the disease process that impacts so heavily on a significant proportion of the population. The material properties of the endplate in degeneration are vital to the understanding of both the mechanical environment within degeneration and the response of the bone to this alteration of forces through the degenerate disc-endplate complex. Integrity of the endplate is crucial to allow the disc to withstand and transmit forces[18].

Work by Lui found a decrease in endplate stiffness (with intact underlying bone) with worsening degeneration[45]. It is worth noting that this work is on cadaveric samples within incidental degeneration on MRI. The indentation in their study was performed with a 3mm spherical indenter and a force of over 200N was required for their 3mm depth indentations. This will therefore act as an analysis of a composite of the structural and material properties of the vertebral body. Their indentation studies were performed on samples in which the cartilaginous endplate had not been removed and therefore represents a combination of the cartilaginous and bony properties.

When compared to non-degenerate samples (according to the Pfirrmann classification[152]) using this technique the endplate in degeneration was found to have a higher mean elastic modulus without a change in the mean hardness. The modulus of elasticity and the hardness are independent measurements but are often closely correlated. Factors affecting these measurements are complex and difficult to isolate from one another, including collagen alignment, collagen crosslinking, mineral content and hydroxyapatite crystal size and orientation[145–147,149].

Zhang[153] used mouse femur, applying indentation, Atomic Force Microscopy (AFM) and inductively coupled plasma optical emission spectroscopy to correlate the mineral properties with the material testing and found strong positive correlations between hardness and modulus for both cortical and trabecular bone. They also found an increase in hardness and stiffness in those bones that reached skeletal maturity, and in this same group was noted a bundle-like arrangement of the collagen fibres with elongated dense crystals (as opposed to a loose fibre arrangement with plate-like crystals). As the ageing process developed the crystals continued to elongate, but the integrity of the composition with the collagen fibres became less stable with more fragility and separation. Elastic modulus and hardness remained static, with these changes suggesting that while the crystal-fibre arrangement has an effect on the material properties of elastic modulus and hardness the relationship is too complex to be

explained by changes in this alone. Examining collagen cross linking they found a negative correlation between this and indentation modulus. Ojanen[71] worked with human femurs, applying nano-indentation and Raman micro spectroscopy. They found that crystallinity correlated positively with the elastic modulus and the hardness measurements but not with age.

In a study of murine bone, using Raman micro spectroscopy and nano-indentation, positive correlations between the crystal size and elastic modulus ($R^2 = 0.14$) were found[154]. An important negative correlation was found between both hardness ($R^2 = -0.35$) and elastic modulus ($R^2 = -0.13$) and the ratio of collagen cross-links in the same work. In another study on dehydrated human femurs, atomic force microscopy and nano-indentation were combined finding elastic modulus to be related to the grain (crystal) size.

Nuclear magnetic resonance investigation by Nikel[155] used knockout mice (for osteocalcin, osteopontin or both). They found the quality of the organic and inorganic components of bone were unaltered, but it is known that the hardness and toughness of these mice is inferior. They conclude therefore that osteocalcin and osteopontin do not change the collagen or mineral components of the bone but rather the links between them.

Samuel et al. [156] used cadaveric femurs to determine the effect of hydration. They found that dry bone had a higher elastic modulus than wet (17.2GPa and 11.2GPa respectively). They explored these effects on the mineral components and the collagen fibrils individually finding that (in compression) they were equally affected. They conclude that dehydration of the bone makes it more brittle and 'presence of water in bone matrix is indispensable for sustaining the viscous behaviour of bone'.

Summarising these works could go some way to explaining the differences seen in my work. It could be theorised that in degeneration crystal size increases. This would increase the hardness and stiffness (but stiffness more so), while the breakdown in collagen cross linking (both collagen-collagen and collagen-hydroxyapatite) as part of the degeneration process (which is also seen in the adjacent disc) reduces the stiffness and hardness (but hardness more so) such that the hardness overall is relatively unchanged while the stiffness is increased overall. Contributing to these changes, relative dehydration of the bone (perhaps linked to the well-known phenomena of disc dehydration in degeneration) makes it stiffer and more prone to failure.

My work found that the same pattern of an increase in stiffness is seen in the presence of degeneration in the underlying trabecular bone as well as the endplate, with both showing statistically significant differences. In the trabecular bone I also found a significant increase in the measured hardness of degenerate samples when compared with our controls. This increased hardness might be explained by the proportionally lesser effect of collagen degeneration than is seen in the endplate while it still exhibits some of the effects of increased crystal size and relative dehydration that are known to increase both the stiffness and the hardness of bone.

5.5.5 Modic changes and indentation properties

The initial description of what became known as Modic changes by Modic[91] was based on analysis of just 3 histological slides of type 1 and type 2 changes. They found type 1 to have increased granular tissue increased Osteoblasts and Osteoclasts as well as fibrous bone marrow replacement, representing a process of inflammation. In type 2 their histology demonstrated replacement of the normal bone marrow with abundant fat with granulation tissue and fissuring at the degenerate endplate, suggesting that this represents a more stable process of fatty infiltration. The underlying mechanism for the development of Modic changes has yet to be conclusively established; they may well represent a range of disease pathologies with the same MRI appearance. The current evidence would support type 1 changes representing inflammation, type 2 representing fatty infiltration and type 3 a process of sclerosis.

In general, sclerosis represents thickening of the subcartilaginous plate of bone as well as an increase in the trabecular volume[157]. In the knee this process is associated with a decrease in mineralisation and therefore a reduction in elastic modulus[158]. Weber[159] suggests this sclerosis is due to a chronic cycle of microfracture inflammation and repair and also due to Osteoblasts producing aberrant type 1 collagen with poor mineralisation capability as a response to the process of inflammation. In keeping with this, Perilli[74] found that the bone formation was higher in Modic type 3 while type 2 Modic changes had a reduced bone turnover index compared to type 1 or type 3.

My mechanical testing has shown type 1 and type 2 Modic changes to be associated with a significant increase in stiffness of both the endplate and trabecular bone, with an additional increase in hardness of the endplate when compared to those without Modic changes. Those with type 3 Modic changes have a significantly reduced stiffness and hardness of both the

endplate and the trabecular bone when compared with those displaying type 1, type 2 or no Modic changes.

Work by Liu[45] found that the presence of Modic changes (of any type) decreased the stiffness and the strength calculated by their 3mm indentations with a load of over 200N. This analysis also included the entire CEP, CCEP and BEP, and, while the results are not consistent with the findings in my work, the conditions of testing and the heterogenous nature of the tissue make comparisons unreliable between this and my work. If we consider the structural analysis in the work by Perilli[74], which showed an increase in trabecular thickness and bone volume in those with type 3 Modic changes, one might expect the increase in thickness to affect the structural stiffness of the bone with micro-scale indentations. My work has assessed the material properties on a scale and with a force small enough that these structural differences will have minimal (if any) contribution to the values produced; therefore the trend in results might not reflect those from previous work.

Based on the limited evidence available, Modic considered that type 1 Modic pathology represents a process of inflammation while type 2 represents fatty infiltration of the bone marrow. Hutton, using longitudinal MRI imaging, showed that type 1 and type 2 changes can transition between each category over time[94]. My results were unable to distinguish between the elastic modulus and hardness of the type 1 and 2 changes. This may indicate that they are an interchangeable representation of the same process or that the process affects the bone in a way that does not alter the properties tested here. At the endplate we see in both type 1 and type 2 changes that the elastic modulus and the hardness are increased. As previously discussed, increases in hardness and stiffness can be associated with an increase in mineralisation and an increase in hydroxyapatite crystal size. Hydration is known to affect the mechanical properties of bone, with an increase in water content leading to a decrease in stiffness and hardness[156]. The MRI changes seen in type 1 Modic changes are in keeping with an increase in water content. This does not necessarily mean that the hydration of the bone itself has changed; the increase in stiffness and hardness that we have seen would suggest this is not the case. If we look to the subchondral degenerate synovial joint for answers we see that inflammation causes marrow oedema rather than increasing the water content of the bone itself[159]; my results do not, therefore, exclude inflammation as a source of Modic type 1 changes, as the changes seen on MRI may simply represent marrow oedema rather than increasing the water content in the bone itself.

Type 2 Modic changes were originally described (by Modic) to represent fatty infiltration of the bone marrow[91], which may be the more established phase of the inflammation seen in type 1 changes. Type 2 changes are the most prevalent in the population which would fit with them representing an established and stable phase of the underlying process. Work by Hutton[94] would suggest that there is some transition between type 1 and 2 Modic changes. In my results the type 2 Modic changes are associated with an increased hardness and modulus at both the endplate and trabecular bone. This is slightly different from those with type 1 changes where the hardness of the trabecular bone did not reach clinical significance when compared to those with no Modic changes. This could simply be due to the sample size (as in the general population, type 2 Modic changes are more common among my samples). An alternative explanation could be that the more established type 2 changes affect the trabecular bone to a greater extent than the type 1 Modic process. The fatty infiltration seen in type 2 Modic changes may be associated with a reduction in water content (which would be in keeping with the MRI changes), which is known to increase the stiffness and hardness of the bone[156]. Fat infiltration is seen in the bone marrow spaces, however, and the results of type 1 changes suggest that the increased water content does not affect the bone. The previously discussed effect of increased hydroxyapatite crystal size and increased mineralisation with alterations of the interaction between the collagen with itself and with the inorganic crystals in a complex relationship with each other may also contribute to the explanation of the increased material stiffness and hardness that have been found in my results. The relationship between these changes and the changes in bone marrow fat and water content remain an avenue of further investigation.

The reduction in nano-indentation stiffness and hardness seen in my results for the samples from those displaying type 3 Modic changes can be explained by combining the work by Perilli[74] with the work from osteoarthritis of synovial joints. Perilli found that in type 3 Modic changes there was higher bone formation (which is in keeping with the process of sclerosis). In the knee, the process of subchondral sclerosis is known to increase the bone formation and trabecular volume but decrease the mineralisation of that bone, therefore reducing its elastic modulus[158]. The results of my study could be explained by applying the same principles; the type 3 Modic changes have a lower indentation modulus of elasticity and are less hard. This is in line with the decrease in mineralisation which we know to reduce both modulus and hardness. In the context of degeneration, breakdown of the collagen fibres

and the intermolecular cross links (as previously discussed) would contribute further to this reduction in material hardness and stiffness that we have identified.

My work has identified differences between those without Modic pathology within degeneration and those with Modic changes of any type. Type 1 and 2 changes display very similar material properties (with type 2 affecting the trabecular bone to a greater extent). This is in line with the observations of MRI interchangeability between type 1 and 2 Modic changes as well as the original description that type 1 and 2 changes may be continuations of the same process. Both increase the hardness and stiffness of the endplate. The exact mechanism for this has not been established but is likely to involve a complex change in the balance between several interacting elements of the structure of the bone. Type 3 changes on a structural scale have an increased trabecular thickness and bone volume, explaining the difference between my results and the larger scale indentation work in the spine. The process of sclerosis and new bone formation produces bone with collagen that reduces mineralisation potential, leading to bone with a lower hardness and elastic modulus.

6 Clinical subsidence study

An X-ray-based retrospective analysis of the subsidence of lumbar interbody devices has been undertaken as a vital addition to the basic science areas of this research into the endplate and trabecular bone. This clinical analysis aims to bridge aspects of the basic science investigation into clinical application. Research and ethical approvals were obtained prior to collection of these data (Reference 18/WM/0388). This study does not include any of the patients included in the other sections of my work.

6.1 Methods

Cage subsidence can be a difficult measurement to quantify. It relies on an initial quality control of the images taken followed by accurate measurement. Widely accepted standards for lumbar spine lateral projection X-ray quality are published by the European Commission [160]. In this document it is recommended that the following standards are met to ensure the quality of the lateral lumbar spine X-ray:

1. Visually sharp reproduction, as a single line, of the upper and lower-plate surfaces with the resultant visualisation of the intervertebral spaces.
2. Full superimposition of the posterior vertebral edges.
3. Reproduction of the pedicles and the intervertebral foramina.
4. Visualisation of the spinous processes.
5. Visually sharp reproduction of the cortex and trabecular structures.

During the collection of data all X-rays assessed will first be scrutinised to ensure these quality criteria are met to allow for accurate measurement values to be taken.

Subsidence according to Rao et al. is a loss of disc height of more than 2mm[161] Other studies also use this 2mm definition[162,163]. Marchi classified subsidence in terms of percentage of disc height loss [164]. Both Rao and Marchi subcategorised it in terms of early and late with 6 weeks being the delineating point. Behrbalk classified subsidence as 1mm loss of disc space height based on work by Strube et al. on the classification of spinal fusion radiologically [165][166]. Therefore, in this study a definition of a loss of height greater than 2mm between the initial post-operative radiograph and radiographs taken at 1 year follow up was employed. An example radiograph showing interbody cage subsidence is seen in figure 6.1.1

Figure 6.1.1 Initial and subsequent radiographs demonstrating interbody cage subsidence

For this study the measurement of disc height was taken using the method described by Dabbs in 1990, in which the measurement of disc height (H) is taken from the measurement of the anterior disc height (a) plus the posterior disc height (p) using the formula;

$$H = \frac{a+p}{2} \text{ [167]}. \quad (6.1\text{-}1)$$

This method is widely used in the literature surrounding cage subsidence[161,165,168,169]. Dabbs method was employed in this work to measure the average disc height at three timepoints. Pre-operative measurement was taken from the most recent radiographic lumbar lateral film prior to surgical intervention; immediate post-operative measurement was taken either prior to discharge or at the initial 6 weeks follow up appointment and finally at the 12 month appointment.

There are alternative methods described for measuring disc height including measurement from the central portion or expressing the height as a ratio of disc diameter (Fanfan's method)[167]. I have employed the measurement described by Dabbs as the average anterior and posterior height measurements provide an accurate measurement of the overall disc height changes before and after the surgery. If one were to measure only posterior this could underestimate changes in disc height, especially in those cases where lordosis is created (hence the anterior portion of the disc will change more than the posterior). A measurement from the central portion of the disc poses two potential issues: the first is that it may well be difficult to identify, especially with the insertion of an all-metal cage; the second is that the central portion of the endplate may well be affected by the very subsidence being measured. Measurement from the anterior aspect alone may overestimate changes in disc height in those where the sagittal alignment changes (lordosis increasing the measurement and kyphosis decreasing).

Therefore, an average measurement is the most effective way of gauging true changes in disc height for the purpose of this study. In the instances where there is a spondylolisthesis (the moving forward of one vertebral body with relation to the next) the height will be measured from the point at which a line perpendicular to the endplate intersects the endplate of the

adjacent vertebra. This is to avoid artificially measuring an increase in disc height in this group of patients, avoiding the diagonal measurement that this translation would cause. X-rays films within both institutions are taken with standard parameters of distance from the source and plate which allows electronic measurement (based on average values for magnification) to be employed.

Disc height measurements require a high level of accurate correlation between films in the same individual, however. To overcome this the measurements were correlated with the height of an adjacent vertebral body (not involved in the surgical procedure). The height of this specified vertebral body was measured on the pre-operative films, and this was then used as a measure of magnification for the subsequent measurements (as a ratio of the first measurement assuming that the height of the vertebral body is unchanged). This ratio was then applied to the measurement produced by the computing software to correct for differences in magnification.

Radiographic measurements were undertaken independantly by two orthopaedic spine surgeons experienced in the interpretation of spinal imaging (TM and DS) for a selection of patients from the study and an intraobserver comparison was made between the two. Statistical analysis has been performed using SPSS version 25 (IBM Corp., Armonk, New York, USA).

To establish the distribution of the date (parametric or non-parametric) a combination of visual analysis with the use of histograms and application of the Kolmogorov-Smirnov test were employed. Normally distributed data has been analysed with the t-test and data not displaying normal distribution analysed with the Mann-Whitney U test. Each interbody cage representing one sample. Analysis of subsidence has been undertaken on the data as a binary form (subsided or not subsided). This data is of course non-parametric. Analysis of other parameters has been based on the mean measurement (through application of the aforementioned dabs method) with each interbody device representing one data point.

For the analysis of the comparison between the two independent observers the mean measured difference between the initial and follow up imaging (ie. Initial measurement – Follow up measurement) has been used for the comparison data with each interbody cage representing one data point for the application of the sample correlation analysis.

Patients have been included from 2 regional spinal surgery tertiary units (The Norfolk and Norwich Hospital and Ipswich Hospital). All of the anterior lumbar interbody fusion (ALIF)

or lateral lumbar interbody fusion (XLIF) procedures were undertaken at the Ipswich Hospital. The transforaminal interbody fusion (TLIF) procedures were undertaken at both hospitals. The interbody cages used in the two institutions included in this study were the Sovereign PEEK cage (Medtronic) for ALIF procedures, the Modulus Titanium cage for XLIF (Nuvasive), the Capstone PEEK cage (Medtronic) (used in Ipswich), Tritanium PL (Stryker) (used in Ipswich and Norwich) and Concorde cages (DePuy Synthes) (used in Norwich) for the TLIF procedures.

6.2 Results

Analysis of the demographics available for the patients included in this study, comparing between those displaying the 3 types of Modic change or no Modic changes, did not show any statistically significant difference in age (p=0.881) or sex (p=0.257) as displayed in Table 6.2.1. The level of fusion (p=0.669 (see Table 6.2.2)) or type of cage (p=0.114 (see Table 6.2.3)) was not significantly different between groups either. T-test analysis of subsidance data comparing the two contributing spinal units also did not reveal a statistically significant difference (p=0.621 (see Table 6.2.4)); this is especially important given the implant used differs in the two institutions.

Table 6.2.1 Age and Gender of subjects included in clinical subsidence study analysis

Modic Type	Mean Age (Standard deviation)	Male:Female
0	46.7 (13.5) (n=57)	23:34
1	47.0 (9.6) (n=17)	3:14
2	46.8 (12.5) (n=27)	14:13
3	45.9 (10.6) (n=7)	2:5

Table 6.2.2 Level of surgery frequencies for each Modic type

Modic Type	L3/4	L4/5	L5/S1
0	3	24	30
1	3	4	10
2	2	8	17
3	0	3	4

Table 6.2.3 Frequencies of interbody cages for each Modic type

Modic Type	ALIF	TLIF	XLIF
0	16	39	2
1	7	8	2
2	3	14	0
3	2	5	0

Table 6.2.4 Subsidence rate for each hospital

Hospital	Subsided Cages	Total	Rate
Ipswich	19	67	0.28
Norwich	12	41	0.29

Analysis of the data from the two independent observers (comparing the measured differences: see Table 6.2.5 showed no significant difference between the two observers (n=67, paired sample correlation agreement 0.918, significance p=<0.00). Therefore, a decision was made not to continue to review the remaining radiographs for correlation, accepting that the difference between the two observers was not significant and there was not one instance in which there was a disagreement in the diagnosis of subsidence. The interobserver reliability of Modic changes has already been well established[170,171].

Table 6.2.5 The measured differences between the independent observations measuring radiological subsidence

Inclusion Number	Difference in measurement (mm)	Inclusion Number	Difference in Measurement (mm)
1	0.10	**34**	0.40
2	0.95	**35**	-0.25
3	0.20	**36**	-0.40
4	0.25	**37**	0.90
5	0.50	**38**	-0.30
6	0.15	**39**	-0.10

7	-0.35	**40**	-0.57
8	0.30	**41**	-0.20
9	-0.75	**42**	0.30
10	0.00	**43**	-0.50
11	0.10	**44**	0.80
12	0.30	**45**	0.25
13	0.25	**46**	-0.05
14	-0.60	**47**	0.00
15	0.05	**48**	0.20
16	-1.25	**49**	-1.15
17	0.65	**50**	00.75
18	-0.80	**51**	-.35
19	0.50	**52**	0.20
20	-0.45	**53**	0.15
21	-0.15	**54**	-0.75
22	0.50	**55**	0.25
23	-0.40	**56**	-0.40
24	-0.05	**57**	0.70
25	0.40	**58**	-0.75
26	-0.10	**59**	-0.11
27	-0.15	**60**	0.08
28	0.15	**61**	0.70
29	-0.15	**62**	-0.05
30	0.30	**63**	-0.20
31	0.30	**64**	0.10
32	0.65	**65**	-0.20
33	-0.35	**66**	0.30
		67	0.55

A total of 108 cages were analysed in 94 individuals. A total of 46 individuals in which an interbody cage was implanted were excluded due to a lack of available follow up imaging (n=37) (patients referred from outside the catchment received follow up at their local institution in outreach clinics) or the quality of the imaging not meeting the previously specified standards (n=9).

To answer the question ‘Do Modic changes affect subsidence of lumbar interbody cages?’, initial analysis of subsidence of those with Modic changes and those without was performed. Testing the null hypothesis that there is no difference between subsidence rate in those displaying no Modic changes and those displaying Modic changes, Mann-Whitney U

analysis produced a p-value of 0.003 indicating the presence of a significant difference (see Table 6.2.6).

Table 6.2.6 Subsidence data for those without and with Modic changes at the adjacent endplates.

	Subsidence/Total	**Subsidence %**
No Modic changes	11/57	19.3
Modic changes	20/51	39.2
p-value	0.003	

Analysis of the rate of subsidence (change over 2mm) dividing the results into individual Modic subtypes and using those displaying no Modic changes (n=57 19.3% subsidence rate) as a control comparison group revealed the following results when analysed with a Mann-Whitney U test; Type 1 (n=17 subsidence rate 35.3%) p= 0.053, type 2 (n=27 subsidence rate 51.9%) (p=0.002), type 3 (n=7 subsidence rate 0%) p=0.001 (see Table 6.2.7).

Table 6.2.7 Subsidence data for the individual Modic subtypes

Modic Type	**Subsidence/Total**	**Subsidence %**	**Comparison with 0**
0	11/57	19.3	
1	6/17	35.3	p=0.053
2	14/27	51.9	p=0.002
3	0/7	0	p=0.001

Comparison of those displaying type 1 with type 2 Modic changes did not reach significance (p=0.288). Comparison of those with type 1 and those with type 3 Modic changes did not reach statistical significance (p=0.187). Comparison of those with type 2 and type 3 Modic changes did reach significance (p=0.035) with application of the Mann-Whitney U test.

Comparison of the amount of correction (the difference in pre-operative and immediate post-operative heights) revealed that there was a significant difference in the amount of correction (in mm) between those that went on to develop subsidence and those that did not (p=0.017 t-test). When expressing the size of the correction as a proportion of the starting (pre-operative) disc height, significance was not reached (mean for those who went on to develop subsidence 121% correction compared to 105.4% in those that did not): see Table 6.2.8. In this sample

the data demonstrated no significant difference in pre-operative disc height and the presence of subsidence (p=0.084 mean in those that did not progress to subside 6.0mm as compared to 5.18mm in the group that did go on to subside).

Table 6.2.8 Operative correction f disc height and subsidence expressed as an absolute value (in mm) and as a percentage of the original height and the starting average disc height.

	Average height correction (mm) (SD)	**Average correction (% initial)**	**Starting height**
Subsided	5.06 (2.07) (n=31)	122 (84)	5.18 (2.01)
Did not Subside	2.35 (2.35) (n=77)	105 (183)	6.00 (2.29)
p-value	0.017	0.472	0.084

The type of interbody device (or cage) did not have a significant effect on the rate of interbody subsidence as measured in this method (see Table 6.2.9).

Table 6.2.9 Cage type and subsidence rate

	Subsidence/Total	**Subsidence %**
ALIF	11/38	28.9
TLIF	18/66	27.3
XLIF	2/4	50

6.3 Discussion

The rate of subsidence for lumbar fusion surgery is variable in the published literature ranging from 7-89% [161,163,164,172]. Subsidence can affect the outcome of surgery by compromising the goals through, for example, loss of alignment, loss of foraminal height and loss of stability [172], as well as pain from the subsidence itself. The correlation between subsidence and clinical outcome, however, is unclear with studies reporting mixed results [173–175].

Cage subsidence is a commonly used assessment in the evaluation of spine interbody cage devices. There are several potential factors that may contribute to the subsidance rate of interbody cages in the lumbar spine. The presence of osteoporosis affects the bone mineral density and therefore the mechanical properties of the vertebral bodies. For this reason no patients with a diagnosis of osteoporosis (treated or untreated) were included in this analysis. Seaman et al. [176] found in their meta-analysis that, while outcomes and fusion rates were similar, titanium cages had a higher rate of subsidance than PEEK cages. The area of contact and shape of the interbody cage has been shown to affect the subsidance rate[166,177–179]. To take this into consideration, the type of interbody cage has been recorded and analysed as separate subsections: Anterior lumbar interbody fusion (ALIF), Transforaminal (TLIF), Extreme lateral (XLIF). Lee et al.[180] found in their analysis of 77 patients that 'subsidence rate 2 years after surgery was 15.4% in the ALIF group, 38.1% in the TLIF group, and 10% in the PLIF group' but did not find a difference in fusion rates, however.

The reported prevalence of Modic changes in the lumbar spine varies from 0.5% to 81% [95,176,181,182] with the rates being higher in symptomatic individuals. Modic changes in the spine have been shown to affect the stiffness and strength of the vertebral endplate [45]. Pinson et al. investigated the factors affecting clinical outcome in their retrospective analysis of ALIF procedures, finding that those displaying type 1 Modic changes progressed to a better outcome than those with no Modic changes[183]. This is contrary to findings of studies investigating the effect of Modic changes on those undergoing discectomy without fusion[184]. In a review of the literature, Laustsen et al.[184] found only 3 studies exploring Modic changes and lumbar fusion and only 1 correlating interbody fusion with pre-operative Modic changes[185]. Kwon et al.[185] found that for PLIF procedures type 3 Modic changes were associated with a lower bone fusion rate based on lumbar radiographs. Ohtori et al.[186] explored type 1 and 2 Modic changes in those with lumbar stenosis, finding no significant

difference between those displaying Modic type 1 or 2 changes when assessing radiological fusion (on lumbar bending films) or outcome scores. There is no published work investigating the effect of Modic changes on cage subsidence in lumbar interbody fusion. Subsidence of the cage has been linked with post-operative Modic changes, however[187]. This perhaps indicates that Modic changes are associated with abnormal mechanical stresses at the endplate.

Posterior instrumentation is optional in some methods of interbody fusion, especially those not performed through a posterior approach to the spine. Work by Van de Kelft et al. found that for anterior lumbar fusion posterior augmentation did not produce significant benefits [188]. All the patients included in this analysis received a posterior pedicle screw augmentation in addition to the interbody fusion device. This is standard practice across both institutions.

The demographics did not differ between the cohorts within these data although the impact of age, sex and weight is unclear. According to Beutler et al.[163] these do not affect subsidence rates which is contrary to the findings of Phan et al.[189] who found a correlation between subsidence and age >64. It was not the aim of this work to explore the effect of age or gender on subsidence rate.

There are several mechanisms proposed as the driver for Modic changes, including mechanical changes as a consequence of disc degeneration resulting in abnormal load and shear stresses [100]. Inflammation can be caused by an autoimmune response to disc material originating from the nucleus pulposus that enters the vertebral body through microfractures in the endplate which are known to occur in degenerative disc disease [101]. Ohtori et al. [104] found markers of inflammation to be increased in Modic changes, supporting the idea that inflammation is important in the process. Albert et al. in two papers suggest a bacterial cause for Modic changes causing inflammation[100,114] and also note an association between Modic changes and back pain.

This study found that those patients displaying Modic changes had a higher rate of cage subsidence of 2mm or more than those that did not display Modic changes on their pre-operative MRI scans. Subgroup analysis showed that those displaying type 2 Modic changes had a statistically significant increase in subsidence when compared to those not displaying any Modic changes.

This is consistent with work by Perilli et al.[74] finding a situation of reduced bone formation in those displaying Modic type 2 changes. Schmid et al.[119] found that both Modic type 1 and

type 2 changes were associated with an increase in the amount of extruded endplate found in disc herniations, suggesting that these changes are associated with either a weakening process or increased mechanical loading.

Type 1 Modic changes did not demonstrate a significant difference when compared with subsidence frequency in those displaying no Modic changes, despite the data seeming to show a higher rate of subsidence on initial inspection (35.3% vs 19.3%). It might be expected, from previous work, including the initial work by Modic et al.[91], who found that Modic type 1 changes were associated with (or as a result of) disruption, microfracture and fissures of the endplate, that the endplate would be more susceptible to subsidence. Perilli et al. [74] found Modic type 1 to display high bone turnover.

This study found that the subsidence rate in those displaying type 3 Modic changes was 0%, which is in keeping with the logical expectation considering the increase in subchondral sclerosis one finds in type 3 Modic changes as noted in their original description [89].

ALIF cages in this study had a subsidence rate of 28.9% with TLIF cages having a very similar subsidence rate of 27.3%. Previous studies (as previously mentioned) have demonstrated a range of subsidence rates and our data fall within this range. Studies have previously found ALIF cages to have a lower subsidence rate; however, that was not the case in our results. One might expect this to be due to the higher mean percentage correction (125% ALIF as compared to 101% TLIF); however, t-test analysis revealed this did not reach statistical significance ($p=0.48$).

While type 1 Modic changes have been demonstrated to be associated with inflammation, endplate fissuring and microfracture, we were only able to demonstrate a strong trend towards an increase in subsidence that did not reach significance. Type 2 Modic changes were associated with a significantly increased rate of radiological interbody cage subsidence in keeping with previous work showing reduced bone formation and inflammation. Type 3 changes were not associated with any incidences of subsidence in this study, in line with the original description of subchondral sclerosis. The relative rarity of type 3 changes meant that the numbers were too small for this to reach statistical significance.

7 Histology

Histological analysis of the samples in this study has been undertaken to answer some key questions that arose during the initial analysis of the project data and has become a key area of the research.

The location and density of the vascular network within the endplate could hold valuable information about the perfusion and nutrition of the disc and therefore provide some indication about the process of degeneration. As discussed in the introduction of the thesis, this may also give further knowledge when considering the advent of regenerative therapies. Histological study enables analysis of the process of calcification of the endplate, and also, using Osteoblasts as a marker of bone turnover, it will contribute to the understanding of the structure of the bone and the effect of degeneration. This will add to the knowledge gained from the biomechanical studies. Also, study of inflammatory cells will not only explore the processes surrounding Modic pathology but also in degeneration.

The details for slide preparation and staining are available in Appendix 11.2 which contains the standard operating procedures for histological slide preparation which were adhered to during the preparation of the samples used in this study. Histological images have been taken using a Zeiss AXIO Observer Z1 automated stage microscope with analysis of the images using Image J software.

7.1 Calcification

7.1.1 Calcification Methods

Haematoxylin and eosin (H&E) staining allows the delineation of the cartilaginous endplate (CEP), calcified cartilaginous endplate (CCEP) and the bony endplate (BEP) (See Figure 1.4.1).

In order to account for the variability of the thickness of the layers of the endplate, measurement of the calcified portion of the endplate has been taken at 10 evenly spaced points across the prepared slide. A mean average value has then been calculated for comparison between the samples. Where the tidemark is broader the central point has been taken for measurement. All measurements have been taken at an angle perpendicular to the axis of the tidemark to account for the variability of the angle at which the samples were trephined.

Statistical analysis has been undertaken using SPSS version 25 (as previously detailed).

7.1.2 Calcification Results

Taking into account the age of the patient at the time of sample collection (split into decades) the average thickness of the CCEP trended towards an increase with age (see Table 7.1.1). The increase was only significant between those in their 30s and 40s (p=0.048). Comparison between those in their 40s and 50s did not show any significant difference (p=1), neither did comparison between those in their 50s and 60s (p=0.8). There was a non-significant decrease in the CCEP thickness between those patients in their 50s and their 60s.

Table 7.1.1 Age and thickness of the CCEP

Age	Mean thickness (µm)	Standard Deviation
30s	33.26 (n=2)	13.59
40s	115.60 (n=2)	50.99
50s	112.06 (n=2)	102.2
60s	75.33 (n=1)	35.21

When the grade of degeneration of the adjacent disc is considered, this study found no significant increase of the average thickness of the CCEP with an increase in the Pfirrmann grade. Comparison between the non-degenerate disc (Pfirrmann 1) and the degenerate disc (Pfirrmann 4 and 5) did show an increase in the mean from 75.32µm for Pfirrmann grade 1 discs to 92.49µm in those classified Pfirrmann grade 4 or 5. This increase did not reach statistical significance (p=0.571). The average CCEP thickness split into individual Pfirrmann grades is displayed in Table 7.1.2, where we see a slight decrease in grade 4 compared to grade 1 but an increase in those with grade 5 Pfirrmann degeneration.

Table 7.1.2 Degeneration and CCEP thickness

Pfirrmann Grade	Mean thickness (µm)	Standard Deviation
1	75.33 (n=1)	35.21
4	63.52 (n=3)	44.24
5	116.65 (n=3)	67.54

Within this cohort of samples there are patients displaying Modic type 1 and type 2 changes as well as those not displaying any Modic changes (the control patient is not included in this analysis). Comparison of the thickness of the CCEP in these patients is summarised in the

Table 7.1.3. The CCEP thickness is decreased in those displaying type 1 Modic changes but increased in those displaying type 2 Modic changes when compared to those samples taken from patients not displaying any Modic changes. Statistical analysis with the Mann-Whitney U test shows no significant difference between Modic 0 and Modic 1 (p=0.643), Modic 0 and 2 (p=0.295) or when comparing those displaying Modic changes of any kind (0) with those not displaying any (1 or 2) (p=0.529).

Table 7.1.3 Modic changes and CCEP thickness

Modic Type	Mean Thickness (µm)	Standard Deviation
0	84.14 (n=3)	60.49
1	40.31 (n=2)	9.50
2	104.76 (n=2)	54.66

7.1.3 Discussion

Calcification of the endplate has been shown to increase with age[43,47,122,128]. My work shows an increasing trend in the thickness of the CCEP with a progression in age. The exception to this is the 60s age group which includes a patient that is not suffering from DDD. As degeneration is also known to increase the calcification of the endplate[47] this lack of degeneration might explain the non-significant decrease in CCEP thickness contrary to the trend between the other decades in the study. With the exception of this patient in their 60s (the control) the trend in increase in thickness in the CCEP is in keeping with previously published work.

Degeneration has been shown to increase the thickness of the calcified portion of the cartilaginous endplate[190] in animal studies and in human cadaveric work[47]. My work also shows this overall increase in CCEP thickness with degeneration. Interestingly, when subcategorised into the individual Pfirrmann grades we see a decrease in the mean thickness when comparing grade 1 with grade 4. Potential explanations for this include the increased age of the sample with the grade 1 disc (as previously discussed CCEP thickness increases with age as well as degeneration). As these are biological samples and the sample size is limited due to the nature of the samples and difficulty with collection this may simply represent the biological variation that is normal between individuals. The standard deviation of these measurements is high indicating the variability between samples. Despite this the CCEP thickness increases overall with degeneration of the disc, which is, reassuringly, in keeping with previous work.

This increase in calcification may represent an increase in force transmission through the endplate (both axial and shear) and will alter the diffusion into and out of the disc.

In his original work Modic described a process of inflammation, fissuring and fibrous tissue formation in type 1 change and yellow (fatty) marrow replacement in type 2[91]. Type 3 changes represent a process of sclerosis and one would therefore expect to see an increase in the thickness of the CCEP. Perilli[74] found Modic type 1 changes to represent an 'active' stage of pathology with high bone erosion and subsequent formation, type 2 changes were associated with reduced bone formation and remodelling and type 3 were found to represent increased bone presence. Applying this to the measurement of the thickness of the CCEP one might conclude that type 1 changes might represent a process of initial erosion of the bone (and perhaps CCEP) therefore reducing its overall thickness. If the process of erosion and formation were in balance, then it would be expected that type 1 changes would not be significantly different from those without Modic changes.

My results have displayed an overall decrease in the thickness of the CCEP in those with type 1 changes (when compared with those without changes). This would seem to be indicative of an imbalance in the processes of erosion and formation of bone in favour of erosion. My results show that type 2 Modic changes are associated with an increased thickness of the CCEP (when compared to either those with type 1 Modic changes or no changes). The hypothesis that Modic type 2 changes are a process of remodelling and reduced bone erosion correlates with this finding. It is worth noting the high standard deviation with these data, which is expected in biological samples of this nature. Interpretation of trends within this limited sample group with such deviation could be due to biological variation. It is notable that the mean thickness for those with type 2 Modic changes is more than twice that of type 1.

My results would support the existing hypothesis that type 1 Modic changes represent an active phase of bone metabolism with erosion prospering over bone formation, while type 2 changes represent a process of bone formation and remodelling with an increase in thickness of the CCEP. The thinning of the CCEP seen in type 1 changes is in keeping with the biochemical mechanism of Modic changes summarised by Zhang[110], where inflammatory mediators from the disc (or perhaps in response to herniation of disc material through the endplate as suggested by Adams[116]) lead to an inflammatory response and the presence of type 1 Modic changes. Thinning of the CCEP would, in theory, make contact with the disc material or diffusion of inflammatory mediators into the bone marrow contact channels more

likely and perhaps explain some of the process by which Modic changes arise. Moore[136] comments that endplate erosions are more common in females once they reach the age of 60.

Calcification of the cartilaginous portion of the endplate has been shown to increase with ageing and degeneration [136,191]. This calcification alters the transfer of forces through the region and affects the transport of nutrients to the disc itself[20,42,191]. An understanding of the calcification of the endplate in disease contributes to an understanding of the more complex multifactorial overall process of disc degeneration.

7.2 Tidemark Variability and Erosions

The tidemark is the boundary between the calcified cartilaginous endplate (CCEP) and the uncalcified portion. It is not a uniformly straight line. The variability of the tidemark is logically linked with the presence of erosions that disrupt the endplate. Variability might indicate an increase in the surface area across which the transfer of metabolites could occur and also an increase in the area over which mechanical loads are transferred. An increase in variability might also confer some mechanical resistance to shear forces between the layers of the endplate. Variability could be increased in response to; localised microtrauma, subsequent remodelling or as part of a process of inflammation or degeneration of the cartilaginous matrix. The variability has been examined here to provide a potential further insight into the changes the degenerate endplate undergoes.

7.2.1 Methods

There is no documented method for assessing the variability of the endplate tidemark. The method used in this study is simple which improves its applicability. Using image processing software 'Image J' the tidemark can be identified and traced easily. The overall length can then be calculated by the software by converting the total length of the traced line in pixels into a measurement of length once the scale has been set determining the value of one pixel. To be able to compare the variability of this line a second straight line is used from the exact same starting and ending points. The ratio of the difference between these two lengths gives an indication of the overall variability of the actual tidemark, as the course of a variable line will be longer than the course of a straight one. These measurements are then converted into a ratio where;

$$Variability\ Ratio = \frac{Variable\ Line}{Straight\ Measurement}.$$

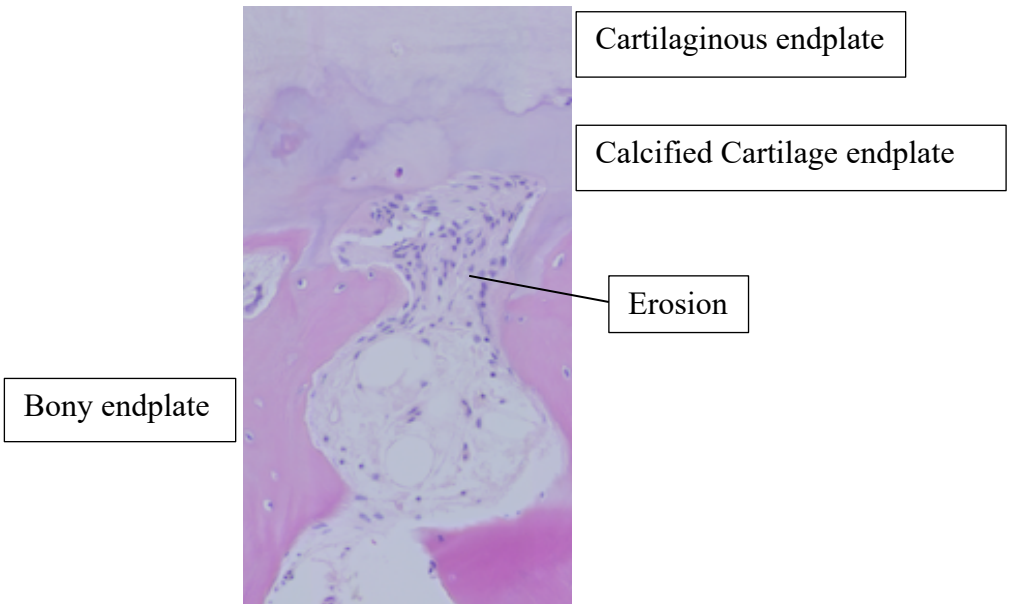

Figure 7.2.1 An example of erosion through the bony endplate

An erosion of the endplate for the purpose of this histological study is any breach in the normal anatomy of the cartilaginous portion of the endplate that communicates with the underlying trabecular spaces. One histological 4μm thick H&E slide was prepared from the central part of the trephined sample perpendicular with the long axis of the samples. The number of erosions has been recorded along with the total length of the endplate and the average size of the erosions seen. Comparison between these points of data collection and the underlying characteristics of the sample has been undertaken. In order to account for the variability in the length of endplate represented between the different samples, a ratio of the total erosion length/total endplate length has been utilised to be able to compare different samples. With the same goal, the number of erosions is reported as erosions per unit length allowing comparison between samples.

7.2.2 Results

The variability ratio data are displayed in Table 7.2.1. It displays a non-significant increase in the variability between those in their 30's and 40's ($p=0.262$) this increase is not sustained into those in their 50's and falls again into the 60's. It should be noted that the patient in their 60's is the patient representing a 'normal' non-degenerate disc. No other significant differences between age groups were found in tidemark variability.

To assess the impact of degeneration on endplate variability, a comparison between the variability ratio and the Pfirrmann classification of degeneration of the adjacent disc has been undertaken. Table 7.2.2 summarises the results of this comparison. There is a significant

increase in variability with the presence of degeneration. A comparison of Pfirrmann grade 1 classified discs and Pfirrmann grades 4 and 5 combined shows a significant increase (p=0.04). Subdividing and comparing type 1 with type 4 classified discs show a non-significant difference (p=0.413). However, comparison with Pfirrmann grade 5 discs does show a statistically significant increase in variability compared to the 'normal' discs (p=0.01).

Table 7.2.1 Tidemark variability by decade of age

Age	Variability Ratio	Standard Deviation
30s	1.1027 (n=2)	0.059
40s	1.3086 (n=2)	0.191
50s	1.1595 (n=2)	0.026
60s	1.0763 (n=1)	0.582

Table 7.2.2 Tidemark variability and degeneration by Pfirrmann classification

Pfirrmann	Variability Ratio	Standard Deviation
1	1.0763 (n=1)	0.582
4	1.1734 (n=3)	0.197
5	1.2686 (n=3)	0.145
4&5 Combined	1.2253 (n=6)	0.169

Applying the endplate variability to the type of Modic changes displayed at each endplate showed an increase in the mean variability ratio for both Modic type 1 and Modic type 2 changes when compared to those endplates not displaying any Modic changes. This increase reached statistical significance for those with type 2 Modic changes (p=0.014) but did not reach significance for those displaying type 1 changes (p=0.492). If we consider those showing Modic changes of any type compared with those not showing any Modic changes, we have a significant increase in the mean variability ratio to 1.2528 (p=0.018). Table 7.2.3 displays these results.

Table 7.2.3 Tidemark variability by Modic subclassification

Modic Classification	Variability Ratio	Standard Deviation
0	1.0848 (n=3)	0.053
1	1.1229 (n=2)	0.067
2	1.2889 (n=2)	0.181
1&2 combined	1.2528 (n=4)	0.174

The number of erosions for a given millimetre in length of endplate divided into age grouped by decade is displayed in Table 7.2.4. There is a clear trend towards an inverse relationship in the number of erosions per millimetre of endplate and age. It should be taken into account that the samples from the patient in their 60s are being used as the normal control and this may some effect on the results. It would not, however, explain why the trend continues throughout the other decades of age. Statistical analysis of this comparison reached significance between those in their 40's and those in their 60's (p=0.016), no other comparisons reached significance.

Table 7.2.4 Endplate erosions and age

Age	Number of Erosions per mm	Standard Deviation
30s	1.5542 (n=2)	0.96471
40s	1.2281 (n=2)	0.49284
50s	0.3865 (n=2)	0.5465
60 s	0.2841 (n=1)	0.21692

To explore the effect of degeneration on the number of erosions in the endplate, the Pfirrmann classification of the adjacent disc was used to group the histological samples. Comparison between the classification of disc degeneration and the average number of erosions seen in the endplate per millimetre is summarised in Table 7.2.5.

Table 7.2.5 Endplate erosions and degeneration

Pfirrmann grade	Number of Erosions per mm	Standard deviation
1	0.2841 (n=1)	0.216
4	1.2833 (n=3)	0.80173
5	1.0646 (n=3)	0.68753
4&5 combined	1.164 (n=6)	0.71169

The number of erosions at the endplate per millimetre in these samples was significantly lower in those with a healthy disc compared to those discs with Pfirrmann 4 or 5 graded degeneration (p=0.01). Comparison between grade 1 and grade 4 Pfirrmann changes in the adjacent disc did reach significance (p=0.016) with Pfirrmann 5 grade not quite reaching statistical significance (p=0.067).

Categorisation of the histological samples into the type of Modic changes found in the endplate and underlying bone and comparison between the respective numbers of endplate erosions seen per millimetre is displayed in Table 7.2.6.

Table 7.2.6 Endplate erosions and Modic changes

Modic changes	Number of erosions/mm	Standard deviation
0	0.6321 (n=3)	1.0121
1	1.0032 (n=2)	0.19931
2	1.1631 (n=2)	0.48167

It is evident that there is a trend towards an increase in the number of erosions/mm at the endplate with both type 1 and type 2 Modic changes. Statistical analysis with the Mann-Whitney U test did not show that either of these perceived increases reached statistical significance (although comparison between types 0 and 2 p=0.051). When comparing those without Modic changes and those with either type 1 or type 2 changes statistical significance was reached (p=0.036).

7.2.3 Discussion

Tidemark variation and Age

When we consider ageing in the disc it is important to consider degeneration. We know that the results include a patient in their 60s that does not have disc degeneration, and therefore caution needs to be employed when making conclusions and including the 60th decade as part of these results. It is also important to highlight that these data represent ageing within degeneration rather than ageing as a separate entity. It is nevertheless important to appreciate the effect of ageing on the measurements given the variation in age between the degenerate and 'normal' sample. My results have not identified a discernible overall trend between age groups when considering the variability of the endplate tidemark. As there is no evidence in the published literature of a previous analysis of the variability of the tidemark or endplate it is difficult to know if this would be expected (especially within a cohort of degeneration). It

may be the case that once the process of degeneration has begun that this has a similar effect across all ages. If the results were to include those with osteopenia/osteoporosis this might give some indication of the underlying driver for variability (an increased variability in this pathology would indicate a mechanical process). We know that the endplate becomes more porous with age[18] and that this might lead to focal weak points and fissures; therefore, ageing might be expected to decrease the uniformity of the endplate structures in addition to the process of degeneration.

Tidemark variation and degeneration

Tidemark variability as a measurement has not been reported elsewhere in the literature, and therefore the significance of this measurement is not yet established. Clinically, endplate erosions on MRI are associated with DDD. Lotz[18] summarises by acknowledging that endplate irregularities are found in asymptomatic populations but are more common in the symptomatic degenerate disc and have been clearly associated with back pain. Adams[151] proposes that damage to the endplate and herniation of the disc through the endplate is one mechanical cause for disc degeneration. Irregularities of the endplate can be indicated by measuring the variability of the tidemark (with a higher variability indicating a higher irregularity). The proposed mechanical failure of the endplate contributing to decompression of the disc and eventual degeneration would be expected to lead to some variation in the uniformity of the structure of the endplate.

My results display an increase in the mean variability of the endplate between those without degeneration and those with degeneration (Pfirrmann 4 or 5). Comparison of those with advanced degeneration (Pfirrmann grade 5) was also significant, indicating that advancing degeneration increases the variability of the tidemark in the human lumbar spine endplate.

There could be potential benefits of an increase in endplate variability. First, it increases the surface area over which nutrients and waste products can diffuse across the endplate (which we know is altered in degeneration[192]). Second, it increases the potential surface area over which the forces are transmitted from compression from the disc (although the trabecular bone beneath will remain unaltered), although this has been shown to alter the stress distribution of the endplate concentrating it in the periphery[193,194]. Third, it may (theoretically at least) offer partial protection from shear forces by increasing the contact area and by increasing the effective friction between layers, effectively interlocking them due to the variations.

Tidemark variability and Modic changes

My results show a significant increase in the variability of the tidemark of those displaying Modic changes when compared to those without. It is worth noting that for this analysis the 'normal' patient was removed so as to remove the confounding factor that degeneration would play. Perilli[74] found type 1 Modic changes to represent a state of high bone turnover and erosion, while type 2 represented a phase of bone formation and remodelling. Zhang[110] reviews Modic changes and describes a biomechanical mechanism and a biochemical

mechanism underlying the process (both involving inflammation). The process of inflammation with erosion and remodelling of the bone and endplate would be expected to decrease the uniformity of the endplate and thus increase the variability measurement used in my work. The potential impact of an increase in variability of the endplate is unclear, as it has not been explored in the published literature previously. We do know that variability is associated with worsening degeneration[18] and that this degeneration alters the concentration of forces regionally within the endplate[193,194]. Given Wolff's law[66], which tells us that bone remodels according to the forces which are applied to it, we might expect the alteration in force concentration in the degenerate endplate coupled with the known increase in bone turnover and remodelling seen in Modic changes to lead to an increase in the variability of the structure of the endplate. My results would therefore support the previous findings in the literature surrounding both degeneration and Modic pathology.

Erosions of the endplate and age

Ageing of the intervertebral disc has been shown to have an established effect from a relatively early decade of life[122]. Changes both within the disc nucleus as well as changes in the endplate have been isolated. Moore[136] comments that erosions of the endplate are more common in females over 60, and Wang[195] found endplate lesions to be correlated with increasing age.

My examination of the effect of ageing on the number of erosions seen histologically at the endplate has not shown a significant difference or trend in this cohort of degenerate samples. The small number of samples is one explanation for the lack of significance, but it is more likely that the process of degeneration has an effect that is much greater than the effect of ageing. This larger effect of degeneration masks any subtle differences in the numbers of erosions secondary to ageing. The effect of degeneration on the number of erosions has also been undertaken, which allows some comparisons to be made.

Further work in this area might include the collection of samples from nondegenerate spines of a variety of ages and an increase in the span of ages from which the samples are collected to include the later decades of life.

Erosions of the endplate and degeneration

Adams[116] described a distinct phenotype of disc degeneration in which the disc herniates through defects in the endplate. In addition to this Schmorl[39] described lesions seen at the

endplate with sclerosis as a reaction to herniation through the endplate of the nucleus pulposus[41]. These lesions are common and not always symptomatic. An erosion of the endplate histologically is a breach in the usual structure of the endplate filled with fibrous, vascular or inflammatory tissue. The pathological process behind the development of erosions is a breach of the endplate secondary to mechanical overload or defects in the endplate (or a combination of the two). These breaches stimulate an inflammatory/healing response and manifest as erosions. Erosions can be seen on MRI and are more common in degeneration. Wang[195] found these to affect the central regions of the endplate more than the peripheral but did not look specifically at the level of degeneration. The same author in another piece of work[196] found an association between the number of endplate lesions and a history of frequent back pain. They also found an association between degeneration of the disc and the number of endplate lesions.

My work found a significant increase in the number of erosions at the endplate histologically when comparing those with disc degeneration to those without ($p=0.01$). This finding is in line with the previously published work and adds to the overall body of work on the matter. It also supports the classification of degeneration and ageing as separate entities. Associations between endplate lesions and pain have been previously described, and Lotz[18] has been able to show a localised increase in neoinnervation in the region of endplate defects, suggesting that not only do they affect the disc and its mechanical environment but they themselves could be a source of pain.

Erosions of the endplate and Modic changes

Modic changes may represent more than one pathological stimulus, resulting in changes that present in the same way on MRI. Zhang[110] summarises this by categorising the stimulus into mechanical and biochemical types. Mechanical overload can cause microfractures and the development of lesions of acute and chronic inflammation as part of the attempted healing process. This can manifest as a defect or erosion at the endplate. Biochemically, defects or erosions in the endplate can lead to the contact of nucleus pulposus tissue (which has been isolated from the immune system since its formation in utero), leading to an inflammatory reaction. Erosions could therefore be part of the stimulus of Modic type changes or a consequence of the process of inflammation.

My work has shown an increase in the number of erosions when comparing those without Modic changes to those with Modic changes. The number of erosions is increased more with

type 2 changes. Type 2 changes are not considered to be representative of a process of inflammation. The presence of erosions here is supportive of the theory that type 1 and type 2 changes are continuations of different stages of the same pathological process with inflammation dominating the appearance of type 1 changes but type 2 representing less acute changes and more established fatty infiltration. My mechanical testing would suggest that the increase in the stiffness and hardness seen in Modic changes represents a process of embrittlement of the endplate, making it less able to adapt to the forces applied to it and predisposing it to micro failure and therefore the formation of erosions. We know these erosions can themselves be a pain source[18], which may contribute to the cause of the pain experienced by some (not all) people with Modic changes.

7.3 CD-31

The CD-31 immunostaining for platelet endothelial cell adhesion molecule (PECAM) is found on the endothelial surface of blood vessels, platelets, circulating leukocytes and is known to play a role in angiogenesis[197]. Figure 7.3.1 provides an example of CD-31 positive vascular structures. This section examines the relative density of CD-31 positive structures at the endplate as a marker of vascularisation (this importance of which has been previously covered) and also the location of these structures with regard the histological layers to further the understanding of the anatomy of the vascular network.

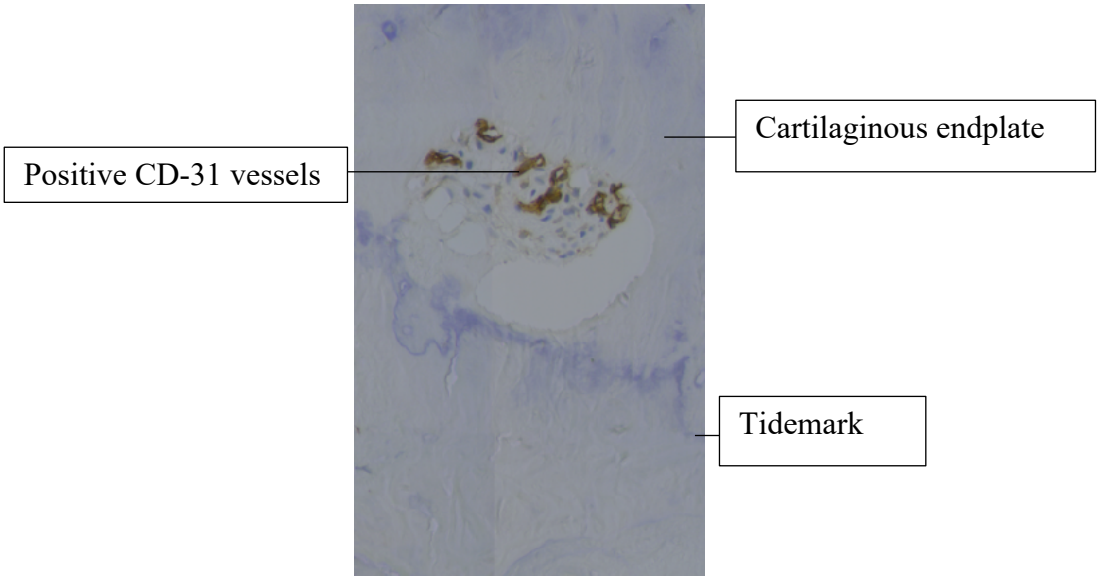

Figure 7.3.1 Histological example of CD-31 positive vessels

7.3.1 Methods

One histological 4μm thick slide of each sample was prepared and stained with the CD-31 immuno-stain. The slide was analysed using Image J software to identify areas of positive stain in keeping with a vascular structure. The overall number of these positively staining vascular structures was recorded for analysis. The size of the vascular structures was not recorded due to the inaccuracies in this kind of measurement that would come with not knowing the exact orientation of the view of the vessel. An oblique section could lead to a false increase in the measurement of the diameter of the vessel. The area of interest of this study is the endplate and immediate surrounding tissue. For reproducibility, the analysis has been undertaken in the area within 500μm of the tidemark; this is the area that encompasses the calcified cartilaginous endplate as well as the bony portion of the endplate.

In order to be able to form a comparison between samples, the number of vessels staining positive with the CD-31 stain within the 500μm distance from the tidemark of the endplate has been converted into a count (or density) per 0.25mm^2. This value is created using a mean across the entire endplate section.

7.3.2 Results

Ageing and blood vessel density of the endplate is displayed in Table 7.3.1. A sharp and maintained decrease is seen between the samples taken from those in their 40s and those in their 50s.

Table 7.3.1 Vascularity and age

Age group	Vascular density/mm^2	Standard Deviation
30s	11.79 (n=2)	7.76
40s	12.32 (n=2)	5.55
50s	4.18 (n=2)	0.61
60s	4.55 (n=1)	3.66

Comparison between the vascularity and the level of degeneration of the adjacent disc is summarised in Table 7.3.2.

Table 7.3.2 Vascularity and degeneration

Pfirrmann Classification	Mean density/mm^2	Standard deviation
1	4.545 (n=1)	3.658
4	9.935 (n=3)	5.737
5	10.791 (n=3)	6.017
4&5 combined	10.363 (n=6)	5.986

Comparison between those samples without any adjacent disc degeneration and those showing degeneration (Pfirrmann grades 4 and 5 combined) revealed an increase in the number of vessels that are present in the samples from endplates adjacent to degenerate disc. Statistical analysis (with the Mann-Whitney U test) did reach significance (p=0.03) indicating that degeneration does affect the density of CD-31 staining vessels at the endplate.

Grouping the samples into classifications based on their expression of Modic type changes on the pre-operative MRI scan reveals that there is a non-significant increase in the mean number of vessels for both those with type 1 changes (p=0.333) and those with type 2 changes (p=0.073) compared to those displaying no Modic changes. Table 7.3.3 displays these results. Comparison of those displaying no Modic changes with those displaying any Modic changes did not quite reach statistical significance (p=0.055).

Table 7.3.3 Vascularity and Modic pathology

Modic change	Vascular density No./0.25mm^2	Standard Deviation
0	5.740 (n=3)	3.471
1	12.354 (n=2)	10.900
2	11.096 (n=2)	6.018

Analysis of the CD-31-stained slides revealed that in 5 slides it is possible to demonstrate structures that, when compared to the corresponding H&E-stained section (which has been taken with consecutive 4μm slices), were within the calcified region of the cartilaginous endplate. There was evidence of vascular structures being identified within the non-calcified portion of the cartilaginous endplate in 5 samples (as illustrated in Figure 7.3.1). All 5 slides that had vessels in the CCEP also had erosions present. These vessels were not seen only

within the erosions themselves, however. There were no vessels seen in the CCEP in those with type 1 Modic changes (there were in those displaying type 2 changes and also those without changes). The slides with vessels within the CCEP were from samples adjacent to discs of Pfirrmann classification 1, 4 and 5.

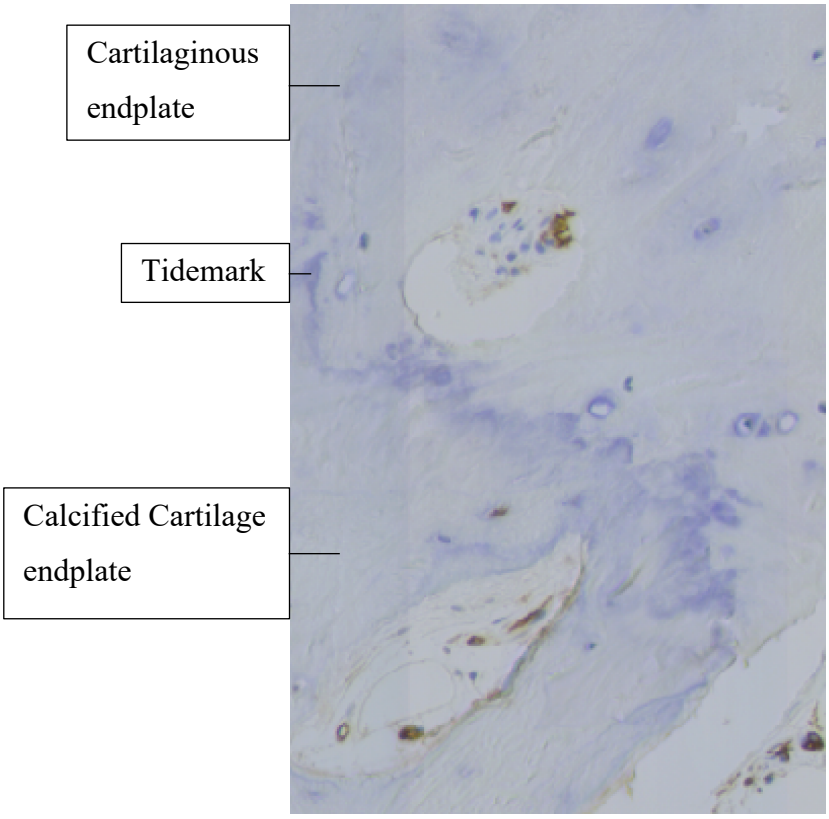

Figure 7.3.2 CD-31 stained vessels (brown) in the calcified and cartilaginous portions of the endplate

7.3.3 Discussion

Considering the effect of age on the vascularity surrounding the endplate these results show a similarity in vascular density in the samples taken from those in their 30s and 40s but a sharp decrease in the samples from those in their 50s which is maintained from the samples taken from the patient in their 60s. This is unlikely to be linked with the process of degeneration as the person in their 60s is actually the control sample and therefore does not have any clinical or radiological degeneration. It would seem likely therefore based on these results that ageing has a detrimental effect on the per-endplate vascularity.

We know that macrovascular atherosclerosis has been associated with DDD[124]. Previously published work into degeneration of the intervertebral disc has shown a process of neovascularisation[126,134], but there is also evidence that this does not translate into an

increase in perfusion[20,22,150]. We also know that perfusion is increased in the central portion of the disc–endplate interface[198]. Tomaszewski[128] showed that occlusion of marrow contact channels in the endplate was associated with DDD. Work by Oki[198] suggests that the structure of the vascular buds themselves are as important as the density.

My results indicate an increase in vascular density with increasing degeneration, with a statistical significance when comparing those with and without degeneration. This is in line with the previously published work. Neovascularisation of the endplate occurs secondarily to an increase in cytokine stimulation[121]. This stimulation is in response to the inflammation associated with degeneration and also the decrease in diffusion that we know happens in degeneration[43,125,199].

Vascular channels around the endplate may not represent entirely the perfusion of the disc, as the thickness of the endplate, the size and density of contact channels and the flow through the vessels are variables that all play a role. The presence of an increased number of vessels at the endplate in degeneration might seem promising when considering regenerative therapies to the disc but one would need to address the other contributing structures to disc perfusion before adequate nutrition to the disc can be achieved.

Modic changes have been shown to involve a process of inflammation, possibly in response to microfracture, herniation of disc material or infection[74,91,107,110,200]. Ohtori[200] demonstrated an increase in inflammatory cytokines and neoinnervation (with associated neovascularisation) in the endplate. Considering this previously published work, one would expect the presence of Modic pathology in these samples in this study to be associated with an increase in the vascularity at the endplate.

While my work demonstrated an increase in the mean density of vessels in those with both Modic type 1 and type 2 changes, the restriction in sample size and the high standard deviation mean that this did not reach significance. Therefore, caution is required when attributing these changes to the Modic pathology. The trend is in keeping with the expected findings with type 1 changes representing the highest vascularisation. The lower deviation of results in those with type 2 changes perhaps indicates that the acute changes (and therefore variability) have become more stable (as expected when considering the original Modic description[91]). It could be hypothesised that in type 2 changes the neovascularisation process is quiescent, and thus there is more uniformity between samples. Vascularisation is associated with degeneration and these results are all in degenerate discs. It may therefore be

the case that the process of vascularisation in degeneration has such an effect that the differences seen between those displaying different types of Modic change cannot reach significance with this number of samples.

Future work might concentrate on Modic vascularity in degenerate and non-degenerate discs with a larger sample size (although this might be difficult to obtain). Also, correlation of Modic vascularity in degenerate and non-degenerate discs with perfusion will be important to try to better appreciate the pathology behind Modic changes and, to explore why not all discs with Modic pathology on MRI become degenerate or symptomatic.

The location of the stained vessels is important to aid the understanding of the nutrition of the disc. Although we do not yet know fully how the presence of vessels affects the nutrition to the disc itself, the location of the vessels in relation to the structure of the endplate did not differ when considering the presence of degeneration. It would therefore seem that while the overall number of vessels at the endplate increases with degeneration the location of these vessels remains confined to the BEP and CCEP. In the one instance where there was a CD-31 positive vascular structure extending past the tidemark, this was associated with an erosion containing fibrous tissue also extending past the tidemark.

Examining vascular structures in the CCEP revealed that not all of these vessels were associated directly with an erosion or fibrous infiltration. In addition to this, vessels within the CCEP were also seen in the samples from those without DDD. This combination of findings would indicate that vessels are normally present in the CCEP (not just as a consequence of neovascularisation). Oki[198] found vessels to extend from the subchondral bone to the surface of the endplate in a ‘capillary coil’. Their light microscopy shows vessels up to the tidemark in the endplate of rabbits. The results from my work would support that this is the case in the human lumbar spine as well as in the rabbit.

Clearly there is more to perfusion than the number of vascular channels; their shape and size affect the perfusion as does the calcification of the endplate, the thickness of the endplate, the number and sizes of the pores in the endplate and the size of the molecule. An insight into the vascular anatomy in degeneration will go part way to helping with the understanding of this. Future work might aim to concentrate on the structure of the end buds in both healthy and degenerate discs as well as the 3-dimensional arrangement of these in the human spine both under normal and degenerate conditions.

7.4 CD-56

Exploration of the CD-56 immunomarker as an indicator of Osteoblast lineage cells has been undertaken in this work to complement and explore the changes seen at the endplate from the biomechanical testing. This work has demonstrated changes taking place at the endplate and the underlying trabecular bone mechanically, and we hypothesise that bone remodelling and turnover will have some contribution to the differences seen. This section aims to explore this further.

7.4.1 Methods

One 4µm thick slice has been taken from each sample and stained with the CD-56 Marker. CD-56 is also known as the Neural Cell adhesion molecule, and, as the name suggests, this is a binding glycoprotein that has a role in the adhesion between cells. The marker, in addition to neural cells, also stains for some Natural Killer Cells and Osteoblasts[201,202].

This analysis focuses on the Osteoblast lineage bone lining cells, as these were the predominant cells staining positive, as well as their function. This focus is in line with the mechanical testing aims of this work.

Histological slides were prepared using 4µm thick slices of decalcified and paraffin embedded tissue. After staining, Image J software has been used. Analysis has been undertaken to cover an area 500µm from the tidemark encompassing the CCEP and the bony endplate. To allow comparison of the results, the data have been converted to represent a standard unit of area of 0.25mm^2 giving a number of positively staining cells/0.25mm^2. Figure 7.4.1 displays an example of CD-56 positive staining cells lining the bone.

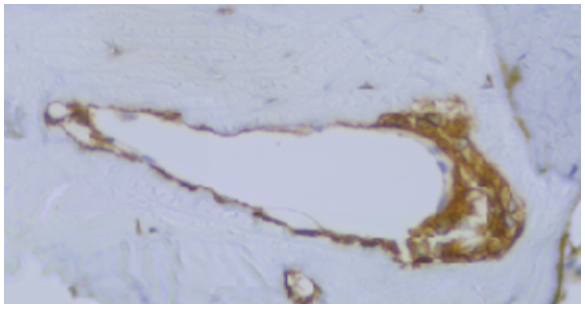

Figure 7.4.1 An example of CD-56 positive cells (brown)

7.4.2 Results

Analysis with samples organised into age categories (by decade) is summarised in Table 7.4.1. It is evident that there is a trend towards an inverse relationship between age and the density of CD-56 positive Osteoblasts. The application of the Mann-Whitney U test to these differences reveals significance is reached when comparing samples from the patients in their 40s with those in their 60s (p=0.01). Other comparisons between groups did not reach significance. It is worth noting that their 60's represents samples from an individual that is considered the control patient in this study.

Table 7.4.1 CD-56 cell density and age

Age	**CD-56 Positive Cell Density (cells/0.25mm^2)**	**Standard Deviation**
30s	265.795 (n=2)	135.775
40s	229.394 (n=2)	83.76
50s	98.636 (n=2)	72.639
60s	63.295 (n=1)	17.731

In order to establish how the process of disc degeneration affects the density of CD-56 staining Osteoblasts, analysis has been undertaken to categorise the samples according to the Pfirrmann classification of the adjacent disc. Table 7.4.2. displays the results of this comparison. The samples from the endplate adjacent to a non-degenerate disc have a significantly lower cell density than those representing the endplate adjacent to degenerate discs (p=0.02). Further analysis shows this is significant between those with no degeneration and those with Pfirrmann grade 4 (p=0.038) but not with grade 5 (p=0.067).

Table 7.4.2 CD-56 cell density and degeneration

Pfirrmann classification	**CD-56 Positive Cell Density (cells/0.25mm^2)**	**Standard Deviation**
1	63.295 (n=1)	17.731
4	240.625 (n=3)	114.618
5	198.561 (n=3)	112.223
4&5 Combined	219.735 (n=6)	110.387

Categorisation of the samples in accordance with the Modic type changes displayed at that endplate are displayed in Table 7.4.3. Those not displaying any Modic changes have a

significantly lower density of CD-56 positive Osteoblasts compared with samples from endplates displaying type 2 Modic changes (p=0.017) but not when compared to those with Modic type 1 (p=0.111). Comparison between those without changes and those with any kind of Modic change was again significant (p=0.008).

Table 7.4.3 CD-56 cell density and Modic changes

Modic type	CD-56 Positive Cell Density (cells/0.25mm^2)	Standard Deviation
0	97.597 (n=3)	97.676
1	340.227 (n=2)	40.819
2	218.052 (n=2)	82.142

7.4.3 Discussion

The CD-56 marker was initially found as a marker of nerve cells. In the bone the same adhesion molecule is involved in the adhesion of Osteoblasts to the surface of the bone. The Osteoblasts function to form new bone (when stimulated) but also to line the bone, preventing the action of Osteoclasts[55]. An increase in the number of Osteoblasts in a region of bone increases its potential for both bone formation but also the activation of Osteoclasts and bone resorption. A reduction in the number of bone lining cells may serve to increase the action of Osteoclasts and therefore bone resorption[55]. Local inflammation and the local release of inflammatory mediators from damaged cartilage[56,58] activate the RANKL pathway of Osteoclast activation and bone resorption. Ageing has been found to affect the number of viable cells within the bone and the number and thickness of the trabeculae and cortical bone[149]. Ageing in the spine has been studied by Boos[122] who found the endplate became disorganised by the age of 31. They found increasing abnormalities with microfractures, endplate lesions and subchondral sclerosis with advancing age.

My work demonstrates a decreasing trend in the mean CD-56 positive cell density with advancing age. This trend is to be expected given the previous work on ageing. This decrease in density can be explained by a reduction in the number of Osteoblasts within the bone, a reduction of the amount of bone (and therefore less cells) with increasing age and a reduction in bone formation (by Osteoblasts with increasing age. This has been discussed by Bosky[149] who noted a decrease in bone formation with every cycle of bone resorption after the age of peak bone mass.

The process of degeneration in my work leads to a significant increase in the CD-56 positive cell density (Osteoblasts). This is the reverse of the trend that we have seen in the analysis of ageing and is in keeping with previous work that ageing and degeneration are distinct processes. Of course, it is worth noting that the patient in the 'normal' aspect of this histological analysis is the oldest, so one might simply conclude that the trend is simply the reverse of this. A counterargument to this explains that in the analysis of ageing, while a trend was seen, there was not a significant difference between even the oldest and youngest age groups. In this analysis of degeneration, we see a significant increase in cell density with degeneration of Pfirrmann grade 4; grade 5 is not quite significant.

Given the previously discussed processes in degeneration, alteration of mechanical loads through the bone due to disc degeneration, microfracture and inflammation, we would expect that the remodelling and formation of new bone (and thus the number of Osteoblasts) would be increased. My results are in line with this expectation, supporting their validity.

Modic changes within degeneration represent processes thought to be due to mechanical stimulation, inflammation or possibly infection (as previously discussed). Alterations in the mechanical environment will lead to the formation of new bone and remodelling to compensate for these mechanical stresses. We know that inflammatory cytokines can affect the RANKL pathway, having action on Osteoblasts and Osteoclasts[56,58]. In addition to this, Perilli[74] demonstrated that the trabecular bone increased in thickness when Modic changes were present. This increase was more prominent in type 2 than type 1 and again in type 3 compared to type 2 changes. We would therefore expect to see an increase in Osteoblasts in the presence of Modic changes, and we might expect those with type 2 changes to have a higher number of Osteoblasts given the trabecular thickening that has been demonstrated. However, if we agree that type 1 Modic changes represent an active phase of the pathology behind Modic changes as described by Modic then type 1 Modic changes might have the higher Osteoblast density.

My results show that samples from those with Modic changes have a significantly higher CD-56 staining cell density at the endplate than those without Modic changes. Although those with Modic type 1 changes had a higher mean cell density, the relative rarity of type 1 samples in this cohort of samples means that significance was not reached when comparing against those with no Modic changes. Comparison of those with type 1 changes and those with type 2 changes did not show a significant difference between the two. The increase in cell density in those with Modic changes in comparison to those without is in line with the

expectations of increases secondary to the alteration of the mechanical environment, thickening of the bony structures associated with Modic pathology and the activation associated with the inflammatory process associated most strongly with type 1 changes. Of course, the presence of Osteoblasts alone does not necessarily indicate that these cells are active, but the work by Perilli et al.[74] would suggest they are.

7.5 CD-20

The CD-20 immunomarker binds to the CD-20 antigen which is present on the surface of B-cells until the point that they complete the final stage of maturation into plasma cells[204]. It is the biological target molecule of the monoclonal antibodies (such as rituximab). B-cells can be present in both acute and chronic inflammatory processes.

Anti-CD-20 therapies are routinely used in the treatment of inflammatory joint conditions[203]. Investigating the presence of CD-20 positive cells in the process of degeneration in the spine might therefore indicate underlying mechanisms contributing to degeneration but also potential therapeutic targets.

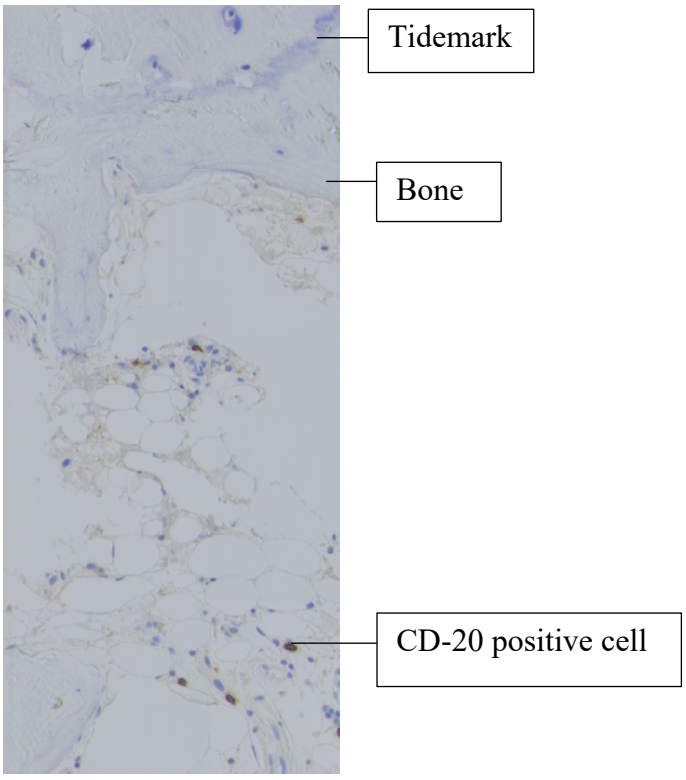

Figure 7.5.1 Histological slide displaying CD-20 positive cells.

7.5.1 Methods

The number of positively staining cells for each 4μm thick histology slide stained with a CD-20 immunomarker has been calculated using the histological image software Image J. To allow comparisons between samples, this count has been converted into a count per 0.25mm^2. The area of measurement has been defined as 500μm from the tidemark which includes the CCEP and the bony endplate.

7.5.2 Results

Categorising the samples into age groups (in decades) based upon the age at the time of sample collection of the individual from whom the sample originated did not reveal any trends in the cell density of CD-20 positive cells. The results are displayed in Table 7.5.1. The application of the Mann-Whitney U test to the data did not reveal any significant differences between the age categories.

Table 7.5.1 CD-20 cell density and age

Age	CD-20 Positive Cell Density (cells/0.25mm^2)	Standard Deviation
30s	7.464	6.972
40s	4.886	2.843
50s	3.281	2.843
60s	8.685	7.045

To consider the effect of the degeneration process on the density of CD-20 positive cells the Pfirrmann classification has been used to categorise the samples. The results of this comparison are seen in Table 7.5.2. There is no significant difference between the samples taken from the endplate of the degenerate or non-degenerate adjacent discs (p=0.446).

Table 7.5.2 CD-20 cell density and degeneration

Pfirrmann grade	CD-20 Positive Cell Density (cells/0.25mm^2)	Standard Deviation
1	8.6859 (n=1)	7.043
4	6.7769 (n=3)	5.603
5	4.1783 (n=3)	2.76130
4&5 combined	5.4776 (n=6)	4.425

Comparison of the CD-20 density/0.25mm^2 between the different types of Modic changes displayed at the endplate of the sample collection on the preoperative MRI is summarised in Table 7.5.3. While the mean CD-20 cell density/0.25mm^2 for those displaying type 1 Modic changes is double that for those without any such changes this does not reach statistical significance due to the variability of the results (p=0.333). The mean cell density falls with those displaying type 2 changes to less than half the value for those with type 1 changes, which does not reach statistical significance (p=0.111). It is not significantly different from those without Modic changes either (p=0.836). Comparison of those without Modic changes and those with any Modic change does not reach significance (p=0.918).

Table 7.5.3 CD-20 cell density and Modic changes

Modic Type	**CD-20 Positive Cell Density (cells/0.25mm^2)**	**Standard Deviation**
0	6.221 (n=3)	5.938
1	12.613(n=2)	5.998
2	4.529 (n=3)	2.762

7.5.3 Discussion

My results have shown no clear trend or any significant difference between the mean density of the CD-20 positive cells and the age of the participant at the time of sample collection. The number and function of B-cells has been shown to reduce with age but predominantly in those over the age of 65 years of age[205,206]. It may be that as the age range in the cohort in this analysis does not cross the threshold of 65 years of age that while ageing does affect the number and function of these CD-20 positive cells this effect cannot be detected between these younger age groups. The absolute number of cells may not correlate with the function of these immune cells that relay on activation by inflammatory cytokines[207].

B cells have little effect on the homeostasis of bone in normal situations; they do, however, contribute to the disruption in homeostasis seen in inflammation. Osteoblast lineage cells have been shown to influence the differentiation of B cells in response to stimulation from factors such as parathyroid hormone (PTH) via multiple cytokine pathways[207]. The RANKL pathway, that is well known to affect the homeostasis of bone by allowing the interaction of Osteoblasts with Osteoclasts, is also essential for the normal function of B cells[207]. We know that degeneration in the spine (as well as synovial joints) affects the structural and

mechanical properties of the bone and also involves a process of inflammation. We therefore expect the process of degeneration to involve B cells or affect their density at the endplate.

Adams[116] described the process of nucleus herniating through the endplate as a cause of localised inflammation and part of the degenerative process causing decompression of the disc. We might expect to see an increase in inflammatory B-cells in response to this stimulus in the degenerate disc.

My work has not shown any significant difference in the mean CD-20 positive cell density and the presence of degeneration of the disc. Inspection of the mean values does show a trend towards an inverse relationship between the number of CD-20 positive cells and the Pfirrmann classification of the adjacent disc. Due to the variation in the results at this sample size, no significance was seen and drawing conclusions is undertaken with caution. The reduction in CD-20 positive B cells that seems apparent in degeneration would suggest that the process of disc degeneration is not associated with a predominantly B-cell mediated inflammatory process (such as those seen in inflammatory arthropathies) and would not suggest that anti-CD-20 type therapies should hold particular promise in the treatment of disc degeneration that is not associated with a pre-existing inflammatory arthropathy.

Inflammation has been shown to be important in the pathological process behind Modic changes ever since Modic described them in 1988 [89,91]. Type 1 changes are considered to represent a process of active inflammation, while type 2 represent a process of fatty infiltration and fibrous tissue formation. Analysis of the CD-20 staining B-cells would be expected to show an increase in these inflammatory cells in type 1 Modic change with a fall when transitioning from type 1 to type 2.

My results show an increase in the mean CD-20 cell density when moving from those with no changes to those with type 1 Modic changes in the degenerate environment and a subsequent fall when transitioning from type 1 to type 2. The increase in B cells in those displaying type 1 Modic changes would indicate an increase in the inflammation surrounding the endplate and is in keeping with the prevailing knowledge underlying Modic changes. The subsequent decrease in those with type 2 changes remains in line with the hypothesis that type 2 changes represent a process of lessening of the inflammatory response[107,110]. Statistical analysis has not shown significance between these changes. The mean values do reflect the expected changes given the underlying knowledge surrounding Modic changes.

The high variability in the data suggests that larger samples sizes would be required to reach significance statistically.

Future work in this area might consider increasing the sample size to further analyse this change, using histological and chemical analysis to investigate the inflammatory mediators involved and perhaps give further indications of the stimulators underlying this process.

7.6 CD-3

The CD-3 marker is a unique marker of the T-Cell [208]. The T-cell is an essential part of the adaptive immune system. T cells can be subdivided into; CD-4 cells which serve to stimulate the maturation of B-cells as well as activating macrophages. CD-4 cells are activated by a complex of an antigen combined with a Major Histocompatibility Complex (MHC) II molecule on the surface of an antigen presenting cell[209]. CD-8 cells are derived from the same lineage as CD-4 cells but have a longer lifespan leading to the oft-used name of memory cells. T cells can only be activated fully when there is presentation of the MHC II and antigen complex and also the presence of pro-inflammatory mediators [210]. This is part of an acute response if the antigen is recognised (i.e., the T-cells have encountered the antigen before). In addition to mounting an acute inflammatory response, T-cell activation has been shown to be present in chronic immune responses (such as in Rheumatoid arthritis)[211]. Figure 7.6.1 is a histological slide illustrating the appearance of CD-3 positively stained cells.

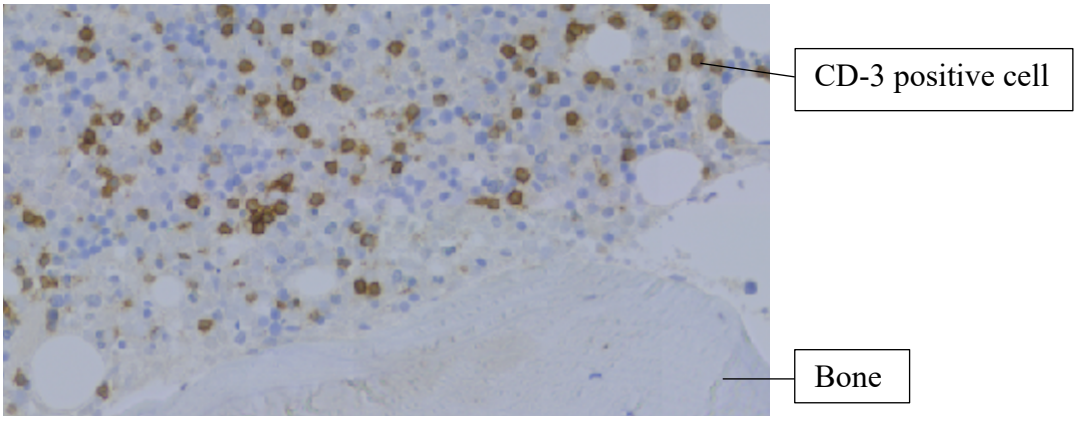

Figure 7.6.1 Histological slide of CD-3 positive cells

The aim of my work was to investigate (by assessing the overall number of CD-3 positive cells) if there might be a contribution to the process of degeneration at the lumbar spine endplate.

7.6.1 Methods

Histological slides were prepared using 4µm thick slices of decalcified and paraffin embedded tissue. Analysis has been undertaken to cover an area 500µm from the tidemark encompassing the CCEP and the bony endplate. To allow comparison of the results, the data have been converted to represent a standard unit of area of 0.25mm^2 giving a number of positively staining cells/0.25mm^2

7.6.2 Results

A comparison of the samples grouped by decade of life is given in Table 7.6.1. Statistical comparison between the decades of life does not reveal any differences that reach significance. There are no clear trends observed with this categorisation.

Table 7.6.1 CD-3 cell density and age.

Age	CD-3 Positive Cell Density (cells per 0.25mm^2)	Standard Deviation
30s	5.685 (n=2)	4.303
40s	2.323 (n=2)	2.301
50s	1.102 (n=2)	0.965
60s	3.256 (n=1)	2.162

Analysis of the CD-3 positive cell count based on the level of degeneration of the disc adjacent to the endplate from which the sample was taken is displayed in the Table 7.6.2. It is not possible to see any recognisable trends in this categorisation of the data. Analysis using the Mann-Whitney U test does not reveal any significant differences between the groups.

Table 7.6.2 CD-3 Cell density and degeneration

Pfirrmann classification	CD-3 Positive Cell Density (cells/0.25mm^2)	Standard Deviation	p-value Compared to Pfirrmann 1
1	3.256 (n=1)	6.696	
4	4.204 (n=3)	8.453	1
5	2.276 (n=3)	2.362	0.610
4&5 combined	3.240 (n=6)	3.317	0.770

The number of CD-3 staining T-cells per 0.25mm^2 categorised by the type of Modic change displayed on the pre-operative MRI scan is displayed in Table 7.6.3. It is evident that there is a noticeable increase in the T-cell density in those displaying type 1 Modic changes. This increase, when compared to those with no Modic changes almost reaches statistical significance (p=0.056). It again does quite not reach significance (p=0.056) when compared to those displaying type 2 Modic changes. There is no significant difference between those displaying no Modic changes and those displaying type 2 changes (p=0.620).

Table 7.6.3 CD-3 cell density and Modic changes

Modic type	CD-3 Positive Cell Density (cells/0.25mm^2)	Standard Deviation
0	2.759 (n=3)	2.036
1	9.118 (n=2)	0.082
2	2.275 (n=2)	2.219

7.6.3 Discussion

T-cells can only be activated fully when there is presentation of the MHC II and antigen complex and also the presence of pro-inflammatory mediators [210]. This is part of an acute response if the antigen is recognised (i.e., the T-cells have encountered the antigen before). In addition to mounting an acute inflammatory response, T-cell activation has been shown to be present in chronic immune responses (such as in Rheumatoid arthritis)[211].

My results do not show any significant differences between groups when considering the age of the participant at the time of sample collection. While there are some initial apparent differences in the mean values, the SD is significant, and in this sample set there is too much variation for any differences to be identified. Studies into the effect of ageing on T-cell populations have shown an overall reduction in T-cells with age[212]; therefore we might have expected to see an overall reduction in the CD-3 positive staining cells as age increases. With the high deviation between the results we would need to significantly increase the number of tested samples in order to expect to reach significance between these age groups. The alternative explanation is that there is no true difference in the number of T-cells at the endplate in these degenerate samples.

T-cells and the cytokines they release have been shown to affect the process of bone homeostasis by activating Osteoclasts, which increases bone resorption and therefore decreases bone density, a process which has been termed 'immunoporosis'[213]. This process is thought to be activated by a process of inflammation. The process has been evidenced to affect patients with osteoarthritis and rheumatoid arthritis as well as contributing to osteoporosis[213].

The degenerative process at the endplate has been established to represent a process of damage, microfracture and healing (which includes an inflammatory response)[129]. Work in

osteoarthritis in synovial joints has shown inflammatory modulation of bone remodelling to be a factor in subchondral sclerosis and a response to abnormal mechanical loading[158,159].

My results show no statistically significant differences between the presence of degeneration and the density of CD-3 positive staining cells (t-cells). The mean density of cells in those with Pfirrmann grade 4 changes was higher than those with type 1 changes at the adjacent disc but due to the high standard deviation in the results no significant difference has been found. Considering the previously published evidence, it was expected that the process of degeneration might be associated with an increase in the number of t-cells at the endplate. It is worth noting that the absolute number of cells does not inform us about the activity of those cells. It could be entirely possible that while the number of cells does not seem to change in the presence of degeneration the function of those cells that are present is altered with an increase in cytokine release and the effects on the bone that this may have. Perhaps an area for further investigation might be the assessment of the activity of the immunomodulating cells in degeneration to add further insight into the process of degeneration of the lumbar intervertebral disc.

My results have shown that the number of CD-3 positive T-cells at the endplate in degeneration is higher in those with type 1 Modic changes (9.118cells/0.25mm^2) than those without Modic changes (2.759) or those with type 2 Modic changes (2.275). This mean increase almost reached the threshold that we have set as significant (0.05) (and that is the accepted standard for biological and medical samples) for comparisons with Type 2 ($p=0.056$) and with no changes ($p=0.056$). Modic type 1 pathology has been associated with microfracture and inflammation ever since its initial description[91]. Type 2 Modic changes have been associated with a decrease in active inflammation and a process of fatty infiltration of the marrow of the bone. Perilli[74] has shown the effects of changes in the structure of the trabecular bone with Modic changes and alterations in the mechanical environment (including microfracture leading to inflammation) have been raised as a potential stimulator for this process of inflammation and bone remodelling. The increase that my work has shown in the density of T-cells present in type 1 Modic changes is in keeping with the trends of the previously published work and supports the existing body of work suggesting type 1 changes are associated with a process of inflammation while type 2 seem to represent resolution of this inflammatory stage.

8 Overall discussion and Future work

The nature of the surgical samples is one of the key novel aspects to this work. We know that it is possible for MRI signs of degeneration of the disc to be present in people without any symptoms. For this reason, the assessment of the degeneration process in cadaveric tissue that shows signs of degeneration may not correlate with the process that produces symptoms. The samples in this study have been collected specifically from people undergoing surgery for symptomatic spinal pathology in the lumbar spine. Such samples that include the endplate are unique to this work. In addition, the work includes analysis of two 'normal' human spines without MRI evidence of degenerate disease, enabling not only a characterisation of the changes seen in degeneration but also a comparison with non-degenerate individuals.

The work has included a study of the clinical implication of the biomechanical testing with a clinical study of interbody cage subsidence.

The mechanical testing of the endplate used in this study has also developed a unique method of nano-indentation testing of fresh bone. Indentation methods have traditionally been applied to dehydrated and embedded specimens. Pawlikowski[68] utilised a method of indentation of femoral trabecular bone that had not been embedded; his specimens had been dehydrated in a high concentration alcohol solution. During my work a method of indentation of fresh (thawed from frozen) vertebral trabecular bone has been developed. No other instances of this have been identified in the literature. This unique method of indentation was developed and trialled on ovine samples before transitioning on to the delicate and valuable human samples.

Previous studies have explored the effect of degeneration on the mechanical properties of the lumbar spine with methodologies using forces that will assess both the structural and the material properties. It was not the aim of this work to make a composite structural/material assessment of the vertebral body/endplate but rather to assess the material properties by using nano-scale indentations small enough that the structural properties will not contribute to the results in any meaningful way.

Given the constraints and difficulties of obtaining surgical samples from those with symptomatic pathology, the number of patients in this study is one of its strengths. Regarding the mechanical testing, the accuracy of the targeting of the indentation process and the low forces (and therefore small indentations) has allowed indentations to be undertaken in both

the endplate and the trabecular regions of the bone while maintaining the hydration of the samples. The number of indentations per sample is high and this has allowed testing to account for the biological variability seen with any bio composite material work. This has, in turn, been critical in the statistical analysis of the mechanical data.

Concurrent histological analysis of a representative selection of the surgical samples has added significantly to the work and furthered the understanding of the pathological processes that are present in symptomatic degeneration. Immunohistochemical staining has been applied to these unique surgical samples, allowing assessments of multiple aspects of the features of the symptomatic degenerate human lumbar spine endplate.

Mechanical testing has shown that the endplate and the trabecular bone display individual properties when exposed to this nano-indentation technique. The endplate has a lower elastic modulus and lower hardness value than the trabecular bone. This is an important finding given that the exact nature of the bone that forms the endplate has been unclear. Previous descriptions have included a continuation of the cortical shell of the vertebral body, a confluence of the trabeculae and a specialised plate of bone (such as that seen in other subchondral regions of bone). While this work does not have results for cortical bone for comparison (due to the nature of the samples), cortical bone has been shown to have a higher elastic modulus and hardness than trabecular bone in other work[50,67]. This study does not therefore support previous conclusions that the bony endplate represents either a confluence of trabecular bone or an extension of the cortical shell of the vertebral body. The results of mechanical testing would suggest that the bony endplate is most likely to represent a specialised region of subchondral bone which can be likened to that of other subchondral regions of bone (the knee for example[158]).

8.1 The effects of age

The analysis of the effects of age have been undertaken in order to answer 2 key questions:

1. Is ageing a separate process from degeneration?
2. Do the relative old and young ages of our control samples affect their comparability?

The control samples obtained during this study were difficult to obtain and as such highly valued in the experimentation process. This rarity means that acceptance (and acknowledgement) of the variation in their age representation has been necessary. One way to try to mitigate this is to explore the effect of age on the experimental results that have been

obtained. In addition to this it has been suggested (and there is some evidence) that ageing and degeneration are not the same process[33,122,214,215]. Analysis of the effect of ageing on the indentation modulus and hardness has shown significant increase in the hardness and elastic modulus of those in the younger cohorts of degenerate samples compared to those older than 50. As this is a comparison between patients that already have degeneration, we can surmise that ageing within degeneration does produce a separate effect to degeneration alone. This indicates that ageing and degeneration do represent separate processes.

Histologically, ageing within degeneration increased the mean thickness of the CCEP (calcified cartilaginous endplate) and decreased the number of CD-56 staining Osteoblasts, a trend towards a non-significant decrease in the number of erosions at the endplate, In addition, CD-20 staining B-cells and CD-3 staining T-cells were also seen. This demonstrates that within degeneration ageing has a separate additional effect on these parameters.

The different ages of the 'normal' samples in this work (29 and 62 years) lie at either end of the spectrum of ages represented by the degenerate samples. Although, from a mechanical analysis point of view, we have shown that ageing does affect our results. The representation from both the older and younger age group should allow the application of a comparison between the overall values represented by the two control samples.

Histological analysis has shown some effect of ageing within degeneration. We see that the trends seen in increasing age within the degenerate samples are disrupted when the non-degenerate samples are included in CD-3 (T-cell) analysis, CD-20 (B-cell) analysis and thickness of the CEEP. Interestingly this is not the case when considering the number of erosions seen at the endplate and the CD-56 staining Osteoblasts. Perhaps this indicated that ageing and degeneration have similar effects on Osteoblasts and erosions at the endplate but not the other histological measurements.

8.2 The effect of degeneration

The analysis of the effect of degeneration on the mechanical properties (as determined by nano-indentation) has shown that in degeneration both the endplate and the underlying trabecular bone display a higher elastic modulus. The trabecular bone (but not the endplate) also shows an increased hardness. The potential explanations for these changes are discussed in section 5.4.

Histological analysis showed the thickness of calcification at the endplate to increase in severe degeneration (Pfirrmann grade 5). In the degenerate endplate, it was noted that the variability of the endplate is increased in degeneration as is the number of erosions affecting the endplate. The two of these measurements would logically be linked and seeing changes in both measurements is therefore to be expected. Application of the mechanical testing results might indicate that this variation is due to changes in the mechanical environment, altering the material properties of the bone (in response to the applied forces) but also creating microfractures and damage to the endplate which decreases its uniformity.

The vascularity of the endplate increases in the presence of degeneration. This work noted a significant increase in the density of vascular channels at the endplate in those with degeneration, perhaps a biological attempt at increasing the nutrition to the disc in response to the increased calcification of the endplate or simply an effect of the healing and remodelling process taking place as a result of the challenging mechanical environment. While the number of vessels is not the sole consideration in perfusion it may give some indication of perfusion potential which is going to be important when considering regenerative therapies as a future method of treatment, indicating the importance of these findings.

Further histological analysis in degeneration showed a significant increase in Osteoblasts in the region of the endplate. The most likely explanation for this is an increase in the new bone formation that we know occurs in response to the mechanical loads placed on bone. Degeneration of the disc increases the transmission of force to the endplate and (according to Wolff's law [66]) subsequent remodelling of the bone to be able to withstand such forces.

In degeneration it was not possible to find a difference in the density of CD-3 staining T-cell populations at the endplate or the density of CD-20 positive B-cells. While the variation was high between these groups (and therefore a larger sample analysis might be able to show some differences) the results suggest that the process of degeneration does not involve these cell lines in a significantly detectable way.

8.3 The effect of Modic changes

The pathology represented by the MRI changes originally described by Modic remains of unclear aetiology and may represent more than one pathological process[110,216,217]. A table summarising the overall findings of this work in relation to Modic changes is available in Table 8.3.1.

Table 8.3.1 Overall findings with regard Modic changes

Modic Changes	0	1	2	3
Hardness (EP) (GPa)	0.141	0.162	0.168	0.120
Hardness (TB) (GPa)	0.158	0.181	0.181	0.103
Modulus (EP) (GPa)	4.368	4.903	5.156	2.645
Modulus (TB) (GPa)	5.002	5.652	5.572	2.172
Subsidence	19.3%	35.3%	51.9%	0%
CD 3 (cells/0.25mm^2)	2.759	9.118	2.275	
CD 20 (Cells/0.25mm^2)	6.221	12.613	4.529	
CD 31 (No./0.25mm^2)	5.740	12.354	11.096	
CD 56 (cells/0.25mm^2)	97.597	340.227	218.052	
CCEP thickness (µm)	84.14	40.31	104.76	
Erosions (Per mm)	0.632	1.003	1.163	

8.3.1 Type 1 Modic changes

The material properties of the endplate in the samples from individuals with type 1 Modic changes had an increased elastic modulus compared to those without Modic changes. Modic type 1 changes were also associated with a higher indentation modulus in the underlying trabecular bone. We might expect the trabecular bone to show similar effects to the endplate, as Modic changes affect the region of trabecular bone adjacent to the endplate. The hardness of the endplate was again increased compared to those without Modic changes, but this was not the case in the trabecular bone.

Histological analysis of the samples from those with type 1 Modic changes showed a non-significant decrease in the thickness of the CCEP. The variability of the endplate and the number of erosions did not show any significant variations in those with type 1 Modic changes. This important lack of variation might be due to the high variability of the measurements but could also indicate that the pathology seen in those with type 1 changes does not significantly alter the endplate above the boundary between the BEP (bony endplate) and CCEP.

Further histological analysis did not demonstrate significant difference in the vascular density of those with type 1 Modic changes (despite a noticeable increase in the mean) or the density of CD-20 positive B cells. It also did not demonstrate a significant difference in CD-3 positive T-cells (although the p-value was close to reaching significance). Inflammation has been postulated as a predominant feature of Modic pathology hypothesis after the initial publication in 1988[91], and therefore it would be expected that cells involved in the inflammatory response (such as B-cells) would be expected to increase in those displaying type 1 Modic changes. The noticeable increases in the mean values for these inflammatory cells did not reach significance, however. The variability of the measurements between samples was high in this work and, coupled with the restriction in sample numbers, this goes some of the way to explaining the failure to reach statistical significance.

8.3.2 Type 2 Modic changes

Similar to those with type 1 Modic changes, type 2 changes were found to be associated with an increase in the elastic modulus and hardness at the endplate and the trabecular bone, with no significant differences between type 1 and type 2 samples. This similarity is in line with the predominant hypothesis that type 1 and type 2 changes represent different stages of the same pathological process and can be interchangeable[94,110,217].

Histological analysis showed Modic type 2 changes were associated with a significant increase in CD-56 staining cells (Osteoblasts) ($p=0.017$). Considering this alongside the mechanical testing, it seems that this represents an increased period of bone turnover and deposition, which is in keeping with the previous work by Pawlikowski[68] who found that the trabecular thickness increases in those with Modic pathology.

The variability of the endplate tidemark was found to be significantly increased in those with type 2 Modic changes. This is accompanied by an increase in the number of erosions that did not quite reach significance ($p=0.051$). The process of type 2 Modic changes would appear to

affect the endplate structure to a greater extent than type 1 changes; this may simply represent a more established continuation of the same pathology (as per the original Modic paper[91]). Further histological analysis did show a non-significant (p=0.073) increase in the vascularity at the endplate but did not show any difference in the number of CD-3 positive T-cells or CD-20 positive B-cells, suggesting that inflammation plays less of a role in type 2 Modic changes, which is again in line with the accepted previous published work[91,110,217].

8.3.3 Type 3 Modic changes

Only one individual is represented in the analysis of type 3 changes due to the lower prevalence of type 3 changes in the population. Analysis of the MRI from this patient shows that while the predominant changes present are those of type 3 changes there is a small focus of type 2 changes anteriorly in the inferior endplate of L5. The analysis of the samples has been undertaken according to the predominant Modic pathology seen, and therefore they have been treated as type 3 changes. We do not have other Modic type 3 pathology with which to compare but we can compare with the type 2 changes. The type 2 changes are significantly different than this type 3 specimen.

Mechanical testing of the samples from the patient with type 3 Modic changes on their MRI showed a significantly decreased indentation modulus and hardness when compared to those without Modic changes and those with either type 1 or type 2 changes. Previous work investigating the effect of Modic changes on the material properties of the bone is limited. Liu[45] found that the presence of Modic changes of any type decreased the stiffness and hardness of the composite cartilaginous and bony endplate that they were testing on a micro (rather than nano) scale. Comparisons between my results and the results of other testing are limited, however, due to the nature of the specimens, the novel fresh, hydrated and not embedded indentation preparation and the small indentation scales. Interestingly, the findings are in keeping with those found in other subchondral bone sclerosis. The results of my work would support the findings of thickening of the bone with a process of sclerosis.

Correlation of the mechanical testing results with a clinical study analysing the rate of lumbar interbody cage subsidence on post-operative radiological imaging shows a significant increase in radiological subsidence in those with type 2 Modic changes and a very near significant increase in subsidence in those with type 1 Modic pathology. Both type 1 and type 2 Modic changes were found to be associated with an increase in the elastic modulus of the endplate and trabecular bone as well as an increase in hardness at the endplate (and trabecular

bone for those with type 2 changes). One might expect stiffer harder bone to be associated with a decrease in the rate of interbody cage subsidence; however, this was not the case in my work. The potential explanation for this is that the increased stiffness and hardness represent a decrease in the ability of the bone to adapt to the force applied, potentially representing a complex process of embrittlement. Although this mechanical testing did not load to failure and therefore did not measure the yield point and ultimate strength, a process of embrittlement would explain a decrease in the ability of the material to withstand forces applied and decrease the load to failure.

The trabecular bone is a complex 3-dimensional structure; there will be factors contributing to the overall mechanical properties in addition to the material properties of the bone or even the thickness of the trabeculae. For example, the orientation and the position of each individual trabeculae will interplay to contribute to the overall ability to adapt to load. Increasing the stiffness and hardness of the bone will alter this complex interrelationship and affect the ability of the bone to maintain integrity. A stiffer and harder trabecula will deform less with an applied force. This change in deformity characteristics will alter the way the force is transmitted from one part of the bone to another. One theory is that less deformity does not allow the 'recruitment' of the adjacent trabeculae and a sharing of the applied force. Once the level of deformation occurs such that adjacent bone units are recruited, the force applied will be higher and therefore closer to the failure (or yield) point of the bone. The bones adaptability has decreased, and the force applied becomes concentrated in localised regions leading to microfracture propagation and eventual failure. This concentration in localised force explains the process of trabecular thickening seen in degeneration and Modic changes by Perilli[74,218] with the application of Wolff's Law, which states the bone remodels according to the nature of the forces applied to it[66].

8.4 Limitations of this work

As has already been discussed, the nature of these surgical samples is both a strength and a limitation of this work. While it has been possible to perform a large number of measurements on each sample, the total number of individuals represented (especially with the less common pathology types) is small. Other pieces of work on such samples have encountered similar issues and a process of collaboration here with 2 specialist spine centres has allowed the sample numbers seen here to be collected. Further widening of this collaboration and a longer collection window could improve these numbers further.

Histological analysis has been undertaken on a representative selection of the surgical samples to provide an insight into the underlying processes investigated. Broadening the histological analysis was beyond the resource and scope of this work. A new nano-indentation sample preparation method has been developed and utilised; this is a strength of the work but limits its applicability and comparability with other pieces of work. The published body of work on vertebral (or bone in general) indentation does, however, include a wide variation of techniques. As novel techniques are developed to more accurately reflect the natural state of the tested tissue, the published literature methodology evolves. The novel methods used here represent a state of the bone as close to that of fresh bone as was possible to recreate. While this is not directly comparable with existing methodologies, it is a useful technique for future applications.

The 'normal' comparison samples included are both limited in number and have some variations from the diseased cohort. They lie at either end of the spectrum of ages for this work which is why age analysis was key to understanding the potential impacts of this. Additionally, they are both female, something which was unavoidable but is to be taken into consideration. The cadaveric spine had a limited medical history available and while this did not include any reference to back pain other co-morbidities existed; the effect of these on the results here is not known. The surgical control subject was having intervention for global malalignment of the spine. While the levels from which these samples were taken did not have any signs of radiological degeneration it is unknown if there are changes in mechanical loading due to the deformity that may affect the results of this work. Regardless of this they are the best available comparisons for this work.

8.5 Direction of future work

A number of potential avenues of research have arisen as a result of this research project and the evolution of the work on these unique samples, together with the ongoing collection of new samples, offers opportunities for future projects.

Mechanical load to failure testing was not undertaken on this occasion mainly due to the destructive nature of such testing and the value of the samples. This deliberate methodological decision was taken to enable the histological analysis of the exact same surgical samples and therefore direct correlation between the two methods. Load to failure testing may, however, aid the understanding of the total energy absorbed by the bone and

further the understanding of the failure mechanisms and how these change in degeneration/Modic changes.

The next logical stage of mechanical/material testing is to apply the nano-indentation material properties to the macrostructural architecture, perhaps through modelling. A thorough analysis of this architecture would need to be undertaken for samples specific to symptomatic degeneration in order for this modelling to be as accurate as possible. It should take into account the complex interplay of the trabecular structure which may in itself need further investigation, as much work on the trabeculae has been undertaken in isolation.

Material analysis of the nanostructure of the bone composition in the different stages of degeneration and Modic pathology would greatly increase the understanding of the processes involved in material level changes affecting the mechanical properties. This would include the collagen alignment, collagen crosslinking, mineralisation of the bone and the orientation and size of the inorganic crystals within the bone.

It has not been possible to accurately quantify the orientation of the osteons within the complex 3-dimensional structure of the endplate with our 2-dimensional histological analysis. This is due to a combination of limited sample physical size and further difficulty recording exact anatomical orientation with a spherical trephine sample. Further work in the analysis of the bony endplate might include analysis of this element of the unique structure of this specialised area of bone.

Histological analysis has given some valuable information in the journey to understanding the process of degeneration and how the perfusion and inflammatory cells change at the endplate with this process. Further work would need to include histological analysis of type 3 Modic changes as well as increasing the analysis of the number of samples in each cohort, including non-degenerate groups. Regarding perfusion, a sequential histological sectioning technique with vascular staining would allow the formulation of a 3-dimensional model of the vascular channels and their morphology. To better understand how this relates to the perfusion of the disc, perfusion analysis techniques in conjunction with this histology may hold answers that aid the understanding of nutrition to the degenerate disc and help to develop cell regeneration/restorative therapies.

Application of these techniques to other levels of the spine may help to further the understanding of degeneration and how it changes throughout the spine, while also increasing the sample numbers. The disc is not an isolated anatomical structure; it forms part of the

‘functional spinal unit’. This includes the facet joints at the posterior aspect of the spinal column, and a complete understanding of the process of spine degeneration will need to incorporate and account for degeneration of these synovial joints.

Alongside this work micro-CT techniques have been employed to analyse these samples further. This analysis has been undertaken by another PhD student within the laboratory and a unifying application of results from mechanical/histological and these architectural data is a planned avenue of future work.

9 Glossary & Abbreviations

AFM	Atomic force microscopy. A high-resolution surface scanning technique in which a small-scale probe scans a material producing an image of the surface.
ALIF	Anterior lumbar interbody fusion.
ALP	Alkaline phosphatase. An enzyme associated with bone metabolism also associated with liver function.
BEP	Bony endplate.
CCEP	Calcified cartilaginous endplate.
CEP	Cartilaginous endplate.
CGRP	Calcitonin gene-related peptide. A cell signalling molecule produced by nerve cells involved in vasodilation and nociception.
CRP	C-reactive protein. A protein measured in the blood which is produced by the liver as part of the acute response to inflammation.
CT	Computed tomography. An imaging technique utilising an X-ray source and detector rotating around an object to measure absorption and construct an image of the structure.
Degenerate disc disease (DDD)	A degenerative phenomenon involving the intervertebral disc of the spine.

DEXA	Dual energy X-ray absorptiometry. The application of a technique to use X-ray absorption to measure the density of bone.
Discography	A process of injecting contrast directly into an intervertebral disc to provide information about its degeneration.
EP	Endplate. The structure between the vertebral bone and the disc consisting of cartilaginous, calcified cartilage and bone layers.
Functional spinal unit	One working section of the spine, including the intervertebral disc, vertebral bodies and facet joints at that level.
G	Giga. A unit of measurement indicating $x10^9$.
H&E	Haematoxylin and Eosin. A method of histological slide staining that is widely used to assess tissues.
Hardness	The ability of a material to resist plastic deformation in response to an applied force.
IL-1	Interleukin 1. A group of cell signalling molecules that play a role in inflammation
Immunohistology	The method of applying specific immunological markers to histological slides to highlight structures of interest.
Lumbar interbody fusion	The placement of a device (or cage) in the space between adjacent vertebral bodies after removal of the

	intervertebral disc to promote fusion while maintaining or restoring mechanical alignment.
m	milli. A unit of measurement indicating $x10^{-3}$.
Micro-indentation	A method of measuring hardness and elastic modulus of a material by applying a force through an indentation tip of micrometre scale and measuring the response.
Micro-CT	Micrometre scale computed tomography.
Modic changes	Signal changes seen adjacent to the intervertebral disc in the spine on MRI.
MRI	Magnetic resonance imaging. A method of imaging using a magnetic field and radiofrequency pulse to alter the phase of water molecules within a tissue and produce a measurable signal.
n	nano. A unit of measurement indicating $x10^{-9}$.
N	Newton. A measure of applied force.
Nano-indentation	A method of measuring the hardness and elastic modulus of a material by applying a measured force through an indentation tip of nanometre scale and measuring the response.
Neoinnervation	a process of new nerve formation or growth within a tissue.
Neovascularisation	a process of new blood vessel formation or growth within a tissue.

NGF	Nerve growth factor. A protein involved in the signalling pathways involved in nerve cell growth.
NHS	National Health Service
NPY	Neuropeptide Y. A cell signalling molecule involved in the central nervous system. Functions include vasoconstriction and promotion fat growth.
Paraboloid of revolution	A shape with one axis of symmetry and no centre of symmetry.
Pa	Pascal. A unit of measurement defined as 1 Newton per square metre of area.
PGP 9.5	Protein gene product 9.5. A protein expressed by nerve cells.
Physiological load	The load and forces applied to an anatomical structure in normal conditions of functioning.
Pfirrmann classification	A radiological classification of intervertebral disc degeneration.
PTH	Parathyroid hormone. A protein secreted by the parathyroid glands.
Raman Spectroscopy	A method of determining molecular structure utilising photon scatter from the application of a laser.
RANK	A surface receptor found on the surface of cells (with reference to this work, osteoblasts specifically).

RANKL	Receptor activator of nuclear factor kappa. This binds to the RANK receptor.
SD	Standard deviation.
Stiffness	The ability of a material to resist elastic deformation in response to an applied force.
Strain	A material measurement of the deformation of a material structure with an applied force as a percentage of its original length.
Strength	The measure of a material's ability to withstand force without plastic deformation or failure.
Stress	A material measurement of the force per unit area applied to a material.
TB	Trabecular bone. A subtype of bone based on its structure.
TLIF	Transforaminal lumbar interbody fusion.
TNF	Tumour necrosis factor. A cell signalling protein which is known to be involved in the process of inflammation.
VEGF	Vascular endothelial growth factor. A signalling molecule involved in the proliferation of new blood vessels.
Volkmann's canals	Nutrient channels within the structure of bone.
Wolff's law	A principle stating that bone will adapt to the loads which are placed on it.

XLIF	Extreme lateral lumbar interbody fusion.
Young's Modulus of Elasticity	A measurement of the elastic properties of a material calculated from the measurement of stress and strain.
μ	micro. A unit of measurement indicating $x10^{-6}$.

10 References

1. Deyo RA, Cherkin D, Conrad D, Volinn E. Cost, Controversy, Crisis: Low Back Pain and the Health of the Public. Annual Review of Public Health. 1991;12:141–56.

2. Dionne CE, Dunn KM, Croft PR. Does back pain prevalence really decrease with increasing age? A systematic review. Age and Ageing. 2006;35(3):229–34.

3. Wynne-Jones G, Cowen J, Jordan JL, Uthman O, Main CJ, Glozier N, et al. Absence from work and return to work in people with back pain: a systematic review and meta-analysis. Occupational and Environmental Medicine. 2014;71(6):448–56.

4. Bevan PS. The Impact of Back Pain on Sickness Absence in Europe. The Work Foundation 2012.

5. Cheung KMC, Karppinen J, Chan D, Ho DWH, Song Y-Q, Sham P, et al. Prevalence and pattern of lumbar magnetic resonance imaging changes in a population study of one thousand forty-three individuals. Spine. 2009;34(9):934–40.

6. O'Sullivan PB, Caneiro JP, O'Keeffe M, Smith A, Dankaerts W, Fersum K, et al. Cognitive Functional Therapy: An Integrated Behavioral Approach for the Targeted Management of Disabling Low Back Pain. Physical Therapy. 2018;98(5):408–23.

7. O'Sullivan P, Caneiro JP, O'Keeffe M, O'Sullivan K. Unraveling the Complexity of Low Back Pain. Journal of Orthopaedic & Sports Physical Therapy. 2016;46(11):932–7.

8. White AA, Panjabi M. Clinical Biomechanics of the Spine (2nd rev. edn.) Philadelphia: Lippincott Williams and Wilkins; 1990.

9. NHS. Clinical commissioning policy statement; spinal surgery for non-specific chronic low back pain. December 2012 Reference NHSCB/D14/a [Internet]. 2012 [cited]. Available from: https://www.engage.england.nhs.uk/consultation/ssc-area-d/supporting_documents/d14astatement.pdf

10. Noshchenko A, Hoffecker L, Lindley EM, Burger EL, Cain CMJ, Patel VV. Long-term Treatment Effects of Lumbar Arthrodeses in Degenerative Disk Disease: A Systematic Review With Meta-Analysis. Journal of Spinal Disorders & Techniques. 2015;28(9):E493-E521.

11. Phillips FM, Slosar PJ, Youssef JA, Andersson G, Papatheofanis F. Lumbar spine fusion for chronic low back pain due to degenerative disc disease: a systematic review. Spine. 2013;38(7):E409-E422.

12. Hou Y, Luo Z. A study on the structural properties of the lumbar endplate: histological structure, the effect of bone density, and spinal level. Spine. 2009;34(12):E427-E433.

13. Hou Y, Yuan W. Influences of disc degeneration and bone mineral density on the structural properties of lumbar end plates. The Spine Journal. 2012;12(3):249–56.

14. Schwab F, Lafage V, Patel A, Farcy J-P. Sagittal plane considerations and the pelvis in the adult patient. Spine. 2009;34(17):1828–33.

15. Taher F, Essig D, Lebl DR, Hughes AP, Sama AA, Cammisa FP, et al. Lumbar Degenerative Disc Disease: Current and Future Concepts of Diagnosis and Management. Advances in Orthopedics [Internet]. 2012:970752–7

16. Iatridis JC, Kang J, Kandel R, Risbud MV. New Horizons in Spine Research: Intervertebral Disc Repair and Regeneration. Journal of Orthopaedic Research. 2017;35(1):5–7.

17. Tendulkar G, Chen T, Ehnert S, Kaps H-P, Nüssler AK. Intervertebral Disc Nucleus Repair: Hype or Hope? International Journal of Molecular Sciences. 2019;20(15):3622.

18. Lotz JC, Fields AJ, Liebenberg EC. The role of the vertebral end plate in low back pain. Global Spine Journal. 2013;3(3):153–63.

19. Adams MA, Roughley PJ. What is intervertebral disc degeneration, and what causes it? Spine. 2006;31(18):2151–61.

20. Holm S, Maroudas A, Urban JP, Selstam G, Nachemson A. Nutrition of the intervertebral disc: solute transport and metabolism. Connective Tissue Research. 1981;8(2):101–19.

21. Wu Y, Cisewski S, Sachs BL, Yao H. Effect of cartilage endplate on cell based disc regeneration: a finite element analysis. Molecular & Cellular Biomechanics : MCB. 2013;10(2):159–82.

22. Nachemson A, Lewin T, Maroudas A, Freeman MA. In vitro diffusion of DYE through the end-plates and the annulus fibrosus of human lumbar inter-vertebral discs. Acta Orthopaedica Scandinavica. 1970;41(6):589–607.

23. Rodriguez AG, Rodriguez-Soto AE, Burghardt AJ, Berven S, Majumdar S, Lotz JC. Morphology of the human vertebral endplate. Journal of Orthopaedic Research. 2012;30(2):280–7.

24. Malandrino A, Lacroix D, Hellmich C, Ito K, Ferguson SJ, Noailly J. The Role of Endplate Poromechanical Properties on the Nutrient Availability in the Intervertebral Disc. Osteoarthritis and Cartilage. 2014;22(7):1053–60.

25. Le Maitre CL, Binch AL, Thorpe AA, Hughes SP. Degeneration of the intervertebral disc with new approaches for treating low back pain. Journal of Neurosurgical Sciences. 2015;59(1):47–61.

26. Smith LJ, Nerurkar NL, Choi K-S, Harfe BD, Elliott DM. Degeneration and regeneration of the intervertebral disc: lessons from development. Disease Models & Mechanisms. 2011;4(1):31–41.

27. Johnson EF, Chetty K, Moore IM, Stewart A, Jones W. The distribution and arrangement of elastic fibres in the intervertebral disc of the adult human. Journal of Anatomy. 1982;135(Pt 2):301–9.

28. Vo NV, Hartman RA, Patil PR, Risbud MV, Kletsas D, Iatridis JC, et al. Molecular Mechanisms of Biological Aging in Intervertebral Discs. Journal of Orthopaedic Research. 2016;34(8):1289–306.

29. García-Cosamalón J, del Valle ME, Calavia MG, García-Suárez O, López-Muñiz A, Otero J, et al. Intervertebral disc, sensory nerves and neurotrophins: who is who in discogenic pain? Journal of Anatomy. 2010;217(1):1–15.

30. Peng B, Wu W, Hou S, Li P, Zhang C, Yang Y. The pathogenesis of discogenic low back pain. Journal of Bone and Joint Surgery. British volume. 2005;87(1):62–7.

31. Stone MA, Williams F, Wolber L, Karppinen J, Maatta J. Twins UK heritability study of candidate low back pain phenotype shows vertebral endplate abnormalities to be heritable. Rheumatology. 2013;52:64–5.

32. Battié MC, Videman T, Levälahti E, Gill K, Kaprio J. Genetic and environmental effects on disc degeneration by phenotype and spinal level: a multivariate twin study. Spine. 2008;33(25):2801–8.

33. Massey CJ, van Donkelaar CC, Vresilovic E, Zavaliangos A, Marcolongo M. Effects of aging and degeneration on the human intervertebral disc during the diurnal cycle: a finite element study. Journal of Orthopaedic Research. 2012;30(1):122–8.

34. Le Maitre CL, Pockert A, Buttle DJ, Freemont AJ, Hoyland JA. Matrix synthesis and degradation in human intervertebral disc degeneration. Biochemical Society Transactions. 2007;35(Pt 4):652–5.

35. Phillips KLE, Jordan-Mahy N, Nicklin MJH, Le Maitre CL. Interleukin-1 receptor antagonist deficient mice provide insights into pathogenesis of human intervertebral disc degeneration. Annals of Rheumatic Diseases. 2013;72(11):1860–7.

36. Ishihara H, McNally DS, Urban JP, Hall AC. Effects of hydrostatic pressure on matrix synthesis in different regions of the intervertebral disk. Journal of Applied Physiology. 1996;80(3):839–46.

37. Rodrigues SA, Thambyah A, Broom ND. A multiscale structural investigation of the annulus-endplate anchorage system and its mechanisms of failure. The Spine Journal. 2014;14(11 SUPPL. 1):S39–S40.

38. Hadjipavlou AG, Tzermiadianos MN, Bogduk N, Zindrick MR. The pathophysiology of disc degeneration: a critical review. The Journal of Bone and Joint Surgery. British volume. 2008;90(10):1261–70.

39. Schmorl G. Über die an den Wirbelbandscheiben vorkommenden ausdehnungs–und zerreisungsvorgange und die dadurch an ihnen und der wirbelspongiosa hervorgerufenen veranderungen. Verhandlungen der Deutschen Pathologischen Gesellschaft. 1927;(22):250–62.

40. Schmorl G, Junghanns H. Schmorl: The human spine in health and disease. Trans. Besemann EF. (2nd American edn.) New York: Grune and Stratton; 1971.

41. Kyere KA, Than KD, Wang AC, Rahman SU, Valdivia–Valdivia JM, La Marca F, et al. Schmorl's nodes. European Spine Journal. 2012;21(11):2115–21.

42. Roberts S, Menage J, Urban JPG. Biochemical and structural properties of the cartilage end-plate and its relation to the intervertebral disc. Spine. 1989;14(2):166–74.

43. Bernick S, Cailliet R. Vertebral end-plate changes with aging of human vertebrae. Spine. 1982;7(2):97–102.

44. DeLucca JF, Cortes DH, Jacobs NT, Vresilovic EJ, Duncan RL, Elliott DM. Human cartilage endplate permeability varies with degeneration and intervertebral disc site. Journal of Biomechanics. 2016;49(4):550–7.

45. Liu J, Hao L, Suyou L, Shan Z, Maiwulanjiang M, Li S, et al. Biomechanical properties of lumbar endplates and their correlation with MRI findings of lumbar degeneration. Journal of Biomechanics. 2016;49(4):586–93.

46. Tosun O, Fidan F, Erdil F, Tosun A, Karaoğlanoğlu M, Ardıçoğlu O. Assessment of lumbar vertebrae morphology by magnetic resonance imaging in osteoporosis. Skeletal Radiology. 2012;41(12):1583–90.

47. Wang Y. The roles of vertebra and vertebral endplate in lumbar disc degeneration [doctoral]. 2012 University of Alberta.

48. Feng X. Chemical and Biochemical Basis of Cell-Bone Matrix Interaction in Health and Disease. Current Chemical Biology. 2009;3(2):189–96.

49. Bromage TG, Goldman HM, McFarlin SC, Warshaw J, Boyde A, Riggs CM. Circularly polarized light standards for investigations of collagen fiber orientation in bone. The Anatomical Record Part B: The New Anatomist 2003;274B(1):157–68.

50. Rho J-Y, Roy ME, Tsui TY, Pharr GM. Elastic properties of microstructural components of human bone tissue as measured by nanoindentation. Journal of Biomedical Materials Research. 1999;45(1):48–54.

51. Jirousek O. Nanoindentation of Human Trabecular Bone – Tissue Mechanical Properties Compared to Standard Engineering Test Methods. In: Nemecek J, ed. Nanoindentation in Materials Science [Internet]. InTech; 2012 [cited 10 August 2018].

52. Parfitt AM. Bone-forming cells in clinical conditions. In: Hall BK ed. Bone, Vol 1: The Osteoblast and Osteocyte. Boca Raton, FL: Telford Press; 1990:351–429.

53. Capulli M, Paone R, Rucci N. Osteoblast and osteocyte: Games without frontiers. Archives of Biochemistry and Biophysics. 2014;561:3–12.

54. Florencio-Silva R, Sasso GR da S, Sasso-Cerri E, Simões MJ, Cerri PS. Biology of Bone Tissue: Structure, Function, and Factors That Influence Bone Cells. BioMed Research International. 2015:421746.

55. Del Fattore A, Teti A. The Tight Relationship Between Osteoclasts and the Immune System [Internet]. Inflammation & Allergy - Drug Targets (Discontinued). 2012;11(3):181–7 [cited 12 March 2020].

56. Boyce BF. Advances in the regulation of osteoclasts and osteoclast functions. Journal of Dental Research. 2013;92(10):860–7.

57. Pacios S, Xiao W, Mattos M, Lim J, Tarapore RS, Alsadun S, et al. Osteoblast Lineage Cells Play an Essential Role in Periodontal Bone Loss Through Activation of Nuclear Factor-Kappa B. Scientific Reports. 2015;5(1):16694.

58. Bertuglia A, Lacourt M, Girard C, Beauchamp G, Richard H, Laverty S. Osteoclasts are recruited to the subchondral bone in naturally occurring post-traumatic equine carpal osteoarthritis and may contribute to cartilage degradation. Osteoarthritis and Cartilage. 2016;24(3):555–66.

59. Bobinac D, Spanjol J, Zoricic S, Maric I. Changes in articular cartilage and subchondral bone histomorphometry in osteoarthritic knee joints in humans. Bone 2003;32(3):284–90.

60. Bellido M, Lugo L, Roman-Blas JA, Castañeda S, Caeiro JR, Dapia S, et al. Subchondral bone microstructural damage by increased remodelling aggravates experimental osteoarthritis preceded by osteoporosis. Arthritis Research & Therapy 2010;12(4):R152.

61. Martel-Pelletier J, Barr AJ, Cicuttini FM, Conaghan PG, Cooper C, Goldring MB, et al. Osteoarthritis. Nature Reviews Disease Primers. 2016;2:16072.

62. Jarvik JG, Hollingworth W, Heagerty PJ, Haynor DR, Boyko EJ, Deyo RA. Three-Year Incidence of Low Back Pain in an Initially Asymptomatic Cohort: Clinical and Imaging Risk Factors. Spine. 2005;30(13):1541–8.

63. Livshits G, Popham M, Malkin I, Sambrook PN, MacGregor AJ, Spector T, et al. Lumbar disc degeneration and genetic factors are the main risk factors for low back pain in women: the UK Twin Spine Study. Annals of the Rheumatic Diseases. 2011;70(10):1740–5.

64. Elfering A, Semmer N, Birkhofer D, Zanetti M, Hodler J, Boos N. Risk factors for lumbar disc degeneration: a 5-year prospective MRI study in asymptomatic individuals. Spine. 2002;27(2):125–34.

65. Hangai M, Kaneoka K, Kuno S, Hinotsu S, Sakane M, Mamizuka N, et al. Factors associated with lumbar intervertebral disc degeneration in the elderly. The Spine Journal 2008;8(5):732–40.

66. Wolff J. The Law of Bone Remodelling [Internet]. Berlin Heidelberg: Springer-Verlag; 1986 [cited 18 June 2020]. Available from:

67. Choi K, Kuhn JL, Ciarelli MJ, Goldstein SA. The elastic moduli of human subchondral, trabecular, and cortical bone tissue and the size-dependency of cortical bone modulus. Journal of Biomechanics. 1990;23(11):1103–13.

68. Pawlikowski M, Jankowski K, Skalski K. New microscale constitutive model of human trabecular bone based on depth sensing indentation technique. Journal of the Mechanical Behavior of Biomedical Materials. 2018;85:162–9.

69. Turunen MJ, Prantner V, Jurvelin JS, Kröger H, Isaksson H. Composition and microarchitecture of human trabecular bone change with age and differ between anatomical locations. Bone. 2013;54(1):118–25.

70. Mandair GS, Morris MD. Contributions of Raman spectroscopy to the understanding of bone strength. BoneKEy Reports. 2015;4:620.

71. Ojanen X, Isaksson H, Töyräs J, Turunen MJ, Malo MKH, Halvari A, et al. Relationships between tissue composition and viscoelastic properties in human trabecular bone. Journal of Biomechanics. 2015;48(2):269–75.

72. Arnold M, Zhao S, Ma S, Giuliani F, Hansen U, Cobb JP, et al. Microindentation – a tool for measuring cortical bone stiffness? Bone & Joint Research. 2017;6(9):542–9.

73. Boughton O, Zhao S, Arnold M, Ma S, Cobb J p., Giuliani F, et al. Measuring cortical bone stiffness using micro-indentation. Orthopaedic Proceedings. 2016;98-B(SUPP_16):31.

74. Perilli E, Parkinson IH, Truong L-H, Chong KC, Fazzalari NL, Osti OL. Modic (endplate) changes in the lumbar spine: bone micro-architecture and remodelling. European Spine Journal. 2015;24(9):1926–34.

75. Oliver WC, Pharr GM. An improved technique for determining hardness and elastic modulus using load and displacement sensing indentation experiments. Journal of Materials Research. 1992;7(6):1564–83.

76. Hoffler CE, Guo XE, Zysset PK, Goldstein SA. An application of nanoindentation technique to measure bone tissue Lamellae properties. Journal of Biomechanical Engineering. 2005;127(7):1046–53.

77. Dall'Ara E, Karl C, Mazza G, Franzoso G, Vena P, Pretterklieber M, et al. Tissue Properties of the Human Vertebral Body Sub-Structures Evaluated by Means of Microindentation. Journal of the Mechanical Behavior of Biomedical Materials. 2013;25:23–32.

78. Hoffler CE, Guo XE, Zysset PK, Goldstein SA. An application of nanoindentation technique to measure bone tissue Lamellae properties. Journal of Biomechanical Engineering. 2005;127(7):1046–53.

79. Wolfram U, Wilke H-J, Zysset PK. Rehydration of vertebral trabecular bone: Influences on its anisotropy, its stiffness and the indentation work with a view to age, gender and vertebral level. Bone. 2010;46(2):348–54.

80. Mittra E, Akella S, Qin Y-X. The effects of embedding material, loading rate and magnitude, and penetration depth in nanoindentation of trabecular bone. Journal of Biomedical Materials Research. Part A. 2006;79A(1):86–93.

81. Zysset P. Indentation of bone tissue: A short review. Osteoporosis International. 2009;20(6):1049–55.

82. Follon E. Micro- and nano-indentation of aged bone from the femoral neck [Doctoral]. University of Cambridge; 2003.

83. Grant JP, Oxland TR, Dvorak MF. Mapping the structural properties of the lumbosacral vertebral endplates. Spine. 2001;26(8):889–96.

84. Hoffler CE, Guo XE, Zysset PK, Goldstein SA. An application of nanoindentation technique to measure bone tissue Lamellae properties. Journal of Biomechanical Engineering. 2005;127(7):1046–53.

85. Hengsberger S, Kulik A, Zysset P. A combined atomic force microscopy and nanoindentation technique to investigate the elastic properties of bone structural units. European Cells & Materials 2001;1:12–7.

86. Zhang J, Niebur GL, Ovaert TC. Mechanical property determination of bone through nano- and micro-indentation testing and finite element simulation. Journal of Biomechanics. 2008;41(2):267–75.

87. Kaye B. The Effects of Freezing on the Mechanical Properties of Bone. The Open Bone Journal. 2012;4(1):14–9.

88. el Barzouhi A, Vleggeert-Lankamp CLAM, Lycklama à Nijeholt GJ, Van der Kallen BF, van den Hout WB, Koes BW, et al. Predictive value of MRI in decision making for disc surgery for sciatica. Journal of Neurosurgery: Spine. 2013;19(6):678–87.

89. Modic MT, Masaryk TJ, Ross JS, Carter JR. Imaging of degenerative disk disease. Radiology. 1988;168(1):177–86.

90. de Roos A, Kressel H, Spritzer C, Dalinka M. MR imaging of marrow changes adjacent to end plates in degenerative lumbar disk disease. American Journal of Roentgenology. 1987;149(3):531–4.

91. Modic MT, Steinberg PM, Ross JS, Masaryk TJ, Carter JR. Degenerative disk disease: assessment of changes in vertebral body marrow with MR imaging. Radiology 1988;166(1 Pt 1):193–9.

92. Kerttula L, Luoma K, Kaapa E, Gronblad M. Modic type I changes predict rapidly progressing disc degeneration at 1-year follow-up. Spine. 2010.

93. Kuisma M, Karppinen J, Niinimäki J, Kurunlahti M, Haapea M, Vanharanta H, et al. A Three-Year Follow-up of Lumbar Spine Endplate (Modic) Changes: Spine 2006;31(15):1714–8.

94. Hutton MJ, Bayer JH, Powell JM. Modic vertebral body changes: The natural history as assessed by consecutive magnetic resonance imaging. Spine. 2011;36(26):2304–7.

95. Arana E, Kovacs M, Royuela A, Estremera A, Asenjo B, Sarasíbar H, et al. Modic changes and associated features in Southern European chronic low back pain patients. The Spine Journal. 2011;11(5):402–11.

96. Kjaer P, Leboeuf-Yde C, Korsholm L, Sorensen J Solgaard, Bendix T. Magnetic resonance imaging and low back pain in adults: a diagnostic imaging study of 40-year-old men and women. Spine. 2005;30(10):1173–80.

97. Esposito P, Pinheiro-Franco JL, Froelich S, Maitrot D. Predictive value of MRI vertebral end-plate signal changes (Modic) on outcome of surgically treated degenerative disc disease. Results of a cohort study including 60 patients. Neuro-Chirurgie 2006;52(4):315–22.

98. Jensen RK, Leboeuf-Yde C. Is the presence of modic changes associated with the outcomes of different treatments? A systematic critical review. BMC Musculoskeletal Disorders. 2011;12:183.

99. Jensen OK, Nielsen CV, Sørensen JS, Stengaard-Pedersen K. Type 1 Modic changes was a significant risk factor for 1-year outcome in sick-listed low back pain patients: a nested cohort study using magnetic resonance imaging of the lumbar spine. The Spine Journal. 2014;14(11):2568–81.

100. Albert HB, Kjaer P, Jensen TS, Sorensen JS, Bendix T, Manniche C. Modic changes, possible causes and relation to low back pain. Medical Hypotheses. 2008;70(2):361–8.

101. Ma X-L, Ma J-X, Wang T, Tian P, Han C. Possible role of autoimmune reaction in Modic Type I changes. Medical Hypotheses. 2011;76(5):692–4.

102. Osti OL, Zahari S, John TC, Truong L, Perilli E, Fazzalari NL. Microstructure and remodelling in modic changes. Spine Journal Meeting Abstracts 2010;1;13

103. Teichtahl AJ, Urquhart DM, Wang Y, Wluka AE, O'Sullivan R, Jones G, et al. Modic changes in the lumbar spine and their association with body composition, fat distribution and intervertebral disc height – a 3.0 T-MRI study. BMC Musculoskeletal Disorders. 2016;17:92.

104. Ohtori S, Inoue G, Ito T, Koshi T, Ozawa T, Doya H, et al. Tumor Necrosis Factor-Immunoreactive Cells and PGP 9.5-Immunoreactive Nerve Fibers in Vertebral Endplates of Patients With Discogenic Low Back Pain and Modic Type 1 or Type 2 Changes on MRI: Spine. 2006;31(9):1026–31.

105. Antonacci MD, Mody DR, Rutz K, Weilbaecher D, Heggeness MH. A histologic study of fractured human vertebral bodies. Journal of Spinal Disorders & Techniques. 2002;15(2):118–26.

106. Rannou F, Ouanes W, Boutron I, Lovisi B, Fayad F, Macé Y, et al. High-sensitivity C-reactive protein in chronic low back pain with vertebral end-plate modic signal changes. Arthritis Care & Research. 2007;57(7):1311–5.

107. Dudli S, Liebenberg E, Magnitsky S, Lu B, Lauricella M, Lotz JC. Modic type 1 change is an autoimmune response that requires a proinflammatory milieu provided by the 'Modic disc'. The Spine Journal. 2018;18(5):831–44.

108. Dudli S, Sing DC, Hu SS, Berven SH, Burch S, Deviren V, et al. ISSLS PRIZE IN BASIC SCIENCE 2017: Intervertebral disc/bone marrow cross-talk with Modic changes. European Spine Journal. 2017;26(5):1362–73.

109. Korhonen T, Karppinen J, Paimela L, Malmivaara A, Lindgren K-A, Bowman C, et al. The Treatment of Disc Herniation-Induced Sciatica With Infliximab: One-Year

Follow-up Results of FIRST II, a Randomized Controlled Trial. Spine. 2006;31(24):2759–66.

110. Zhang Y-H, Zhao C-Q, Jiang L-S, Chen X-D, Dai L-Y. Modic changes: a systematic review of the literature. European Spine Journal. 2008;17(10):1289–99.

111. Khot A, Bowditch M, Powell J, Sharp D. The Use of Intradiscal Steroid Therapy for Lumbar Spinal Discogenic Pain: A Randomized Controlled Trial. Spine. 2004;29(8):833–6.

112. Buttermann GR. The effect of spinal steroid injections for degenerative disc disease. The Spine Journal. 2004;4(5):495–505.

113. Stirling A, Worthington T, Rafiq M, Lambert PA, Elliott TS. Association between sciatica and Propionibacterium acnes. The Lancet. 2001;357(9273):2024–5.

114. Albert HB, Lambert P, Rollason J, Sorensen JS, Worthington T, Pedersen MB, et al. Does nuclear tissue infected with bacteria following disc herniations lead to Modic changes in the adjacent vertebrae? European Spine Journal. 2013;22(4):690–6.

115. Mclorinan GC, Mcmullan MG, Mcdowell A, Glenn J, Cooke EA, Eames N, et al. The role of bacterial infection in sciatica? Orthopaedic Proceedings. 2005;87-B(SUPP_III):244–244.

116. Adams MA, Dolan P. Intervertebral disc degeneration: evidence for two distinct phenotypes. Journal of Anatomy. 2012;221(6):497–506.

117. Dudli S, Fields AJ, Samartzis D, Karppinen J, Lotz JC. Pathobiology of Modic changes. European Spine Journal. 2016;25(11):3723–34.

118. Campbell LK. Protein Gene Product 9.5 (PGP 9.5) Is Not a Specific Marker of Neural and Nerve Sheath Tumors: An Immunohistochemical Study of 95 Mesenchymal Neoplasms. Modern Pathology. 2003;16(10):963–9.

119. Schmid G, Witteler A, Willburger R, Kuhnen C, Jergas M, Koester O. Lumbar Disk Herniation: Correlatlon of Histologic Findings with Marrow Signal Intensity Changes in Vertebral Endplates at MR Imaging. Radiology. 2004;231(2):352–8.

120. Adams MA. Biomechanics of back pain. Acupunct Med Br Med AcupunctSoc. 2004;22:178–88.

121. Gruber HE, Ashraf N, Kilburn J, Williams C, Norton HJ, Gordon BE, et al. Vertebral endplate architecture and vascularization: application of micro-computerized tomography, a vascular tracer, and immunocytochemistry in analyses of disc degeneration in the aging sand rat. Spine. 2005;30(23):2593–600.

122. Boos N, Weissbach S, Rohrbach H, Weiler C, Spratt KF, Nerlich AG. Classification of age-related changes in lumbar intervertebral discs: 2002 Volvo Award in basic science. Spine. 2002;27(23):2631–44.

123. Horner HA, Urban JP. 2001 Volvo Award Winner in Basic Science Studies: Effect of nutrient supply on the viability of cells from the nucleus pulposus of the intervertebral disc. Spine. 2001;26(23):2543–9.

124. Kauppila LI. Atherosclerosis and disc degeneration/low-back pain – a systematic review. European Journal of Vascular & Endovascular Surgery. 2009;37(6):661–70.

125. Benneker LM, Heini PF, Alini M, Anderson SE, Ito K. 2004 Young investigator award winner: Vertebral endplate marrow contact channel occlusions and intervertebral disc degeneration. Spine. 2005;30(2):167–73.

126. LA Binch A, Cole AA, Breakwell LM, Michael AL, Chiverton N, Cross AK, et al. Expression and regulation of neurotrophic and angiogenic factors during human intervertebral disc degeneration. Arthritis Research Therapy. 2014;16(5):416.

127. Johnson WEB, Caterson B, Eisenstein SM, Roberts S. Human intervertebral disc aggrecan inhibits endothelial cell adhesion and cell migration in vitro. Spine. 2005;30(10):1139–47.

128. Tomaszewski KA, Adamek D, Konopka T, Tomaszewska R, Walocha JA. Endplate calcification and cervical intervertebral disc degeneration: the role of endplate marrow contact channel occlusion. Folia Morphologica. 2015;74(1):84–92.

129. Vernon-Roberts B, Pirie CJ. Healing trabecular microfractures in the bodies of lumbar vertebrae. Annals of the Rheumatic Diseases. 1973;32(5):406–12.

130. Wang H, Ma L, Yang D, Wang T, Liu S, Yang S, et al. Incidence and risk factors of adjacent segment disease following posterior decompression and instrumented fusion for degenerative lumbar disorders. Medicine. 2017;96(5):e6032.

131. Zigler JE, Blumenthal SL, Guyer RD, Ohnmeiss DD, Patel L. Progression of Adjacent-level Degeneration After Lumbar Total Disc Replacement: Results of a Post-hoc Analysis of Patients With Available Radiographs From a Prospective Study With 5-year Follow-up. Spine. 2018;43(20):1395–400.

132. Antonacci MD, Mody DR, Heggeness MH. Innervation of the human vertebral body: a histologic study. Journal of Spinal Disorders. 1998;11(6):526–31.

133. Freemont A, Peacock T, Goupille P, Hoyland J, O'Brien J, Jayson M. Nerve ingrowth into diseased intervertebral disc in chronic back pain. The Lancet. 1997;350(9072):178–81.

134. Brown MF, Hukkanen MVJ, Mccarthy ID, Redfern DRM, Batten JJ, Crock HV, et al. Sensory and Sympathetic innervation of the vertebral endplate in patients with degenerative disc disease. The Journal of Bone and Joint Surgery. 1997;79(1):147–53.

135. Niv D, Gofeld M, Devor M. Causes of pain in degenerative bone and joint disease: a lesson from vertebroplasty. Pain. 2003;105(3):387–92.

136. Moore RJ. The vertebral end-plate: what do we know? European Spine Journal 2000;9(2):92–6.

137. Sneddon IN. The relation between load and penetration in the axisymmetric boussinesq problem for a punch of arbitrary profile. International Journal of Engineering Science. 1965;3(1):47–57.

138. Thavarajah R, Mudimbaimannar VK, Elizabeth J, Rao UK, Ranganathan K. Chemical and physical basics of routine formaldehyde fixation. Journal of Oral and Maxillofacial Pathology. 2012;16(3):400–5.

139. Zhang G-J, Yang J, Guan F-J, Chen D, Li N, Cao L, et al. Quantifying the Effects of Formalin Fixation on the Mechanical Properties of Cortical Bone Using Beam Theory and Optimization Methodology With Specimen-Specific Finite Element Models. Journal of Biomechanical Engineering. 2016;138(9).

140. Andrade MGS, Sá CN, Marchionni AMT, de Bittencourt TCBSC, Sadigursky M. Effects of freezing on bone histological morphology. Cell and Tissue Banking. 2008;9(4):279–87.

141. Turner CH, Rho J, Takano Y, Tsui TY, Pharr GM. The elastic properties of trabecular and cortical bone tissues are similar: results from two microscopic measurement techniques. Journal of Biomechanics. 1999;32(4):437–41.

142. Hart NH, Nimphius S, Rantalainen T, Ireland A, Siafarikas A, Newton RU. Mechanical basis of bone strength: influence of bone material, bone structure and muscle action. Journal of Musculoskeletal & Neuronal Interactions. 2017;17(3):114–39.

143. Fonseca H, Moreira-Gonçalves D, Coriolano H-JA, Duarte JA. Bone Quality: The Determinants of Bone Strength and Fragility. Sports Medicine. 2014;44(1):37–53.

144. Burr DB. The contribution of the organic matrix to bone's material properties. Bone. 2002;31(1):8–11.

145. Wang X, Bank RA, TeKoppele JM, Mauli Agrawal C. The role of collagen in determining bone mechanical properties. Journal of Orthopaedic Research. 2001;19(6):1021–6.

146. Oxlund H, Barckman M, Ørtoft G, Andreassen TT. Reduced concentrations of collagen cross-links are associated with reduced strength of bone. Bone. 1995;17(4, Supplement):S365–71.

147. Wang X, Shen X, Li X, Agrawal C. Age-related Changes in the Collagen Network and Toughness of Bone [Internet]. Bone. 2002;31(1):1–7

148. Follet H, Boivin G, Rumelhart C, Meunier RJ. The Degree of Mineralization Is a Determinant of Bone Strength: A Study on Human Calcanei [Internet]. Bone. 2004;34(5):783–9 [cited 20 May 2020].

149. Adele Boskey. Bone mineral crystal size. Osteoporosis International. 2003;14(5):16–21.

150. DeLucca JF, Cortes DH, Jacobs NT, Vresilovic EJ, Duncan RL, Elliott DM. Human cartilage endplate permeability varies with degeneration and intervertebral disc site. Journal of Biomechanics. 2016;49(4):550–7.

151. Adams MA, Lama P, Zehra U, Dolan P. Why do some intervertebral discs degenerate, when others (in the same spine) do not? Clinical Anatomy. 2015;28(2):195–204.

152. Pfirrmann CW, Metzdorf A, Zanetti M, Hodler J, Boos N. Magnetic resonance classification of lumbar intervertebral disc degeneration. Spine. 2001;26(17):1873–8.

153. Zhang R, Gong H, Zhu D, Ma R, Fang J, Fan Y. Multi-level femoral morphology and mechanical properties of rats of different ages. Bone. 2015;76:76–87.

154. Raghavan M, Sahar ND, Kohn DH, Morris MD. Age-specific profiles of tissue-level composition and mechanical properties in murine cortical bone. Bone. 2012;50(4):942–53.

155. Nikel O, Laurencin D, McCallum SA, Gundberg CM, Vashishth D. NMR investigation of the role of osteocalcin and osteopontin at the organic–inorganic interface in bone. Langmuir. 2013;29(45):13873–82.

156. Samuel J, Park J-S, Almer J, Wang X. Effect of water on nanomechanics of bone is different between tension and compression. Journal of the Mechanical Behavior of Biomedical Materials. 2016;57:128–38.

157. MacKay JW, Murray PJ, Kasmai B, Johnson G, Donell ST, Toms AP. Subchondral bone in osteoarthritis: association between MRI texture analysis and histomorphometry. Osteoarthritis & Cartilage. 2017;25(5):700–7.

158. Donell S. Subchondral bone remodelling in osteoarthritis. EFORT Open Reviews. 2019;4(6):221–9.

159. Weber A, Chan PMB, Wen C. Do immune cells lead the way in subchondral bone disturbance in osteoarthritis? Progress in Biophysics & Molecular Biology. 2019;148:21–31.

160. Carmichael JHE, Maccia C, Moores BM, Oestmann JW, Schibilla H, Teunen D, et al. (European Commission, Directorate-General XII: Science, Research and Development). European guidelines on quality criteria for diagnostic radiographic images. Luxembourg: Office for Official Publications of the European Communities; 1996.

161. Rao PJ, Phan K, Giang G, Maharaj MM, Phan S, Mobbs RJ. Subsidence following anterior lumbar interbody fusion (ALIF): a prospective study. Journal of Spine Surgery. 2017;3(2):168–75.

162. Kim M-C, Chung H-T, Cho J-L, Kim D-J, Chung N-S. Subsidence of Polyetheretherketone Cage After Minimally Invasive Transforaminal Lumbar Interbody Fusion. Journal of Spinal Disorders and Techniques. 2013;26(2):87–92.

163. Beutler WJ, Peppelman WC. Anterior lumbar fusion with paired BAK standard andpaired BAK Proximity cages: subsidence incidence, subsidence factors,and clinical outcome. The Spine Journal. 2003;3(4):289–93.

164. Marchi L, Abdala N, Oliveira L, Amaral R, Coutinho E, Pimenta L. Radiographic and clinical evaluation of cage subsidence after stand-alone lateral interbody fusion. Journal of Neurosurgery: Spine. 2013;19(1):110–8.

165. Behrbalk E, Uri O, Parks RM, Musson R, Soh RCC, Boszczyk BM. Fusion and subsidence rate of stand alone anterior lumbar interbody fusion using PEEK cage with recombinant human bone morphogenetic protein-2. European Spine Journal 2013;22(12):2869–75.

166. Strube P, Hoff E, Hartwig T, Perka CF, Gross C, Putzier M. Stand-alone Anterior Versus Anteroposterior Lumbar Interbody Single-level Fusion After a Mean Follow-up of 41 Months: Journal of Spinal Disorders & Techniques. 2012;25(7):362–9.

167. Dabbs VMD, Dabbs LGD. Correlation Between Disc Height Narrowing and Low-Back Pain. Spine. 1990;15(12):1366–8.

168. Choi JY, Sung KH. Subsidence after anterior lumbar interbody fusion using paired stand-alone rectangular cages. European Spine Journal. 2006;15(1):16–22.

169. Lang G, Navarro-Ramirez R, Gandevia L, Hussain I, Nakhla J, Zubkov M, et al. Elimination of Subsidence with 26-mm-Wide Cages in Extreme Lateral Interbody Fusion. World Neurosurgery. 2017;104:644–52.

170. Jensen TS, Sorensen JS, Kjaer P. Intra- and interobserver reproducibility of vertebral endplate signal (modic) changes in the lumbar spine: the Nordic Modic Consensus Group classification. Acta Radiologica Scandinavica. 2007;48(7):748–54.

171. Peterson CK, Gatterman B, Carter JC, Humphreys BK, Weibel A. Inter- and Intraexaminer Reliability in Identifying and Classifying Degenerative Marrow (Modic) Changes on Lumbar Spine Magnetic Resonance Scans. Journal of Manipulative and Physiological Therapeutics. 2007;30(2):85–90.

172. Malham GM, Parker RM, Blecher CM, Seex KA. Assessment and classification of subsidence after lateral interbody fusion using serial computed tomography. Journal of Neurosurgery: Spine. 2015;23(5):589–97.

173. Oh KW, Lee JH, Lee J-H, Lee D-Y, Shim HJ. The Correlation Between Cage Subsidence, Bone Mineral Density, and Clinical Results in Posterior Lumbar Interbody Fusion. Clinical Spine Surgery. 2017;30(6):E683–E689.

174. Bocahut N, Audureau E, Poignard A, Delambre J, Queinnec S, Flouzat Lachaniette C-H, et al. Incidence and impact of implant subsidence after stand-alone lateral lumbar interbody fusion. Orthopaedics & Traumatology: Surgery & Research. 2018;104(3):405–10.

175. Nemani VM, Aichmair A, Taher F, Lebl DR, Hughes AP, Sama AA, et al. Rate of Revision Surgery After Stand-alone Lateral Lumbar Interbody Fusion for Lumbar Spinal Stenosis. Spine. 2014;39(5):E326–E331.

176. Seaman S, Kerezoudis P, Bydon M, Torner JC, Hitchon PW. Titanium vs. polyetheretherketone (PEEK) interbody fusion: Meta-analysis and review of the literature. Journal of Clinical Neuroscience. 2017;44:23–9.

177. Palepu V, Helgeson M, Molyneaux-Francis M, Nagaraja S. The effects of bone microstructure on subsidence risk for ALIF, LLIF, PLIF and TLIF spine cages. Journal of Biomechanical Engineering. 2018;141(3).

178. Choi W-S, Kim J-S, Hur J-W, Seong J-H. Minimally Invasive Transforaminal Lumbar Interbody Fusion Using Banana-Shaped and Straight Cages: Radiological and Clinical Results from a Prospective Randomized Clinical Trial. Neurosurgery. 2018;82(3):289–98.

179. Faizan A, Kiapour A, Kiapour AM, Goel VK. Biomechanical analysis of various footprints of transforaminal lumbar interbody fusion devices. Journal of Spinal Disorders & Techniques 2014;27(4):E118-E127.

180. Lee N, Kim KN, Yi S, Ha Y, Shin DA, Yoon DH, et al. Comparison of Outcomes of Anterior, Posterior, and Transforaminal Lumbar Interbody Fusion Surgery at a Single Lumbar Level with Degenerative Spinal Disease. World Neurosurgery. 2017;101:216–26.

181. Wang Y, Videman T, Battié MC. Modic Changes: Prevalence, Distribution Patterns and Association with Age in Caucasian Men. The Spine Journal. 2012;12(5):411–6.

182. Jensen TS, Karppinen J, Sorensen JS, Niinimäki J, Leboeuf-Yde C. Vertebral endplate signal changes (Modic change): a systematic literature review of prevalence and association with non-specific low back pain. European Spine Journal. 2008;17(11):1407–22.

183. Pinson H, Hallaert G, Herregodts P, Everaert K, Couvreur T, Caemaert J, et al. Outcome of Anterior Lumbar Interbody Fusion: A Retrospective Study of Clinical and Radiologic Parameters. World Neurosurgery. 2017;103:772–9.

184. Laustsen AF, Bech-Azeddine R. Do Modic changes have an impact on clinical outcome in lumbar spine surgery? A systematic literature review. European Spine Journal. 2016;25(11):3735–45.

185. Kwon Y-M, Chin D-K, Jin B-H, Kim K-S, Cho Y-E, Kuh S-U. Long Term Efficacy of Posterior Lumbar Interbody Fusion with Standard Cages alone in Lumbar Disc Diseases Combined with Modic Changes. Journal of Korean Neurosurgical Society. 2009;46(4):322–7.

186. Ohtori S, Yamashita M, Yamauchi K, Inoue G, Koshi T, Suzuki M, et al. Change in Modic Type 1 and 2 Signals After Posterolateral Fusion Surgery: Spine. 2010;35(12):1231–5.

187. Salgado R, Van Goethem JWM, van den Hauwe L, Parizel PM. Imaging of the Postoperative Spine. Seminars in Roentgenology. 2006;41(4):312–26.

188. Van de Kelft E, Van Goethem J. Trabecular metal spacers as standalone or with pedicle screw augmentation, in posterior lumbar interbody fusion: a prospective, randomized controlled trial. European Spine Journal. 2015;24(11):2597–606.

189. Phan K, Thayaparan GK, Mobbs RJ. Anterior lumbar interbody fusion versus transforaminal lumbar interbody fusion--systematic review and meta-analysis. British Journal of Neurosurgery. 2015;29(5):705–11.

190. Peng B, Hou S, Shi Q, Jia L. The relationship between cartilage end-plate calcification and disc degeneration: an experimental study. Chinese Medical Journal. 2001;114(3):308–312.

191. Roberts S, Urban JP, Evans H, Eisenstein SM. Transport properties of the human cartilage endplate in relation to its composition and calcification. Spine. 1996;21(4):415–20.

192. Rajasekaran S, Babu JN, Arun R, Armstrong BRW, Shetty AP, Murugan S. ISSLS Prize Winner: A Study of Diffusion in Human Lumbar Discs: A Serial Magnetic Resonance Imaging Study Documenting the Influence of the Endplate on Diffusion in Normal and Degenerate Discs: Spine. 2004;29(23):2654–67.

193. Adams MA, Freeman BJ, Morrison HP, Nelson IW, Dolan P. Mechanical initiation of intervertebral disc degeneration. Spine. 2000;25(13):1625–36.

194. Adams MA, McNally DS, Wagstaff J, Goodship AE. Abnormal stress concentrations in lumbar intervertebral discs following damage to the vertebral bodies: a cause of disc failure? European Spine Journal. 1993;1(4):214–21.

195. Wang Y, Videman T, Battie MC. Lumbar vertebral endplate lesions: Prevalence, classification, and association with age. Spine. 2012;37(17):1432–9.

196. Kovacs M, Royuela A, Arana E, Estremera A, Amengual G, Asenjo B, et al. Re: ISSLS prize winner: lumbar vertebral endplate lesions associations with disc degeneration and back pain history. Spine 2012;37:1490-6. Spine. 2013;38(1):93.

197. Woodfin Abigail, Voisin Mathieu-Benoit, Nourshargh Sussan. PECAM-1: A Multi-Functional Molecule in Inflammation and Vascular Biology. Arteriosclerosis, Thrombosis, and Vascular Biology. 2007;27(12):2514–23.

198. Oki S, Matsuda Y, Shibata T, Okumura H, Desaki J. Morphologic Differences of the Vascular Buds in the Vertebral Endplate: Scanning Electron Microscopic Study. Spine. 1996;21(2):174.

199. Rodriguez AG, Slichter CK, Acosta FL, Rodriguez-Soto AE, Burghardt AJ, Majumdar S, et al. Human disc nucleus properties and vertebral endplate permeability. Spine. 2011;36(7):512–20.

200. Ohtori S, Inoue G, Ito T, Koshi T, Ozawa T, Doya H, et al. Tumor necrosis factor-immunoreactive cells and PGP 9.5-immunoreactive nerve fibers in vertebral endplates of patients with discogenic low back Pain and Modic Type 1 or Type 2 changes on MRI. Spine. 2006;31(9):1026–31.

201. Wickramasinghe S, Porwit A, Erber W. Normal bone marrow cells: Development and cytology [Internet]. In: Porwit A, McCullough J, Erber WN, eds. Blood and Bone Marrow Pathology (2nd edn.). Edinburgh: Churchill Livingstone; 2011:19–44

202. Ely SA, Knowles DM. Expression of CD56/Neural Cell Adhesion Molecule Correlates with the Presence of Lytic Bone Lesions in Multiple Myeloma and Distinguishes Myeloma from Monoclonal Gammopathy of Undetermined Significance and Lymphomas with Plasmacytoid Differentiation. The American Journal of Pathology. 2002;160(4):1293–9.

203. Jacobi AM, Dörner T. Current aspects of anti-CD20 therapy in rheumatoid arthritis. Current Opinion in Pharmacology. 2010;10(3):316–21.

204. Naeim F, Nagesh Rao P, Song SX, Phan RT. Chapter 2 - Principles of Immunophenotyping [Internet]. In: Naeim F, Nagesh Rao P, Song SX, Phan RT, eds. Atlas of Hematopathology (2nd edn.). Academic Press; 2018:29–56 [cited 22 April 2020].

205. Frasca D, Blomberg BB. Effects of aging on B cell function. Current Opinion in Immunology 2009;21(4):425–30.

206. Hagen M, Derudder E. Inflammation and the Alteration of B-Cell Physiology in Aging. Gerontology. 2020;66(2):105–13.

207. Horowitz MC, Fretz JA, Lorenzo JA. How B Cells Influence Bone Biology in Health and Disease. Bone. 2010;47(3):472–9.

208. Chetty R, Gatter K. CD3: Structure, function, and role of immunostaining in clinical practice. The Journal of Pathology. 1994;173(4):303–7.

209. Alberts B, Johnson A, Lewis J, Raff M, Roberts K, Walter P. Lymphocytes and the Cellular Basis of Adaptive Immunity [Internet]. Molecular Biology of the Cell (4th edn.) 2002 [cited 22 April 2020].

210. Moro-García MA, Mayo JC, Sainz RM, Alonso-Arias R. Influence of Inflammation in the Process of T Lymphocyte Differentiation: Proliferative, Metabolic, and Oxidative Changes. Frontiers in Immunology [Internet]. 2018;9:339 [

211. Cope AP. Studies of T-cell activation in chronic inflammation. Arthritis Research. 2002;4(Suppl 3):S197–S211.

212. Salam N, Rane S, Das R, Faulkner M, Gund R, Kandpal U, et al. T cell ageing: Effects of age on development, survival & function. Indian Journal of Medical Research. 2013;138(5):595–608.

213. Srivastava RK, Dar HY, Mishra PK. Immunoporosis: Immunology of Osteoporosis—Role of T Cells. Frontiers in Immunology [Internet]. 2018;9:657

214. Nerlich AG, Schleicher ED, Boos N. 1997 Volvo Award winner in basic science studies. Immunohistologic markers for age-related changes of human lumbar intervertebral discs. Spine. 1997;22(24):2781.

215. Thomsen JS, Bruel A, Hauge EM. Human vertebral bone microstructure from infancy to senescence. Bone. 2012;50:S56.

216. Albert HB, Manniche C, Sorensen JS, Deleuran BW. Antibiotic treatment in patients with low-back pain associated with Modic changes Type 1 (bone oedema): a pilot study. British Journal of Sports Medicine. 2008;42(12):969–73.

217. Dudli S, Fields AJ, Samartzis D, Karppinen J, Lotz JC. Pathobiology of Modic changes. European Spine Journal. 2016;25(11):3723–34.

218. Perilli E, Briggs AM, Wark JD, Kantor S, Parkinson IH, Fazzalari NL. Whole human vertebral body BMD and bone volume fraction examined by DXA and micro-CT. Bone. 2009;44:S375.

219. Sterchi DL. Bone. In: Suvarna SK, Layton C, Bancroft JD, eds. Bancroft's Theory and Practice of Histological Techniques (8th edn.). 2019:280–305.

11 Appendix

11.1 Previous work on material creep of bone with indentation

Previous work with human femoral bone in this institution has explored the effects of creep with nano-indentation [82]. Figure 10.1.1 displays the results of indentation testing on human femoral bone with a constant load over time. Creep continues at a constant rate for the duration of the hold time of 3600 seconds. Figure 10.1.2 displays load displacement indentation curves with a maximum load of 1.1mN with different hold periods (ranging from 0 to 3600 seconds). Figure 10.1.3 displays indentation modulus and hardness results based on hold time at maximum load. Analysis of the results showed no significant difference between the results of hold period 10-240 seconds with a constant rate of creep throughout this time.

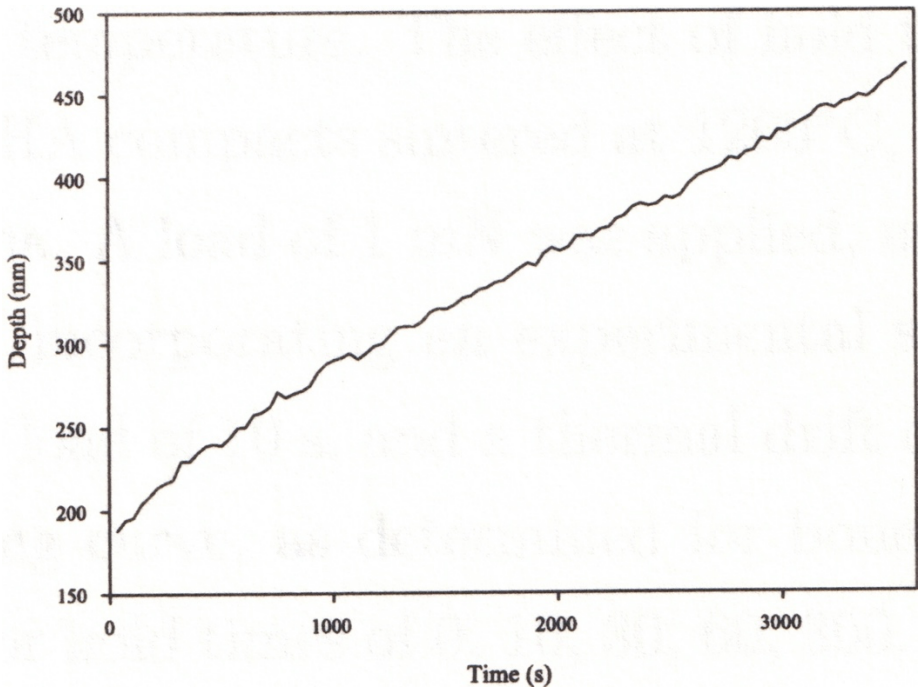

Figure 11.1.1 Indentation depth over time at a constant load.

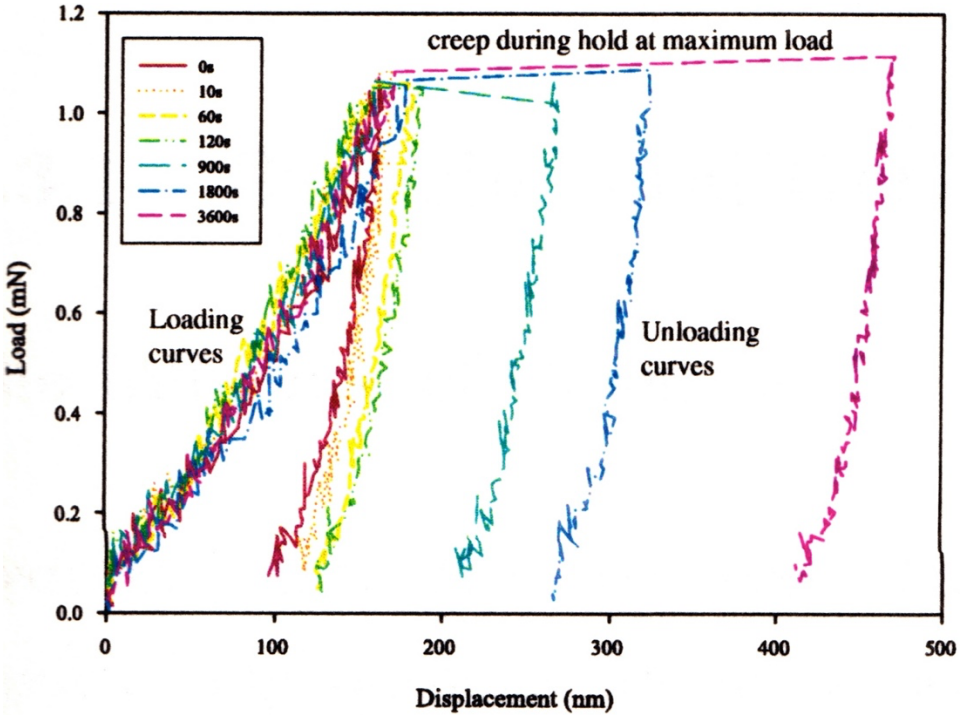

Figure 11.1.2 Load displacement curves demonstrating results after variable hold periods.

Hold Time (s)	Mean Hardness (GPa)	Mean Elastic Modulus (GPa)
0	1.29	40.3
10	1.07	22.4
30	1.09	19.5
60	1.06	22.8
120	1.01	19.8
240	0.95	19.7
420	0.74	18.7
900	0.52	16.1
1800	0.45	15.2
3600	0.29	12.6

Figure 11.1.3 Hardness and modulus results for cortical bone based on hold times at maximum load.

11.2 MRI images for donor patients.

These figures display representative cuts of the MRI scans for the donor patients included in this study.

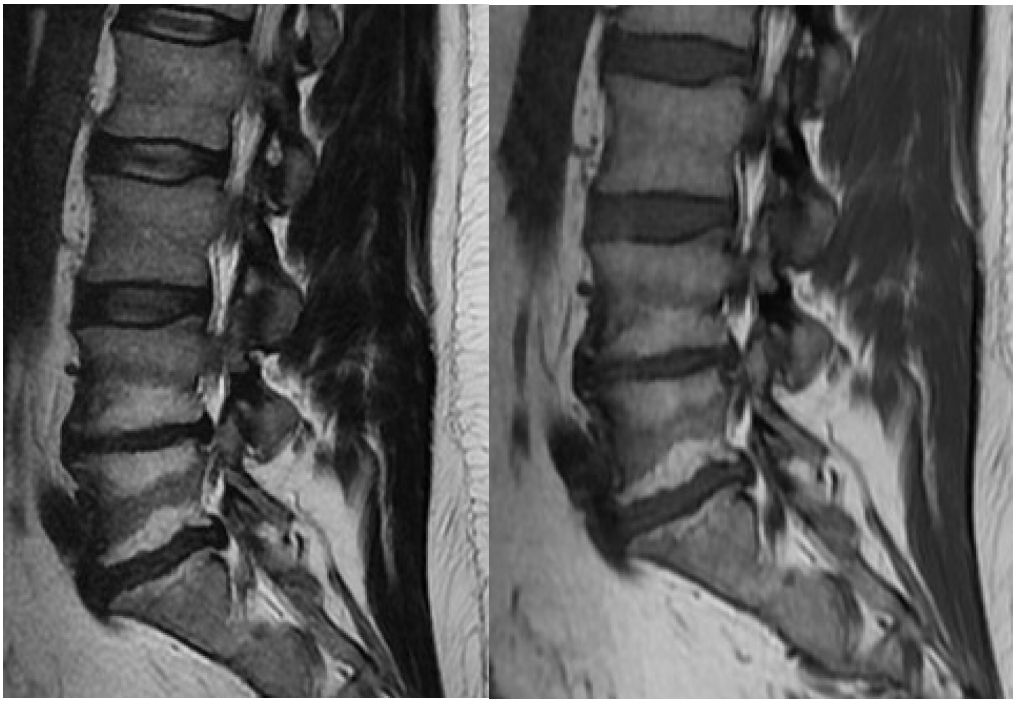

Figure 11.2.1 T1 and T2 MRI images of participant 01

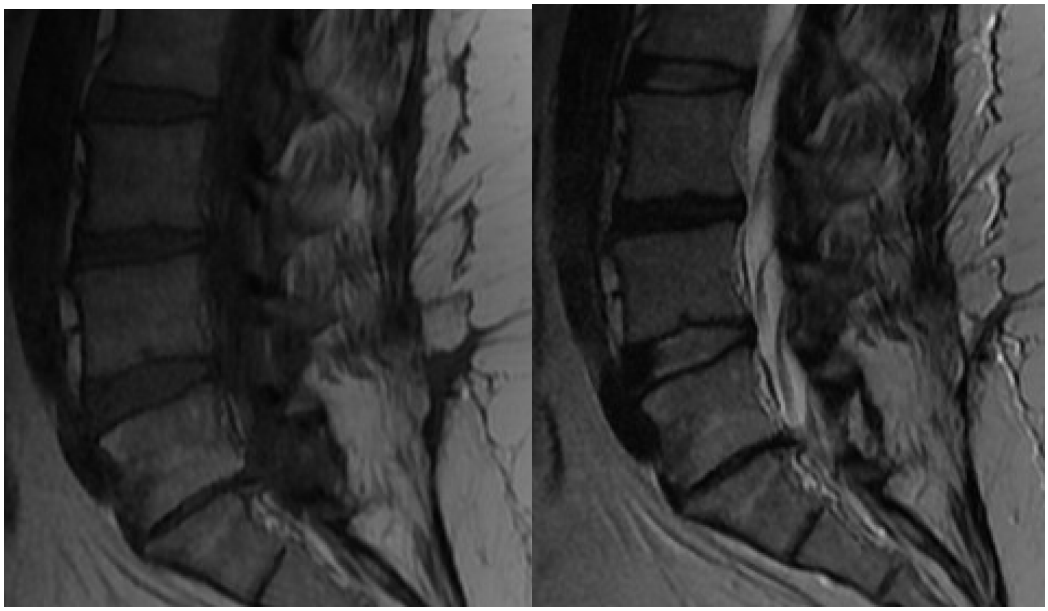

Figure 11.2.2 T1 and T2 MRI images of participant 02

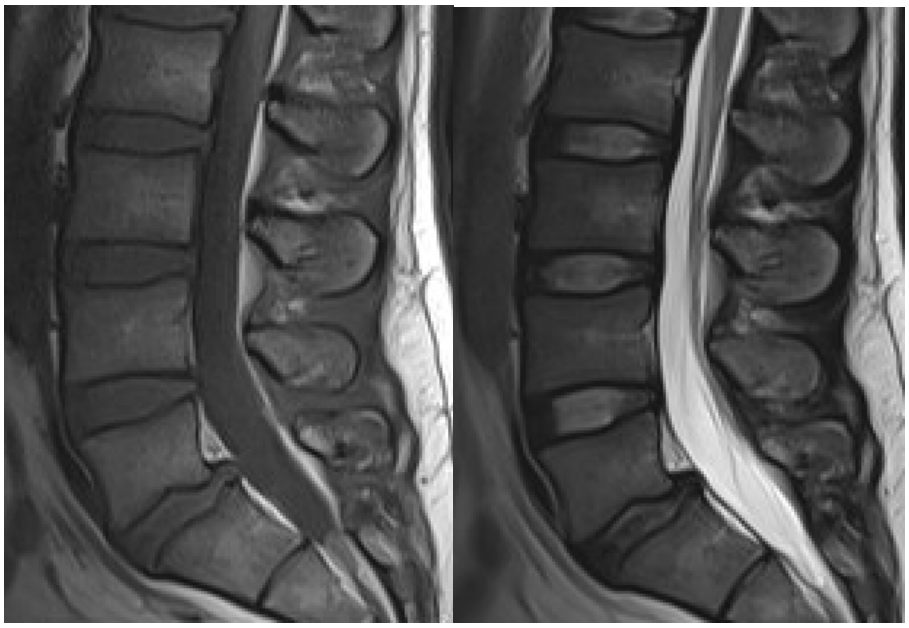

Figure 11.2.3 T1 and T2 MRI images of participant 03

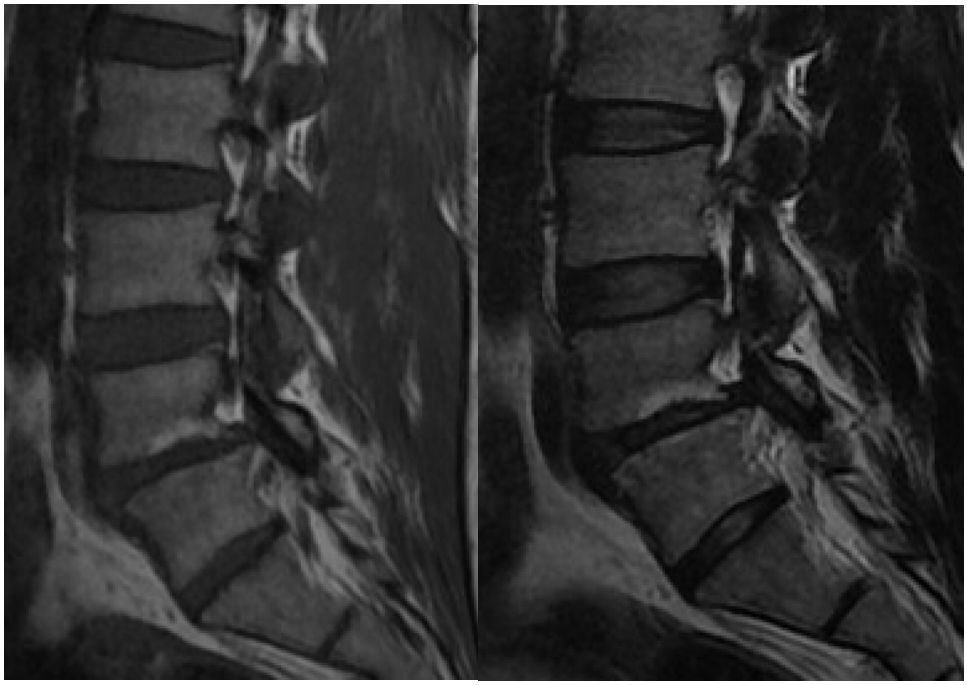

Figure 11.2.4 T1 and T2 MRI images of participant 04

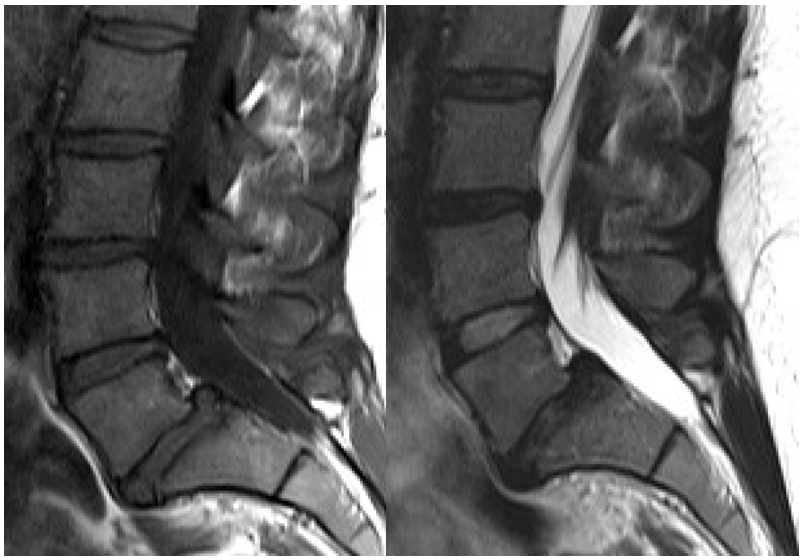

Figure 11.2.5 T1 and T2 MRI images from participant 06

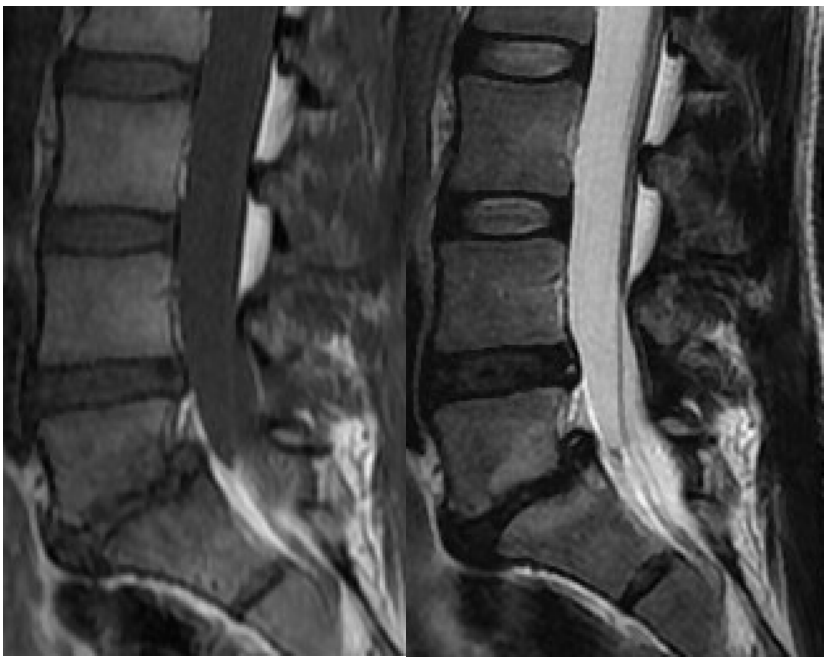

Figure 11.2.6 T1 and T2 MRI images from participant 07

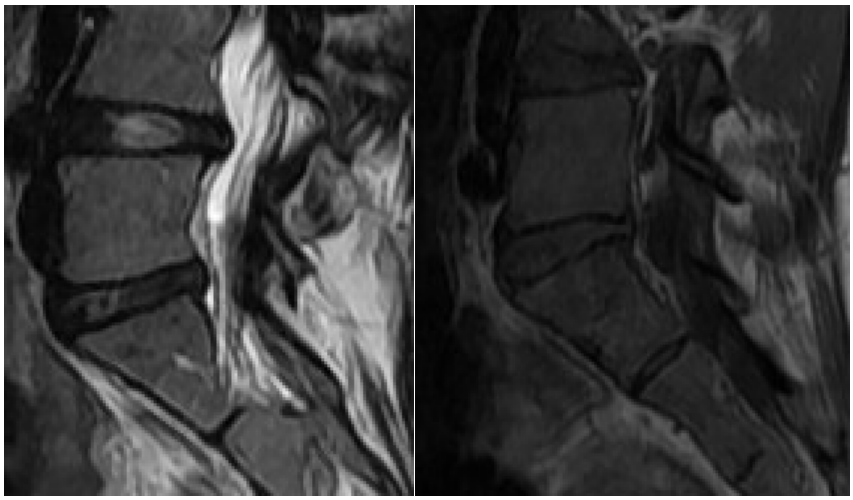

Figure 11.2.7 T1 and T2 MRI images from participant 08

Figure 11.2.8 T1 and T2 MRI images from participant 09

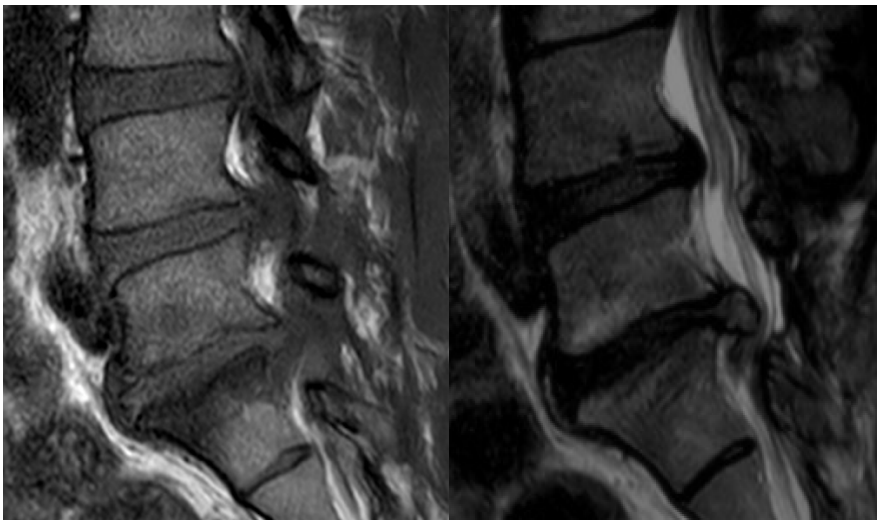

Figure 11.2.9 T1 and T2 MRI images from participant 10

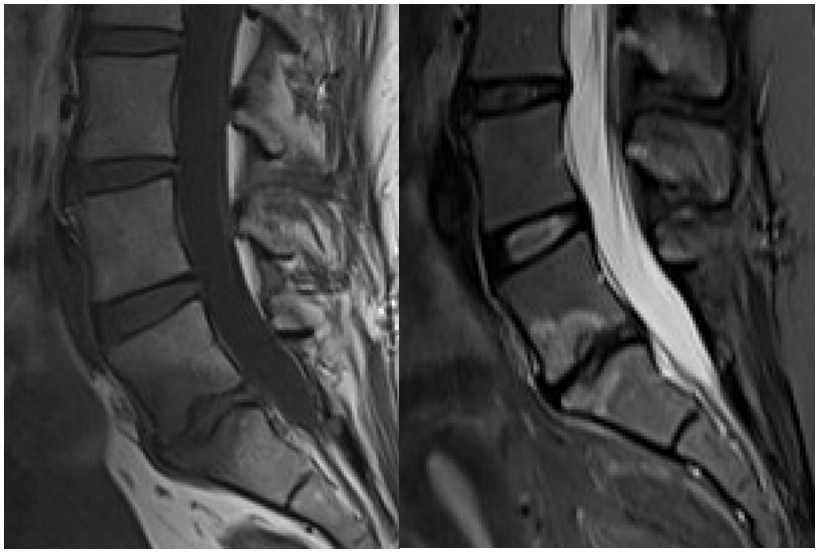

Figure 11.2.10 T1 and T2 MRI images from participant 11

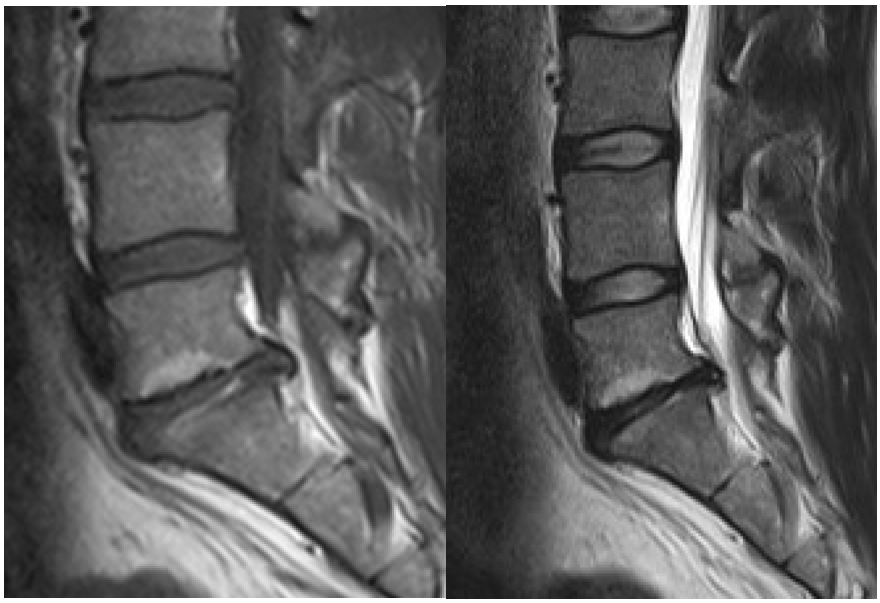

Figure 11.2.11 T1 and T2 MRI images from participant 12

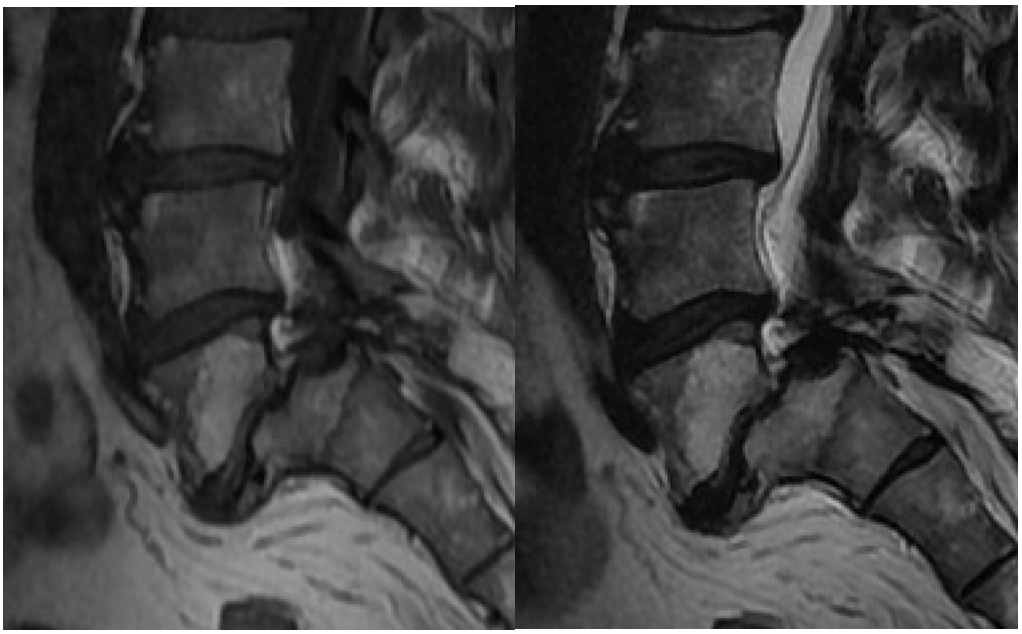

Figure 11.2.12 T1 and T2 MRI images from participant 13

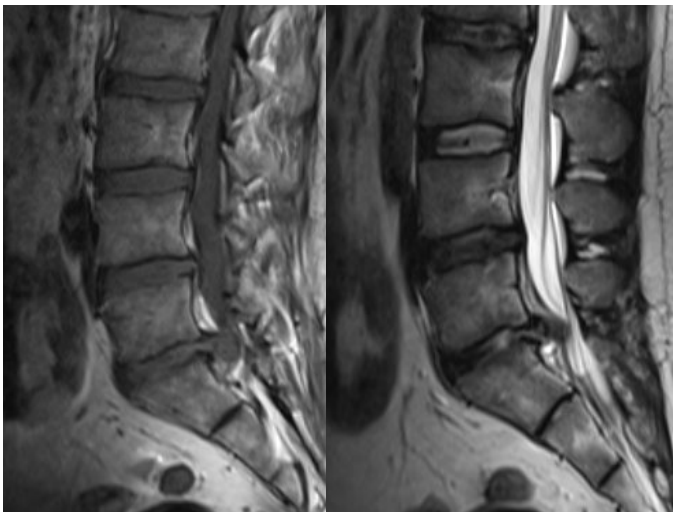

Figure 11.2.13 T1 and T2 MRI images from participant 14

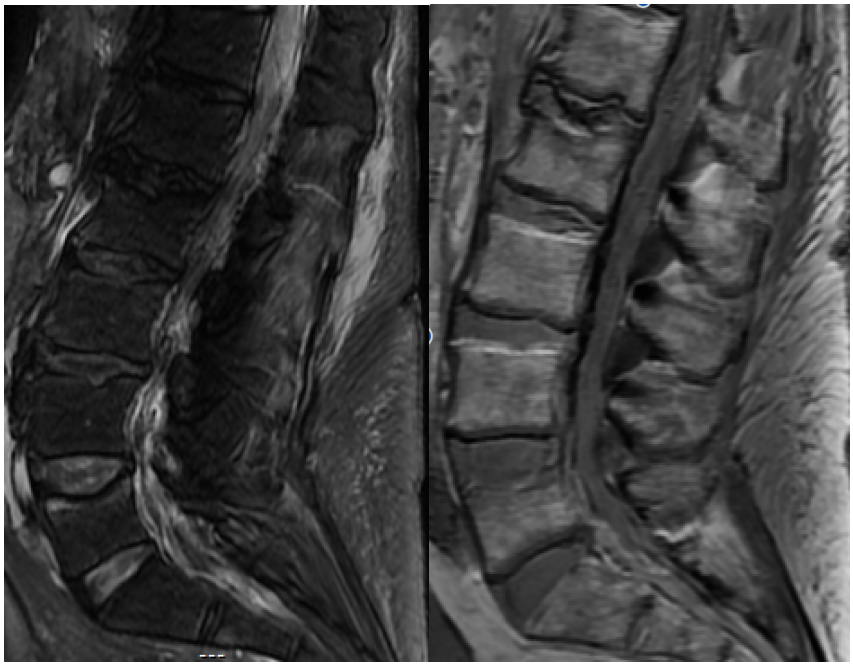

Figure 11.2.14 T1 and T2 MRI images from Participant 22

11.3 Histology sample preparation standard operating procedures

11.3.1 Fixation

All samples prior to transportation from the department of material science at Cambridge University are fixed in neutral buffered formalin, comprising of a solution of 4% formaldehyde and a phosphate buffer at pH7. They are kept in this solution for a minimum of 48 hours to allow completion of the fixation process.

11.3.2 Decalcification

Decalcification of the samples using 4% ethylenediamine tetracetic acid (EDTA) is undertaken after the fixation process. EDTA is a chelating agent and as such has a lower mechanism of action but also gives better preservation of the tissue especially when using immunohistochemical staining. It works by binding to the calcium ions on the outer surface of the hydroxyapatite crystals which are then replaced with calcium ions from the inner aspect of the crystal [219].

All samples after fixation are placed in a solution of 4% EDTA with a pH of 7.2. The volume of solution is to be at least 10 times the estimated volume of the sample.

Samples are left in this solution for 24 hours and then assessed for the adequacy of decalcification.

A chemical test for decalcification is utilised. This involves removing 0.5ml of the EDTA solution, mixing this with citric acid to reduce the pH and then adding ammonium oxalate which causes the precipitation of any calcium.

If the solution is clear after 20 minutes (i.e., minimal calcium precipitation has taken place) then the decalcification process is complete.

At each stage, if a further period is required it is increased in 24 hours increments by washing the sample in distilled water and adding a new volume of EDTA.

11.3.3 Embedding

The principle of embedding is to support the tissue to allow the cutting of thin microscope sections. Paraffin wax is heated to 60°C to keep it in a liquid state. An embedding cassette for each sample is labelled with the unique identification number. A small amount of wax is placed into a mould and the tissue is placed into the mould in the designated orientation.

Tissue is held in place while the mould is placed onto a cooling plate while the paraffin wax sets solid. Once the tissue is stable the labelled cassette is placed on top of the mould, and the mould is then topped up with wax until full and left on the cooling plate until solid.

Once solid the wax can be removed from the mould and the cassette closed.

All samples from the same batch are to be stored together.

Equipment (moulds, cooling plate and forceps) are cleaned between each sample.

Once embedded samples are sectioned to a thickness of 4μm for staining.

11.3.4 H&E staining

Haematoxylin binds to the basophilic elements of the tissue. After application the tissue is washed with an acidic alcohol to remove the non-bound stain. Eosin is then used to stain acidiophilic elements of the tissue.

The H&E slide staining has been automated using the Leica ST5020 Multistainer.

Table 10.3.1 below (H&E auto stain) details the programme used for the H&E staining of the tissue. At the end of this procedure a coverslip is also automatically applied to the slide.

Step	Station	Duration min
1	1 (Xylene)	1:30
2	2 (Xylene)	1:30
3	3 (100% IDA)	1:00
4	4 (100% IDA)	1:00
5	5 (70% IDA)	1:00
6	8(Wash 1)	0:30
7	6 (Haematoxylin)	2:00
8	7 (Haematoxylin)	2.00
9	9(Wash 2)	0:30
10	24 (Acid Alcohol)	0:20
11	12(Wash 3)	0:30
12	23 (Borax)	0:20
13	11(Wash 4)	0:30
14	22 (Eosin)	2:00
15	10(Wash 5)	0:30
16	20 (70% IDA)	0:30
17	19 (100% IDA)	1:00
18	18 (100% IDA)	1:00
19	17 (100% IDA)	1:00
20	16 (Xylene)	0:30
21	15 (Xylene)	0:30
22	14 (Xylene)	0:30
23	13 (Xylene)	0:30
24	Exit (Xylene)	end

Table 11.3.1 H&E auto stain sequence

11.3.5 Immunohistochemical staining.

The Leica Bond III automated immunohistochemistry stainer has been used for the immunostaining of the slides in this project. This has the benefit of being a semi-closed system, limiting the contact with potentially harmful chemicals during the process. After the application of the stain it applies a cover slip automatically. It also ensures a uniform process for all of the tested samples, which is especially useful in comparison studies.

11.3.6 CD-3

The CD-3 staining is performed with Epitomics (Epitomic inc. USA) Concentrated Rabbit anti-human CD-3 monoclonal antibody at a dilution of 1:80.

The manufacturer has clear recommended procedures for the use of these antibodies that are detailed below:

Pretreatment: using sodium citrate buffer 10mM Ph6.0 at 60°C for 20 minutes
Endogenous peroxidase block: blocking for 10 minutes at room temperature using peroxidase solution
Protein block: blocking for 10 minutes at room temperature using blocking solution
Primary antibody: incubate for 30 minutes.
Counterstain: haematoxylin for 5 minutes.

11.3.7 CD-20

CD 20 staining is performed with Dako (Denmark) monoclonal mouse anti-human CD-20 antibody at 1:800 dilution

The following procedure was adhered to (as per the manufacturers guidance) for the staining process:

Pretreatment: using sodium citrate buffer 10mmol/L (pH6.0) at 60°C for 20 minutes
Rinse; with de-ionised water
Primary antibody: application of the antibody at room temperature and incubation for 30 minutes.
Counterstain: haematoxylin for 5 minutes.

11.3.8 CD-31

CD-31 staining is performed with the Dako (Denmark) Monocloncal mouse anti-human CD-31 antibody at a concentration of 1:200

The following procedure was adhered to (as per the manufacturers guidance) for the staining process:

Pretreatment: with tromethamine buffer 10mmol/L (pH7.3) at 60°C for 20 minutes.
Rinse: with de-ionised water.
Primary Antibody: application of the antibody solution at room temperature for 30 minutes.
Counterstain: haematoxylin for 5 minutes.

11.3.9 CD-56

CD-56 antibody staining is performed with the Cell Marque (USA) Rabbit Monoclonal Anti-human CD-56 antibody at a concentration of 1:200.

The following procedure was adhered to (as per the manufacturers guidance) for the staining process:

Pre-treatment: with tromethamine buffer 10mmol/L (pH7.3) at 90°C for 20 minutes.
Rinse: with de-ionised water
Endogenous peroxidase block: blocking for 10 minutes at room temperature using peroxidase solution
Primary Antibody: application of the antibody solution and incubation at room temperature for 20 minutes.
Counterstain: haematoxylin for 5 minutes

11.4 Sample Hydration Data

Table 10.4.1 contains the initial and final prepared weights of the samples. This is used as a marker of weight loss as a result of dehydration of the sample during the process. Hydration of the samples can have a measurable effect on the indentation properties recorded; thus it is vital that the hydration status is maintained to ensure maximum accuracy of the results.

Sample	Level	Initial weight (g)	Prepared weight (g)	Change (g)
01	L4 Caudal	6.7343	6.7310	0.0033
	L5 Caudal	6.7289	6.7283	0.0006
	S1	6.7000	6.6948	0.0052
02	L5 Caudal	6.7019	6.7000	0.0019
	S1	6.6710	6.6706	0.0004
03	S1	6.6972	6.6971	0.0001
04	L4 Caudal	6.6969	6.6960	0.0009
	L5 Cranial	6.7103	6.7099	0.0004
06	S1	6.6901	6.6879	0.0022
07	L5 Caudal	6.7203	6.7197	0.0006
	S1	6.6819	6.6810	0.0009
08	L5 Caudal	6.8770	6.8762	0.0008
	S1	7.1201	7.1183	0.0018
09	L5 Caudal	6.7411	6.7401	0.0010
	S1	6.9387	6.9376	0.0011
10	L5 Cranial	6.8149	6.8136	0.0013
	L5 Caudal	6.9621	6.9612	0.0009
	S1	6.6932	6.6913	0.0019
11	L5 Caudal	6.9945	6.9934	0.0011
	S1	6.7021	6.7010	0.0011
12	L5 Caudal	6.8147	6.8144	0.0003
	S1	6.7034	6.7030	0.0004
13	L4 Caudal	6.8541	6.8511	0.0030
	L5 Caudal	7.0130	7.0111	0.0019
14	L5 Caudal	6.6574	6.6565	0.0009
	S1	6.9118	6.9099	0.0019
22	L4 Caudal	7.2322	7.2313	0.0009
	L5 Cranial	7.0042	7.0023	0.0019
	L5 Caudal	6.9782	6.9775	0.0007
	S1	6.8786	6.8771	0.0015

Table 11.4.1 Sample weights at the start and end of the preparation process used to indicate the maintenance of hydration

11.5 Publications

As part of the work undertaken as part of the preparation and review of the body of existing of work on this subject the following article has been published in the peer-reviewed journal Springer Nature Comprehensive Clinical Medicine. Citation:

Marjoram, T. The Endplate and Trabecular Bone in Lumbar Degenerative Disc Disease: A Narrative Review. SN Comprehensive. Clinical Medicine. 2020;2(3):332–337. Available from: https://doi.org/10.1007/s42399-020-00234-y.